A STUDY OF STRONG MOTION ACCELEROGRAMS FROM HIMALAYAN EARTHQUAKES

A Thesis Submitted
in Partial Fulfillment of the Requirements
for the Degree of
MASTER OF TECHNOLOGY

by

NAVIN N. CHANDAK

to the

DEPARTMENT OF CIVIL ENGINEERING

INDIAN INSTITUTE OF TECHNOLOGY KANPUR

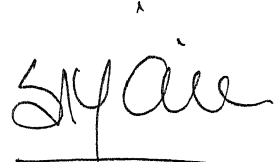JANUARY, 1994

DEDICATED
TO MY
GRAND PARENTS

CERTIFICATE

It is certified that the work contained in the thesis entitled "A Study of Strong Motion Accelerograms from Himalayan Earthquakes" by Navin N. Chandak, has been carried out under my supervision and that this work has not been submitted elsewhere for a degree.

January, 1994

(Sudhir Kumar Jain)
Associate Professor
Department of Civil Engineering
Indian Institute of Technology
Kanpur

ABSTRACT

Ground motion characteristics of the Himalayan earthquakes have been studied from the 198 horizontal component records and 99 vertical component records from six earthquakes in the region that are now available. The characteristics studied are the peak parameters, duration of strong shaking, shape of elastic response spectrum and ductility reduction factor. It is found that mean A/V ratio is quite high in the region and does not vary much with the distance from the shock-source. A study of shape of elastic acceleration response spectra revealed that: (1) shape varies somewhat insignificantly with the distance, (2) shape of spectra in the intermediate period range highly depends on earthquake magnitude, (3) there is a urgent need to revise the shape of response spectra recommended in IS:1893-1984, and (4) shape of "standard spectra" suggested by AERB for rock sites is comparable with the mean-plus-one-standard-deviation shape from the data. Both, the ratios of peak parameters and elastic response spectra indicate that with distance the attenuation of waves of different frequencies is not so different as elsewhere. Based on the data, shape of ductility reduction factor spectrum to be used in design is also proposed.

ACKNOWLEDGEMENTS

LIST OF CONTENTS

LIST OF TABLES

LIST OF FIGURES

LIST OF SYMBOLS

A	Peak ground acceleration
A_V	Peak vertical acceleration
A_H	Larger peak horizontal acceleration
D	Peak ground acceleration
E_1	Location of epicentre by IMD
E_2	Location of epicentre by USGS
E_3	Location of epicentre by Chandrashekharan and Das
E_4	Revised estimate of epicentre location by IMD
M	Magnitude of earthquake
R	Epicentral distance
R_μ	Ductility reduction factor
T	Natural period
V	Peak ground velocity
g	Acceleration due to gravity
u(t)	Relative displacement
$\dot{u}(t)$	Relative velocity
$\ddot{u}(t)$	Relative acceleration
ω	Natural frequency
ζ	Fraction of critical damping

LIST OF ABBREVIATION

AERB	Atomic energy regulatory board
ATC	Applied Technology Council
COV	Coeffecient of variation
DRF	Ductility reduction factor
EPP	Elastic-perfectly plastic
IMD	India meteorological department
IS	Indian standard code
MPOF	Multi degree of freedom system
NEHRP	National earthquake hazards reduction program
NRC	Nuclear regulatory commission
PGA	Peak ground acceleration
PGD	Peak ground displacement
PGV	Peak ground velocity
PSA	Pseudo-acceleration spectra
PSV	Peak ground velocity
SD	Spectral displacement
SDOF	Single degree of freedom system
SEAOC	Structural engineers association of california
UBC	Uniform building code
USGS	United States geological survey

CHAPTER I
INTRODUCTION

1.1 GENERAL

Earthquake-resistant design of structures requires estimate of the expected ground motions at the site in future earthquakes. In order to develop ability to reasonably assess the expected ground motion due to future earthquakes, it is essential to study the characteristics of strong ground motions recorded in the past earthquakes.

Design of engineering structures is usually governed by building codes and standards of design practices. The recommendations in these codes are often based on the analysis of records from major earthquakes. For example, the seismic design spectrum, specified in the codes, takes into consideration characteristics of recorded ground motions. As more records become available, these recommendations are updated and improved for better earthquake-resistant design. Unfortunately, until recent years, time history records of strong ground motion in the Indian earthquakes were almost non-existing. As a result, for instance, the shape of design spectrum in the Indian seismic code (IS:1893 - 1984) is based mainly on some earlier earthquakes in California.

Since 1986, a number of strong motion records have become available from earthquakes in Himalayas. These need to be studied and analysed to understand the peculiarities of ground motion in the Himalayan region.

1.2 SCOPE OF THE STUDY

In the present work, strong motion instrument data from Himalayas, recorded during the period 1986-1991, are examined. In all, 198

horizontal component and 99 vertical component records from six different earthquakes with magnitude varying from 5.2 to 7.2 and epicentral distance in the range of 5 km to 320 km are now available. These have been analysed to understand the characteristics of earthquake ground motion in the Himalayas. The characteristics studied are the peak parameters, duration of strong shaking, shape of response spectrum, and ductility reduction factor. Results obtained are compared with those from published studies based on earthquakes elsewhere and with currently adopted design practices.

1.3 ORGANIZATION

Apart from this introductory chapter, the thesis comprises of five more chapters to cover the present work. Chapter II gives details about the strong motion records used in this study. Chapter III presents the characteristics of the data in terms of ratios of peak ground motions and duration of strong shaking. Chapter IV presents the study on shape of response spectra obtained from the data. Chapter V presents the study on ductility reduction factor for elasto-plastic model. Summary and conclusions from the present work are given in Chapter VI. Appendix A gives the details of the records used in the study with regard to name of stations triggered in each earthquake, epicentral distances, peak ground acceleration, peak ground velocity, peak ground displacement, duration of strong shaking (Trifunac and Brady 1975), and spectrum intensity (Housner 1959) for 5% damping.

CHAPTER II
STRONG MOTION RECORDS

2.1 INTRODUCTION

Ground motion during an earthquake is measured by a seismograph which is essentially a single degree of freedom system with its mass, stiffness, and damping characteristics appropriately designed. Instruments with large natural period (flexible oscillator) usually record ground displacement; these being flexible are very sensitive and can record even the slightest motions in ground. Such instruments, normally termed as seismographs, are useful for recording very small earthquakes or for recording large earthquakes taking place at large distance away from the instrument. However, these go off-scale in case of a strong shaking, which is of primary interest for engineering applications. On the other hand, instruments with a stiff oscillator (large natural frequency) measure ground acceleration and are not sensitive to weak ground motions. Such instruments, often termed as strong motion accelerographs, provide the realistic levels of ground acceleration that an engineering structure may be subjected to during a strong shaking. In normal operations, these instruments lie in a passive state, and get triggered, to operate, when the ground motion exceeds a threshold value set for the instrument.

The acceleration versus time records obtained from such instruments are called accelerograms. Usually, an accelerogram is in the form of an analog record, such as a photographic film. However, in recent years, digital instruments have also become available. The analog records obtained from the accelerograph films have to be digitized at closely spaced time intervals. The digital time history, obtained directly or

from digitizing the analog record, is then corrected through appropriate filtering to control the digitization errors and baseline distortion; also certain accelerograph transducer corrections are applied. The records thus processed are termed as the "corrected" accelerograms. The corrected accelerogram can then be integrated with respect to time to obtain a velocity versus time record, which can be further integrated to obtain a displacement versus time record.

2.2 CHARACTERISATION OF STRONG GROUND MOTION

Fig. 2.1 shows some typical accelerograms obtained from epicentral region of different earthquakes. A visual comparison of these records suggests that the characteristics of earthquake ground motion may vary significantly with regard to the peak acceleration, number of significant peaks in the time record, and duration of shaking.

Fig.2.2 shows the acceleration, velocity, and displacement time histories derived from a typical accelerogram. Not surprisingly, the integration of record changes its frequency content; while the acceleration record has large high frequency content, the displacement record shows motion of high period, and the velocity record shows an intermediate frequency content. A structure is expected to achieve resonance (or multifold increase in response) when frequency of ground motion matches with natural frequency of the structure. Hence, structures with different natural period are expected to respond differently in the same earthquake.

The earthquake ground motion, which is somewhat random with time, can be characterized by several parameters depending on the application. The parameters of most interest are the peak parameters (peak ground

acceleration, velocity, or displacement), duration of strong shaking, and its frequency content. The frequency content is somewhat more difficult to quantify and is usually represented through a Fourier spectrum or a response spectrum.

Traditionally, in the earthquake-resistant design, peak ground acceleration has been the single most frequently used parameter for describing the severity of ground motion. A rigid structure subjected to a given earthquake ground motion experiences a total earthquake force equal to its mass times the peak ground acceleration. Thus, peak ground acceleration gives a good physical feel of the ground motion and is a convenient rule of thumb for scaling different accelerograms. The difficulty with peak ground acceleration is that, sometimes, it gives a very misleading indication of the earthquake ground motion. For instance, an earthquake of rather low magnitude (say M = 4 or 5) may give a rather large peak ground acceleration, even though the overall motion may not be very damaging to structures.

The peak ground velocity is associated with waves of intermediate frequencies (mostly between 0.3 to 3.0 Hz), which is also the range in which most civil engineering structures lie. Hence, peak ground velocity is a much better indicator of the damage potential of a ground motion than the peak ground acceleration. Peak ground displacement is associated with waves of low frequencies (0.1 to 0.3 Hz); in this frequency range very few structures lie, hence this parameter is not very useful for engineering applications. However, peak ground displacement is an important parameter for seismological studies, because, amplitudes of ground displacement are propagated more coherently than amplitudes of ground velocity and acceleration. This due

to the fact that their low-frequency spectral composition is not very sensitive to scattering by small geologic inhomogeneities. Also, peak ground displacement gives a somewhat better indication of the fault displacement.

2.3 STRONG MOTION INSTRUMENTATION IN HIMALAYAS

The arc-shaped Himalayan belt extending from Pamirs in erstwhile USSR to Arkans in Burma has long been regarded as a highly seismic area in the world. The Himalayan belt is believed to have formed due to collision of Indo-Australian and Eurasian plates in past several million years. The area has experienced several destructive earthquakes of magnitude greater than 8.0. The notable among these earthquakes are the Assam earthquake of 1897 (M = 8.7), the Kangra earthquake of 1905 (M = 8.6), the Bihar-Nepal earthquake of 1934 (M = 8.4), and the Assam-Tibet earthquake of 1950 (M = 8.7) (Fig 2.3). Numerous earthquakes of magnitudes ranging between 6.0 and 7.0 have also occurred in the region.

An international workshop on strong motion earthquake instrument arrays held in Honolulu, Hawaii, in May 1978 (Iwan 1978) identified the area around Shillong in the north-eastern India as the highest priority site for deployment of a strong motion array. Subsequently, three strong motion arrays, listed below, have been deployed in the Himalayan region:

(a) An array of fifty strong motion accelerographs (SMA-1 of m/s Kinemetrics, USA) is located in north-west Himalayas in the state of Himachal Pradesh. This array is identified as Kangra array.

(b) An array of fortyfive SMA-1 is located in north-east Himalayas in the states of Assam and Meghalaya. This array is identified as Shillong array.

(c) An array comprising of forty SMA-1 instruments is located in the central Himalayas in the state of Uttar Pradesh. This is identified as Uttar Pradesh array.

Fig. 2.4 shows the location of these arrays. There are also plans to instrument the Himalayas of Bihar-Nepal border region. Thus, the Himalayan zone is now better instrumented to record the strong-motion data from future earthquakes.

Besides the above three arrays, the region also has a number of indigenous strong motion accelerographs and structural response recorders (EQ 88-16 1988, EQ 93-16 1993); these have also provided records of strong ground motion. However, the data from these instruments has not been considered in the present study.

2.4 STRONG MOTION DATA USED IN THE PRESENT STUDY

The Kangra array registered an event of magnitude 5.5 on April 26, 1986. This is the only significant event recorded so far by this array. The Shillong array has registered four events during 1986-1988, while the Uttar Pradesh array has registered one event in October 1991. The details of these events with regard to their date, magnitude, maximum peak ground acceleration, and the range of epicentral distance are presented in Table 2.1. This table also gives the abbreviation used in rest of this study for describing different events (e.g., "Sept" for the earthquake of September 10, 1986). The magnitudes indicated in table are as per estimates of the United States Geological Survey (USGS); these differ somewhat from those by the India Meteorological Department (IMD). Thus, the present study is based on 99 sets of strong motion records (198 horizontal components and 99 vertical components) obtained from six

earthquakes (magnitude ranging from 5.2 to 7.2) that have occurred in three different regions of the Himalayas. The epicentral distance for these records varies from about 5 km to 320 km. Detailed description on site geology of stations is not available. However, Chandrashekharan and Das (1990) indicate that the stations are located on "reasonably firm ground", "soil", or on "soft sedimentary rock". In the absence of more specific information about the local soil conditions, all stations are assumed to have almost similar ground conditions, i.e., the records have not been classified on the basis of soil conditions. Moreover, while comparing with other data, the stations are assumed to be at rock sites.

Figures 2.5 to 2.10 show the location of instruments triggered during the different earthquake events. Also shown in these figures is the location of epicenter. Figs. 2.5 to 2.9 show three locations of epicentre: E1 is the estimated location by the IMD, E2 is that by the USGS, and E3 is the location suggested by Chandrashekharan and Das (1990) based on records from the array. For "April" (Fig. 2.5), revised estimate of epicentre by IMD, E4, is also shown. For each of the events, Appendix A gives the name of the stations triggered and three different estimates of epicentral distance for each station. Also presented in Appendix is the peak ground acceleration, peak ground velocity, peak ground displacement, spectrum intensity (Housner 1959) for 5% damping and duration of strong shaking (Trifunac and Brady 1975) for each of the records used in the study. The different estimates of epicentre in these earthquakes vary by as much as 68 km for "Sept" and 85 km for "Feb". Such large variation rules-out the possibility of using epicentral distance as a criteria for classifying the records for low, medium, and large epicentral distances. Moreover, for most of these events, neither

an indication of rupture zone (based on aftershock data) nor the isoseismals are available. Thus, the distance of recording station from the zone of energy release also cannot be used as a criteria for classifying the records. However, in this study, epicentral distance refers to the epicentral location suggested by Chanshekhran and Das (1990) based on the analysis of strong motion records. The location of epicentre for the "Oct" event (Fig. 2.10) is fairly accurate.

To account for the variation in epicentral distance, each set of records has been classified into one of the three groups on the basis of the value of larger horizontal peak ground acceleration (PGA). Records with larger horizontal peak ground acceleration less than 0.05g are classified into the low PGA group, whereas those with greater than 0.1g PGA are classified into the high PGA group; records with larger horizontal peak ground acceleration between these two limits are classified into the medium PGA group. Thus, once the larger horizontal PGA from a set falls in one group, all the three components of that set are included in that group. The limits of PGA for classification were chosen so that in each group a reasonable number of accelerograms could be included. Table 2.2 shows the summary of number of records included in each of the groups from different events.

Table 2.1 Summary of the earthquake events considered in this study.

Array region	Date of event	Abbreviated as	M	NS	R (km)		PGA (g)	
					Min.	Max.	Horz	Vert
Kangra	April 26, 1986	April	5.5	9	5	29	0.250	0.082
Shillong	September 10, 1986	Sept	5.2	12	15	181	0.138	0.062
	May 14, 1987	May	5.7	14	46	179	0.086	0.005
	February 6, 1988	Feb	5.8	18	35	176	0.114	0.103
	August 6, 1988	Aug	7.2	33	100	324	0.343	0.180
Uttar Pradesh	October 20, 1991	Oct	6.6	13	25	151	0.310	0.294

M   : Magnitude of earthquake
NS   : Number of stations triggered
R   : Epicentral distance (approximate)
PGA : Peak ground acceleration
Horz : Horizontal component
Vert : Vertical component

Table 2.2 Summary of number of records in the three PGA groups.

Array region	Event	High PGA group		Medium PGA group		Low PGA group	
		Horz	Vert	Horz	Vert	Horz	Vert
Kangra	April	10	5	4	2	4	2
Shillong	Sept	6	3	8	4	10	5
	May	0	0	12	6	16	8
	Feb	2	1	12	6	22	11
	Aug	28	14	32	16	6	3
Uttar Pradesh	Oct	8	6	12	4	6	3
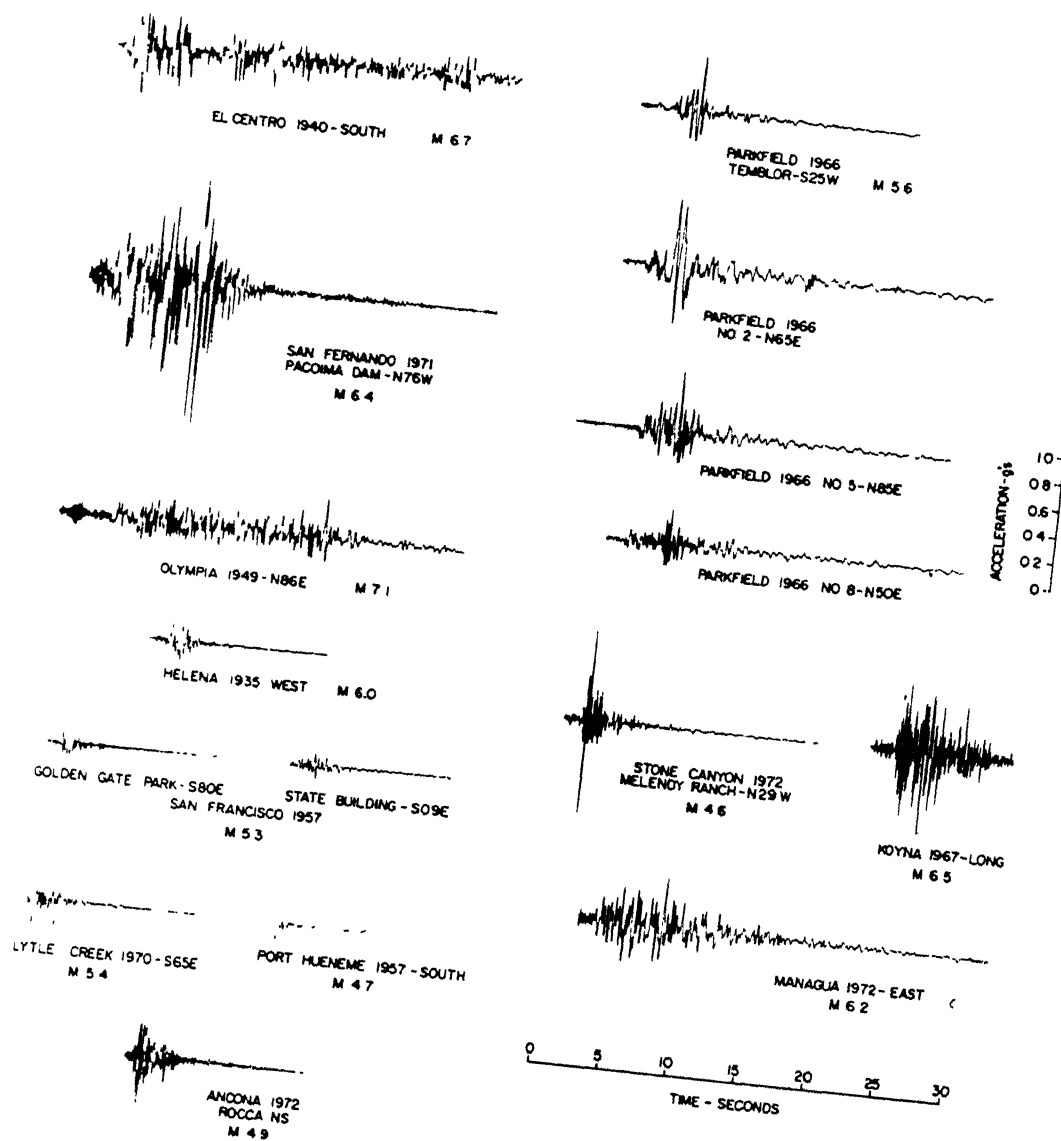
Fig. 2.1   Typical accelerograms obtained from epicentral region of different earthquakes (Hudson 1979).
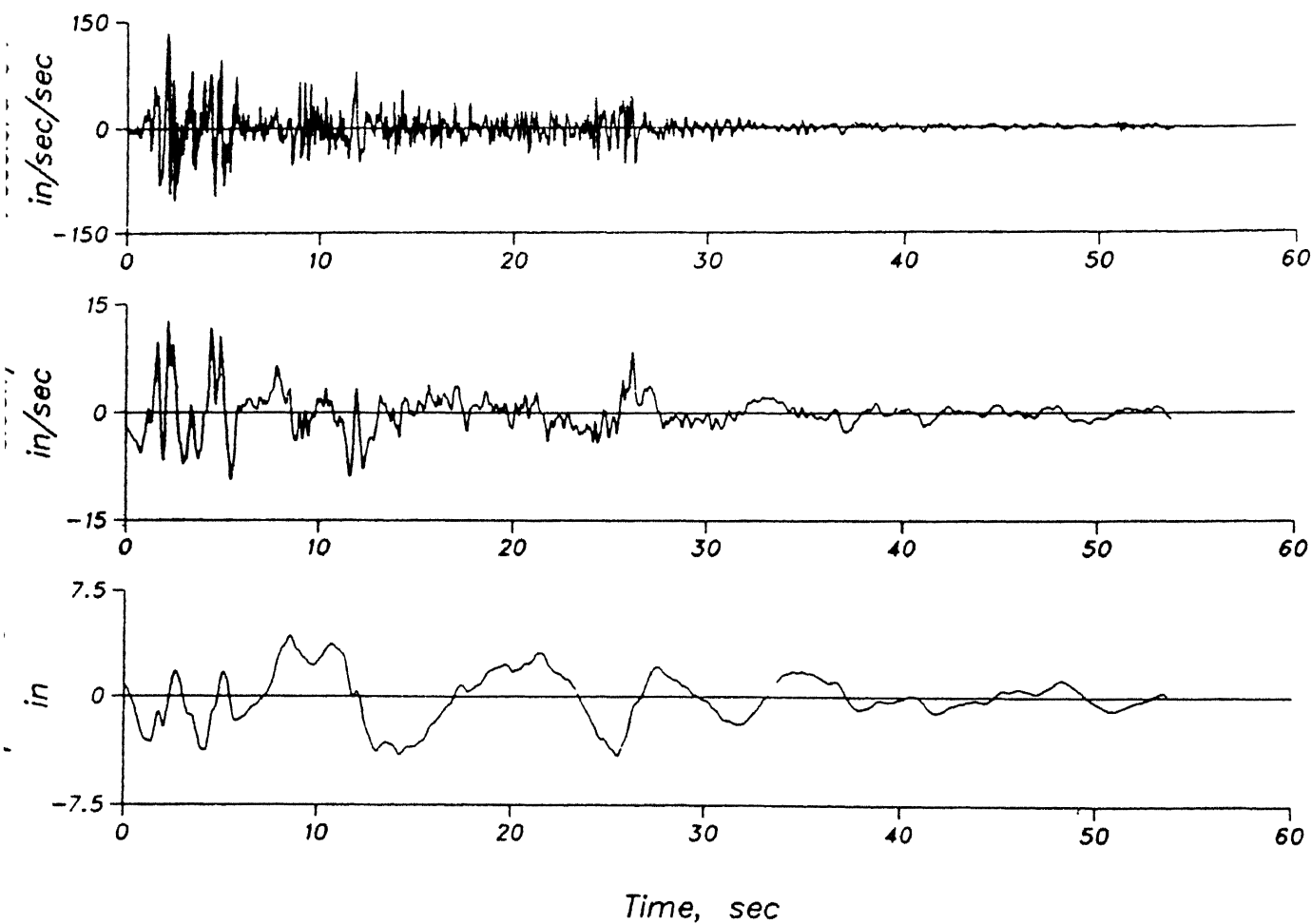
Fig. 2.2   Acceleration,   velocity,   and   displacement   time
            histories   for   the   SOOE   component   of   El   Centro
            earthuake of 1940 (Mohraz and Elghadamsi 1989).
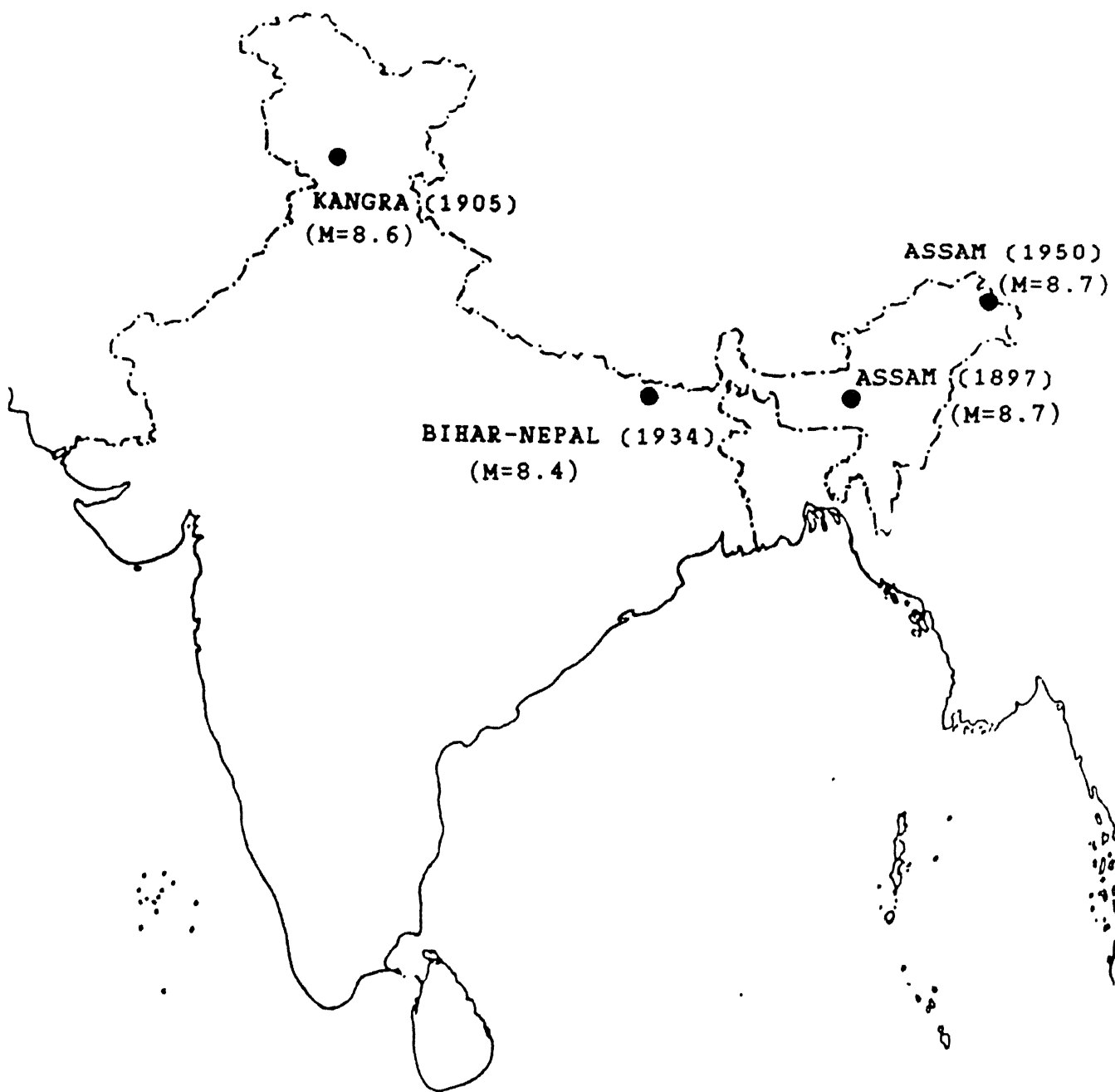
Fig. 2.3   Some great Himalayan earthquakes.
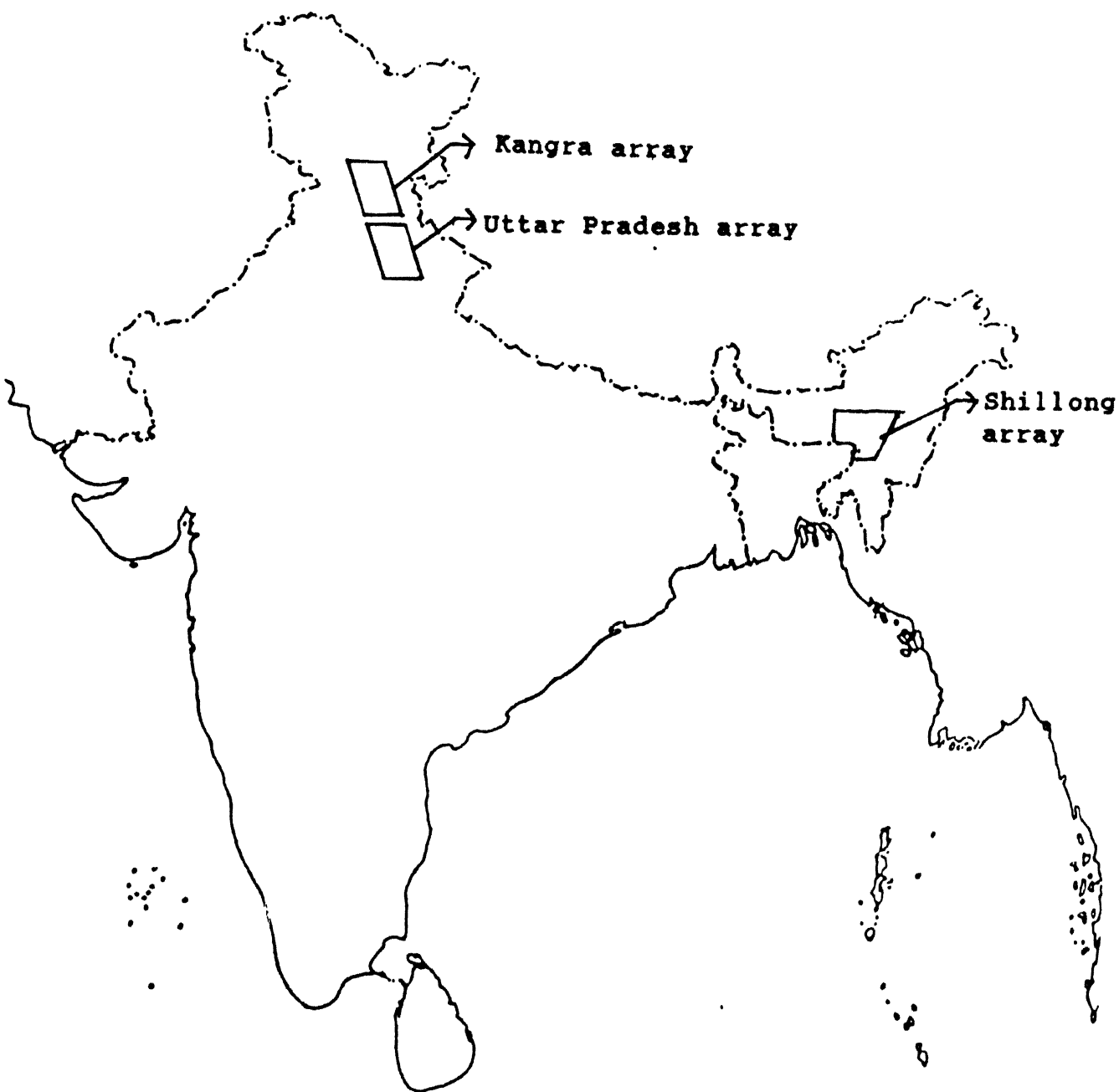
Fig. 2.4   Location of strong motion instrument arrays in Himalayas.
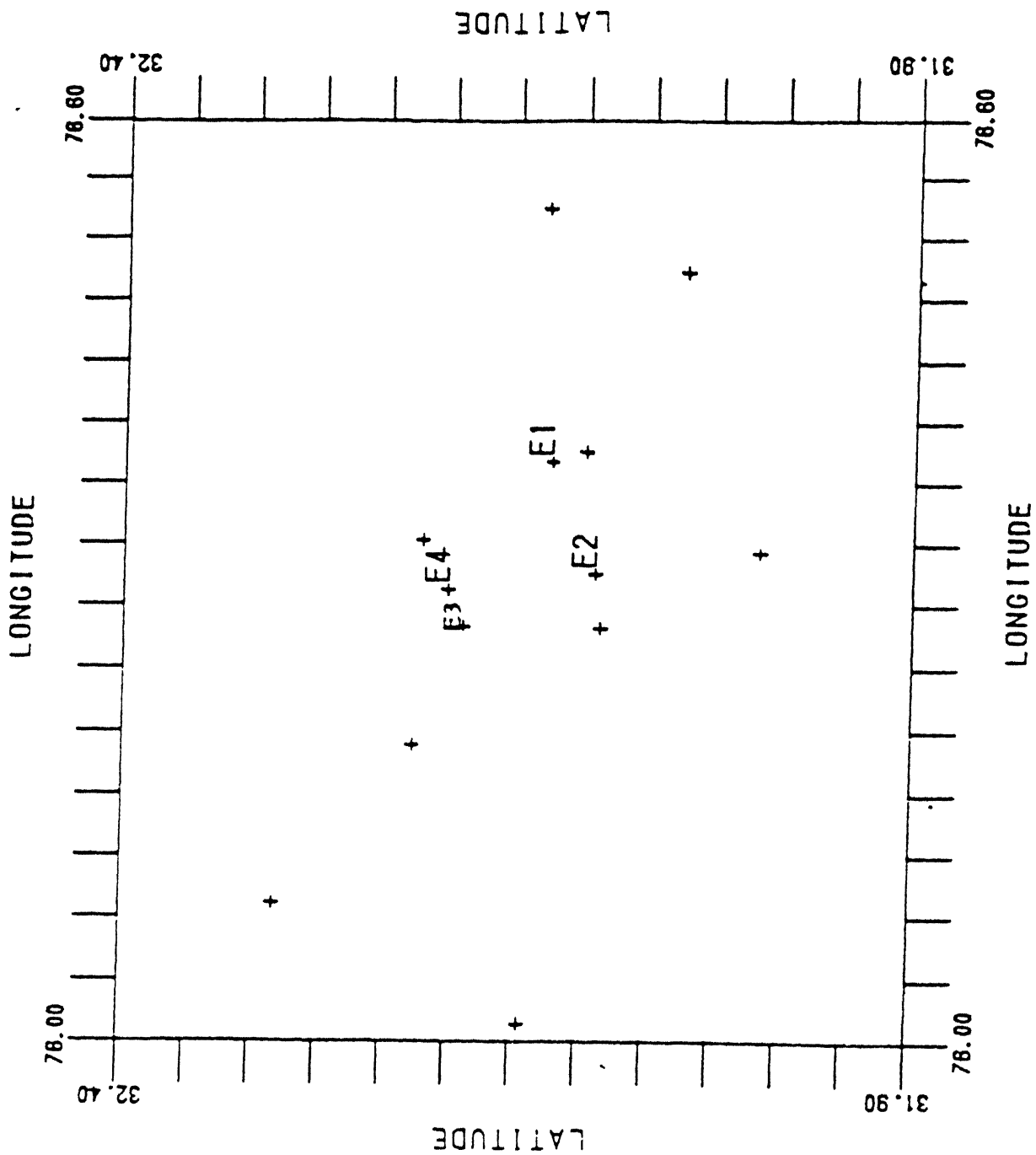
Fig. 2.5   Location of instruments triggered and epicentre for the April 26, 1986 earthquake. (Chandrasekaran and Das 1990).
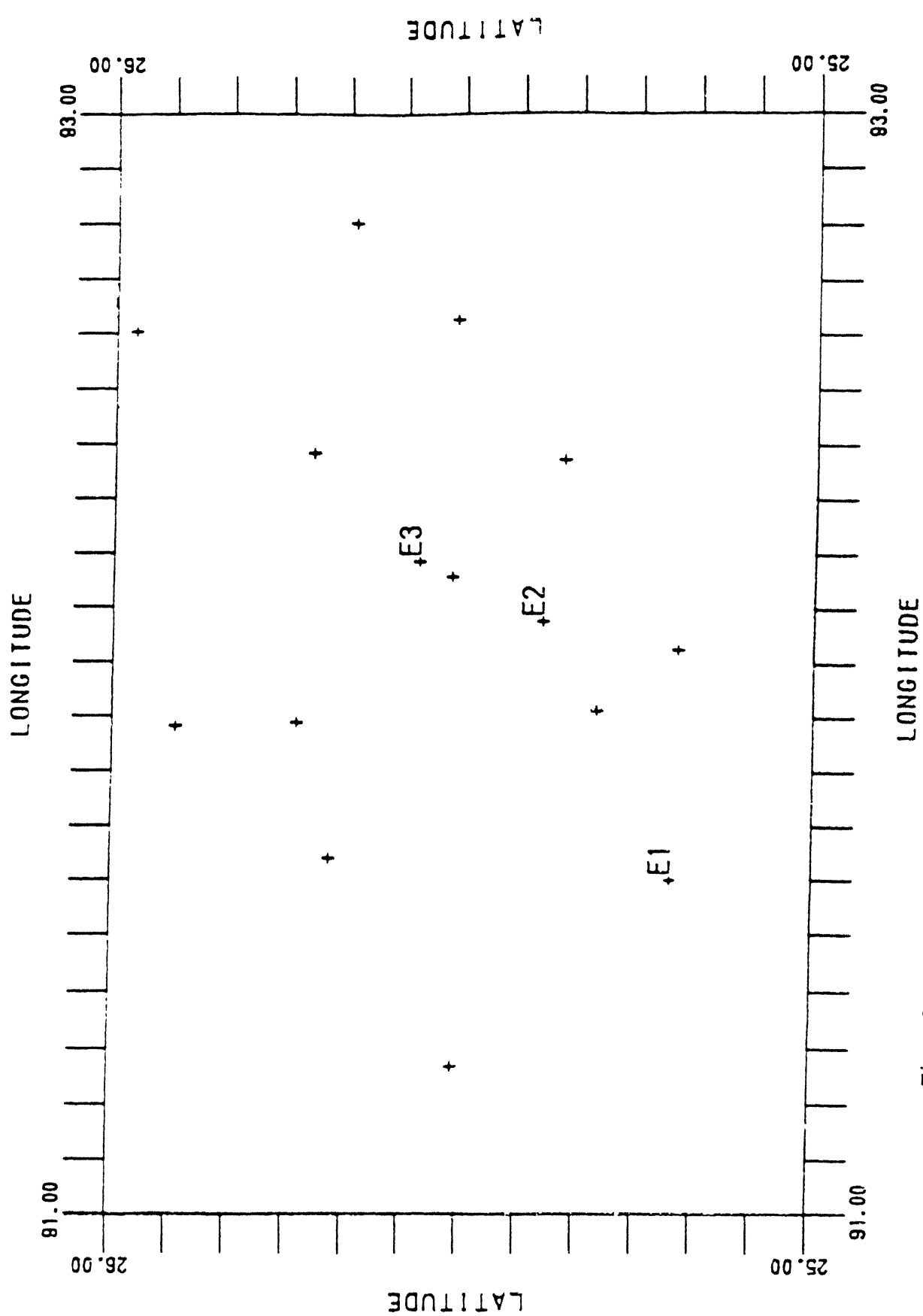
Fig. 2.6   Location of instruments triggered and epicentre for the September 10, 1986 earthquake. (Chandrasekaran and Das 1990).
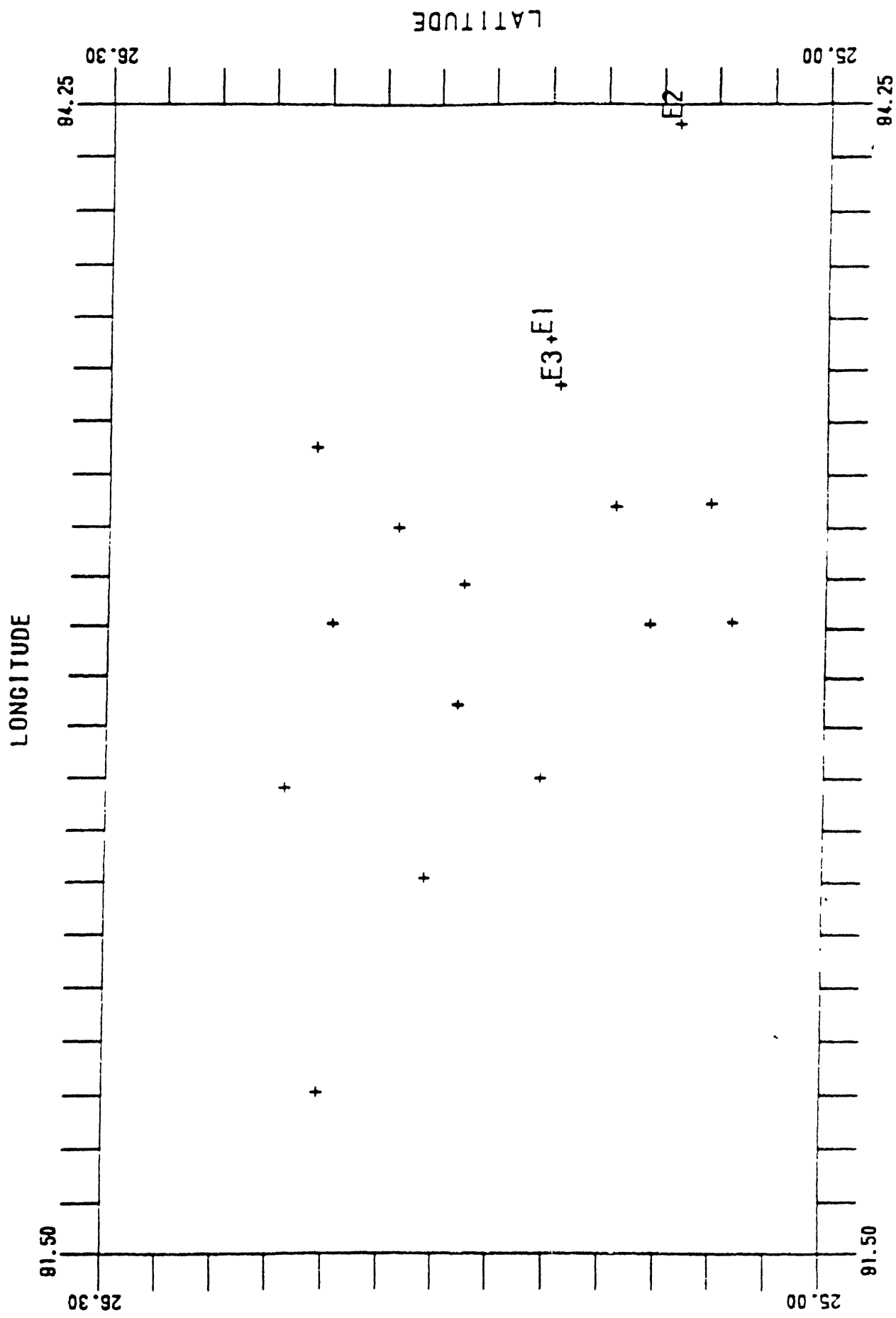
Fig. 2.7   Location of instruments triggered and epicentre for the May
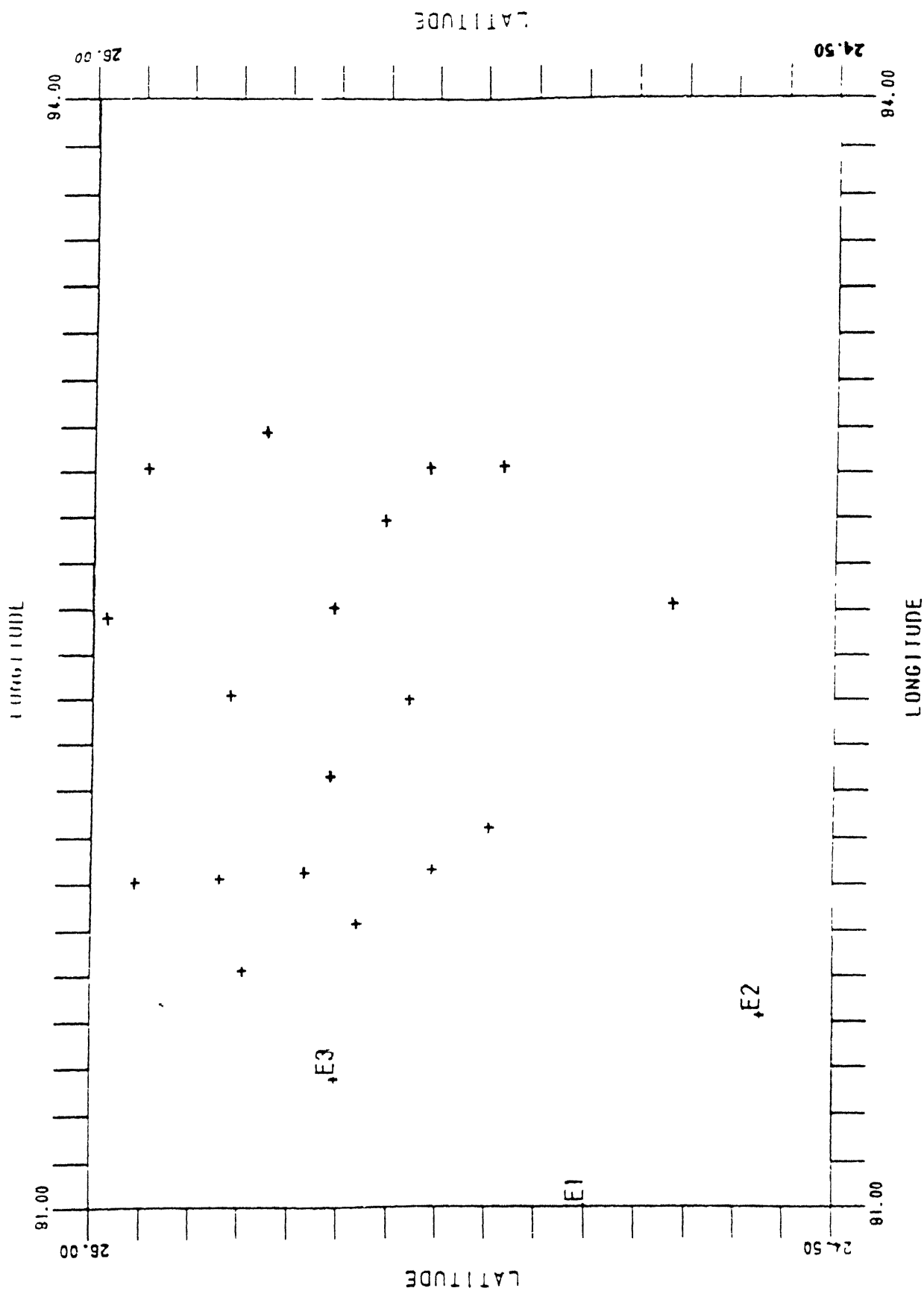
Fig. 2.8 Location of instruments triggered and epicentre for the February 6, 1988 earthquake. (Chandrasekaran and Das 1990).
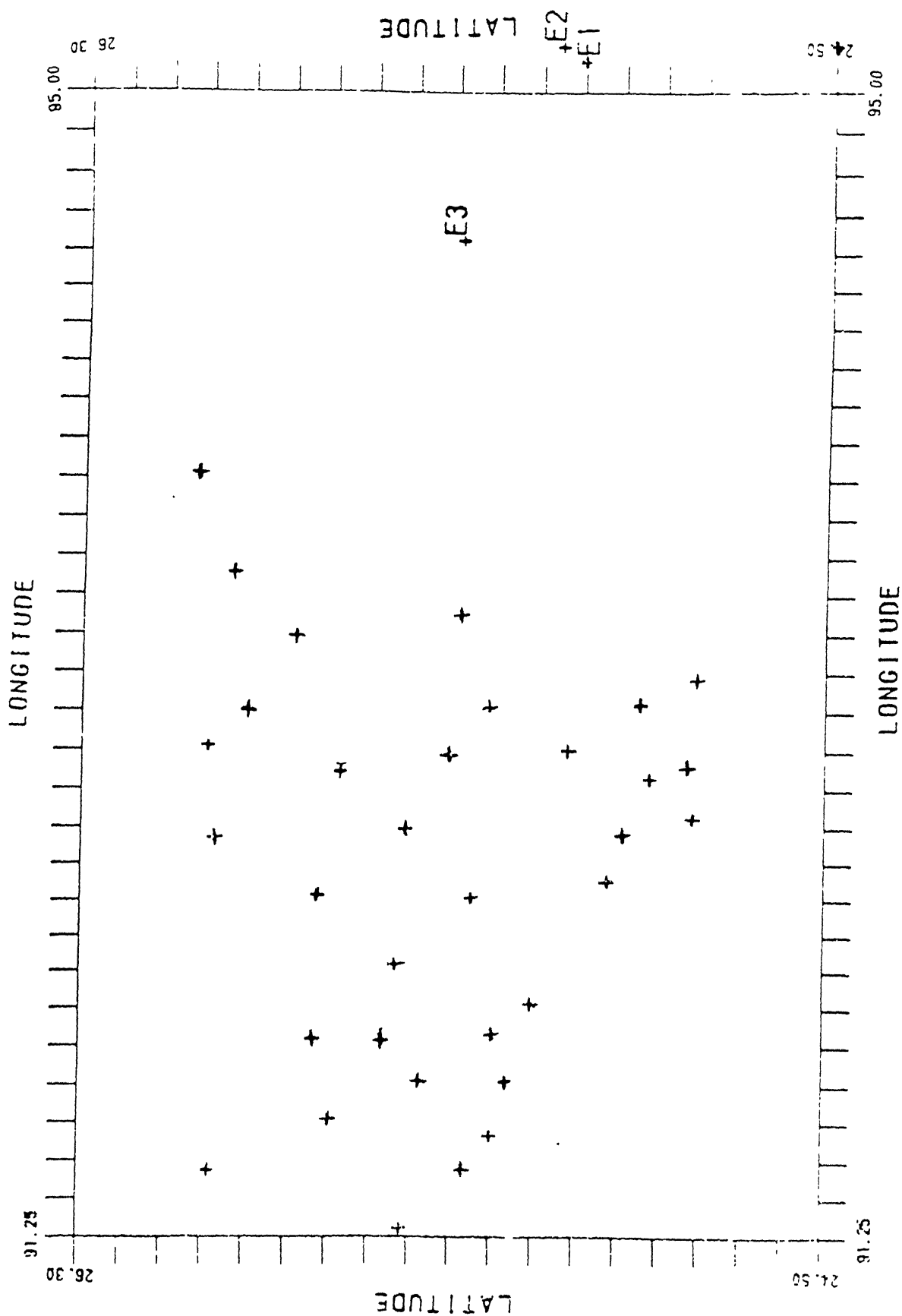
Fig. 2.9 Location of instruments triggered and epicentre for the August 6, 1988 earthquake. (Chandrasekaran and Das 1990).
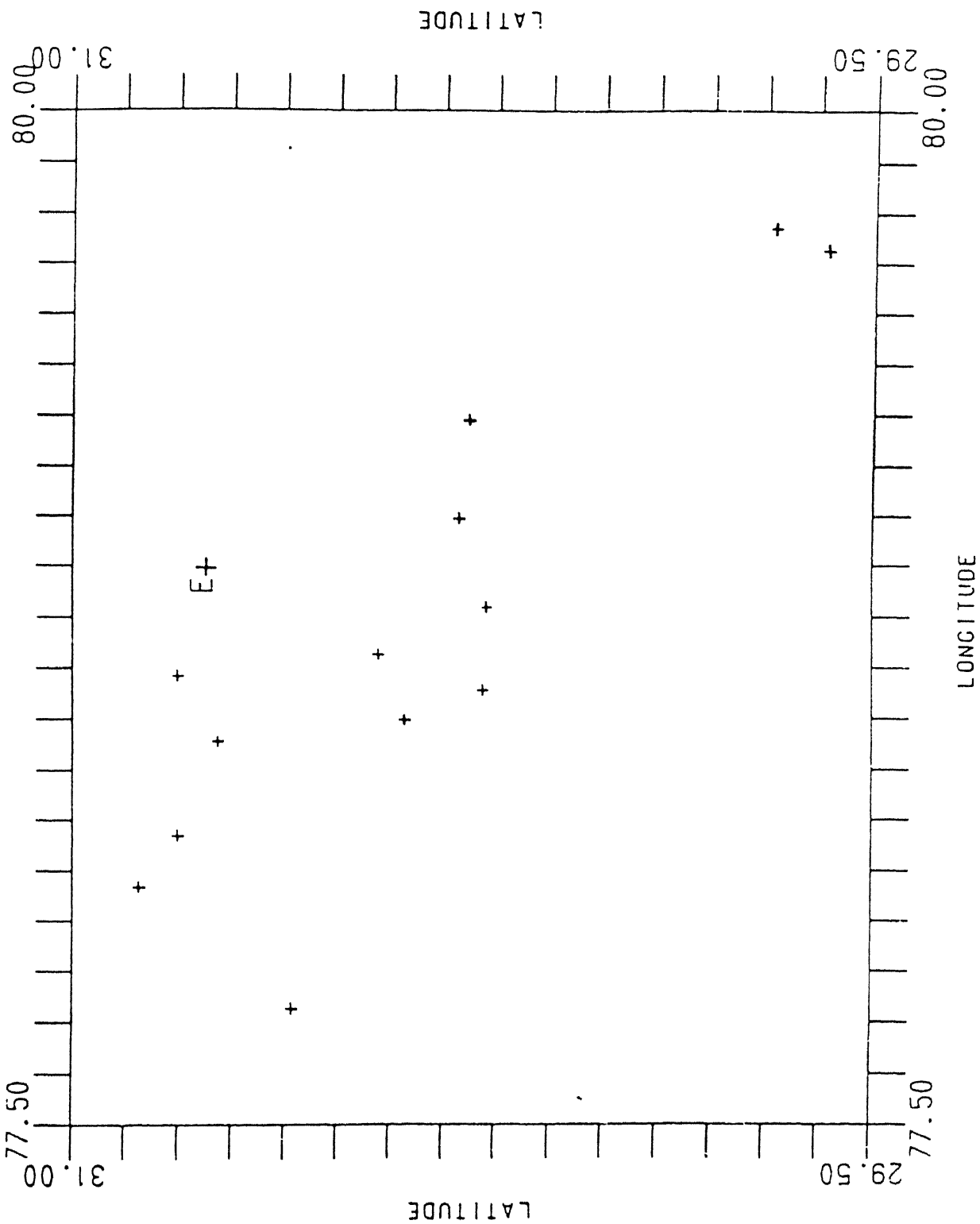
Fig. 2.10 Location of instruments triggered and epicentre for the
October 20, 1991 earthquake. (Chandrasekaran and Das 199).

CHAPTER III

RATIOS OF PEAK GROUND MOTION AND DURATION OF STRONG SHAKING

3.1 INTRODUCTION

Given an estimate of horizontal peak ground acceleration (PGA) at a given site, the values of peak ground velocity (PGV) and displacement (PGD) are often obtained by using average values of ratio of peak parameters. Two ratios, A/V and AD/V^2 (A: peak ground acceleration, V: peak ground velocity, D: peak ground displacement) are most often used for this purpose. Similarly, vertical peak ground acceleration is usually estimated by using an average value of the ratio A_V/A_H (A_V : vertical peak ground acceleration, A_H : horizontal peak ground acceleration). A number of studies are available which indicate the average value of these ratios for a given type of site condition, based on ground motions recorded elsewhere in the world (e.g., Mohraz et al. 1972, Mohraz 1976, Mohraz 1991).

Seismological studies show that attenuation of seismic waves is frequency dependent; high frequency waves attenuate more rapidly with distance than moderate or low frequency waves. Since, peak ground acceleration, peak ground velocity, and peak ground displacement are associated with waves of different frequencies, these ratios of peak parameters happen to be good indicators of ground motion characteristics at different sites. For example, ground motions experienced near an earthquake source are expected to have higher value of A/V than ground motions at a large distance from the source of seismic energy release. This is so because the high frequency waves (and hence the PGA)

attenuate faster with distance than the intermediate frequency waves (and hence the PGV).

It can be seen that for harmonic oscillations, $AD/V^2 = 1.0$. With distance, the ground motion tends to become harmonic with ever-increasing period; hence as epicentral distance increases, the AD/V^2 ratio must reduce and approach to unity (Newmark and Rosenblueth 1971). Also, certain response spectrum characteristics can be correlated to the AD/V^2 ratio.

This chapter presents a study of the peak parameter ratios and duration of strong shaking from strong motion data of the six Himalayan earthquakes.

3.2 REVIEW OF THE PAST STUDIES

3.2.1 A/V Ratio

Mohraz et al. (1972) conducted the first study on V/A ratio. They obtained the average values of V/A from a data set, mostly consisting of records obtained from the San Fernando earthquake of 1971. They recommended the value of V/A ratio as 48 in/sec/g (A/V ratio as 8.1 sec^{-1}) for firm ground, and 32 in/sec/g to 36 in/sec/g (A/V ratio in the range 11.7 sec^{-1} to 12.1 sec^{-1}) for rock sites.

Mohraz (1976) studied the variation of V/A ratio with different site conditions using 54 earthquake records obtained in 16 seismic events in California. The records were classified into four categories depending on the geological conditions at site. For each site category, the ratios were obtained for three groups; the first group consisted of horizontal component records with larger PGA, the second of horizontal component records with smaller PGA, and the third of vertical component

records. Table 3.1 summarises these results. It can be seen that A/V ratio is higher for rock sites than for alluvium. Also, A/V ratio for horizontal component group with larger PGA is higher than that for the lower PGA group. A/V values for the vertical component are close to those for horizontal component group with larger PGA.

Variation of V/A ratio (and hence A/V ratio) with distance from the ruptured surface (R) has been studied by Mohraz (1991) from records of the Loma Prieta earthquake of 1989 (Table 3.2). It is seen that at rock sites A/V ratio for near-field records (R < 20 km) can be more than twice that for mid-field records (50 km > R > 20 km). At alluvium sites, the difference is about 30 %. However, as the site distance increases beyond 50 km, A/V ratio shows a slight increase.

Using 36 records from rock sites, Zhu et al. (1988) studied the effect of ground motions with low, normal, and high A/V ratio on the damage of single degree of freedom stiffness-degrading systems. They demonstrated that if a system is subjected to ground motions with same PGA as that of the design spectrum, the ground motions with low A/V ratio can cause much more significant peak inelastic deformation, stiffness deterioration, and hysteretic energy dissipation than is the case for ground motions with high A/V ratio. This is consistent with the general expectation that given two ground motions with the same PGA, the motion with higher PGV will be more damaging to the structures.

Tso et al. (1992) have examined the engineering implications of A/V ratio on the ground motion characteristics. A data set consisting of 45 records obtained from rock sites during 23 events having magnitude ranging between 5.2 to 8.1 was used. The records were classified as low, normal, or high A/V when this ratio was less than 0.8 g/m/s (= 7.9

sec^{-1}), between 0.8 g/m/s and 1.2 g/m/s (= 11.8 sec^{-1}), and more than 1.2 g/m/s. The study concluded the following:

- Ground motions in the vicinity of small or moderate earthquake usually have high A/V ratio, whereas those distant from large earthquakes have low A/V (Fig. 3.1).

- Ground motions with high A/V ratio usually have seismic energy in the high frequency range, whereas those with low A/V ratio have energy in low frequency range. It was seen that ordinates in acceleration spectra for periods longer than about 0.5 sec for low A/V records could be more than twice as high as those for high A/V group (Fig. 3.2).

- Peak ground velocity correlates well with the spectrum intensity (Housner 1959) over earthquake records having drastically different A/V ratio.

3.2.2 AD/V^2 Ratio

The AD/V^2 ratio was first introduced by Esteva (1969). The ratio is primarily used to estimate PGD from known PGA and PGV. He suggested an empirical equation for estimating AD/V^2 for a known epicentral distance (R in km):

$$\frac{AD}{V^2} = 1 + \frac{400}{R^{0.6}}$$

Newmark and Rosenblueth (1971) suggest that choice of AD/V^2 to evaluate PGD is preferable as compared to D/A or D/V ratios because the integrated velocities and displacements are sensitive to baseline adjustment and large errors may accumulate during the integration. By selecting AD/V^2, the error which may arise is distributed among the

ground motion parameters. According to Newmark and Rosenblueth, for most earthquakes of practical interest AD/V^2 ranges from approximately 5 to 15.

Mohraz et al. (1972) recommend an "adequately conservative" value of 6.0 for AD/V^2 ratio. Further, they observed that AD/V^2 is a measure of sharpness or flatness of pseudo velocity spectrum, i.e., higher the value of AD/V^2 ratio, flatter will be the pseudo velocity spectrum. Table 3.1 clearly shows that AD/V^2 is higher for rock sites than for the alluvium; however, this is not so obvious from the Loma Prieta earthquake data (Table 3.2). Also, Table 3.2 does not show any specific trend in the value of AD/V^2 ratio with site distance from the ruptured surface.

3.2.3 A_V/A_H Ratio

Table 3.3 shows the mean and 84.1 percentile values of the vertical to larger horizontal PGA ratio (A_V/A_H) obtained by Mohraz (1976). For rock sites the mean value is around 0.52 while the 84.1 percentile value is around 0.69. He observes that "The ratio of the vertical to larger peak horizontal acceleration of 2/3, which is currently employed in seismic design corresponds to 84.1 percentile ratio and not the mean. Although this value is conservative, its use has been justified to account for variations greater than the median and mean". The Indian code (IS:1893-1984) recommends that the ratio of vertical to horizontal seismic coefficient be taken as 0.5.

3.3 RESULTS FROM THE DATA

For each of the six events, mean and mean-plus-standard deviation

values of the A/V and AD/V^2 ratios for high, medium, and low PGA groups have been computed; these are summarized in Table 3.4. The ratio for vertical PGA to the larger horizontal PGA (A_V/A_H) for different events is given in Table 3.4. The trends for the Himalayan earthquakes from these tables are discussed here.

3.3.1 A/V Ratio

Table 3.4 clearly shows that the A/V ratio for the Indian earthquakes is unusually high. For the horizontal components, the mean value for different events ranges from 13.3 sec^{-1} to 32.5 sec^{-1} with an overall mean value of 20.2 sec^{-1}. These values are to be compared with mean values of 12 sec^{-1} to 15 sec^{-1} for rock sites suggested by different studies of Mohraz based on data for elsewhere. For instance, Mohraz (1972) suggests the value as around 12 sec^{-1}; Table 3.1 indicates a value of 14.5 sec^{-1}, and the data of the Loma Prieta earthquake (Table 3.2) indicates a mean value of 14.8 sec^{-1} for near-field (and significantly lower values for site distance exceeding 20 km). Similarly, the data studied by Tso et al. (1992) pertains to epicentral distance ranging from 4 km to 379 km; of all these the data pertaining to "high" A/V ratio of 11.7 sec^{-1} or more comes from motions recorded within 27 km of the epicentre.

Table 3.4 also shows that A/V ratio is generally higher for the high PGA group data than for the medium or low PGA group data; i.e., the expected trend of decrease in A/V ratio with increase in the epicentral distance is generally seen. The only exception to this are the horizontal ground motion records of event "Oct" and the vertical ground motion records of event "April". However, the variation in A/V ratio

with distance is not so significant for the Indian data as it is for the other earthquakes. For instance, in the present case, the epicentral distance ranges from about 5 km to 320 km; for such distances, A/V ratio for earthquakes elsewhere could vary by more than 100%, which is not the case in the Himalayan data.

Generally, the A/V ratio for vertical component of ground motion is comparable to that for the horizontal components.

On the whole, a value of around 20 sec^{-1} could be considered as an appropriate mean value and 12 sec^{-1} as the mean-minus-one-standard-deviation value for the Himalayan earthquake records. This is much higher than the values recommended in the literature based on records elsewhere. This has very serious implications for earthquake-resistant design of important structures in the Himalayas. This means that the earthquake ground motion in the Indian Himalayas are associated with (a) unusually low value of ground velocity and hence are far less damaging, (b) unusually high value of ground acceleration and hence are more damaging (particularly to the stiffer structures), or (c) a combination of the possibilities (a) and (b) above. To resolve this issue, systematic studies on attenuation relationships for the Himalayan earthquakes are required for which far more authentic information on the earthquake source parameters is needed. In the meanwhile, for seismic risk studies in India, a great deal of caution is required while using the empirical relationships (relating PGA and/or PGV with the earthquake magnitude and epicentral distance) developed for data from elsewhere.

Table 3.5 shows the mean value of A/V ratio obtained in each of the six Himalayan earthquakes. The results are tabulated in increasing order

of earthquake magnitude. It is readily apparent from the table that mean A/V value decreases with the increase in magnitude. This is probably because, for a given PGA, the value PGV increases with the increase in earthquake magnitude. For the three earthquake magnitude ranges; (1) small magnitude (M < 5.5), (2) moderate magnitude (5.5 ≤ M ≤ 6.5), and (3) large magnitude (M > 6.5), the mean A/V value are also presented in the same table.

3.3.2 AD/V^2 Ratio

Table 3.4 also shows the values of mean AD/V^2 for the three groups in each event. AD/V^2 for vertical component is higher than it is for the horizontal component; this is consistent with the data analysed by Mohraz (1976) and seen in Table 3.1. On the whole, the mean value of AD/V^2 ratio for the horizontal component is 4.6; this is lower than the value of around 7.0 for rock sites in Table 3.1, but higher than 2.3 to 3.8 based on the Loma Prieta data (Table 3.2). The data for "April" has one record with unusually high value of AD/V^2 (equal to 85.6) which could be due to a typographical error in the paper by Chandrasekaran and Das (1990). This gives unusually high values of the mean and mean-plus-one-standard-deviation for low PGA group of this event. Hence, in arriving at the overall mean and mean-plus-one-standard-deviation values for the vertical components (5.2 and 8.8, respectively), this single value has been disregarded. The data of Table 3.4 show no clear trend in the variation of AD/V^2 with distance, except for the event "Aug".

3.3.3 A_V/A_H Ratio

A statistical summary of the ratio of A_V/A_H, in the three PGA groups is presented in Table 3.4. This table shows that, except the event "Oct", the mean value of ratio A_V/A_H is around 0.5 and mean-plus-one-standard-deviation value is around 0.70. This event shows a rather strong vertical component of ground motion with a mean value of A_V/A_H as 0.66 and mean-plus-one-standard-deviation value of 0.9. For the entire data, the mean value of A_V/A_H is 0.51 and the mean-plus-one-standard-deviation value is 0.70. These values are similar to those reported by Mohraz (1976) for data from elsewhere (Table 3.3). Thus, to be on the conservative side, the design for vertical acceleration should be based on A_V/A_H ratio as around 0.67 or 0.75 as against the value of 0.5 presently being used in the Indian code.

3.4 DURATION OF STRONG SHAKING

3.4.1 Definition

The total duration of a complete accelerogram represents the duration during which a earthquake ground acceleration exceeded a threshold or critical acceleration value set for the instrument. However, this duration may not represent the duration during which the structure was subjected to severe shaking. In the past, several procedures have been suggested for extracting a strong motion segment from an accelerogram; each of these give different value of the duration as seen in Fig. 3.3. As yet, no universally accepted definition for duration of strong motion is available.

Bolt (1969) and Page et al. (1972) have suggested a "bracketed duration"; this is the duration between the first and the last acceleration peaks exceeding a specified value (usually 0.05g). Since

PGA decreases with increase in distance from epicenter, this definition leads to a decrease in the duration of strong motion with an increase in distance from the source.

Trifunac and Brady (1975) define the duration of strong shaking as the time duration during which the middle 90 percent (i.e., 5% to 95%) contribution of the "acceleration intensity" (defined as $\int A^2 dt$) takes place. They observe that the average duration for soil is approximately 10-12 sec longer than that for rock, and that it increases at the rate of 1.0 - 1.5 sec for every 10 km increase in distance from the shock-source.

McCann and Shah (1979) define the duration of strong ground motion based on the concept that the strong motion part can be defined as the period during which the RMS, or average rate of energy, is highest relative to the rest of the record. In this method, first the root mean square (RMS) value is evaluated at each of the digitized points in the accelerogram, this is referred to as cumulative root mean square function (CRF). Rate of change of CRF during total duration of the record is then examined to give two cut-off points. The final cut-off time is obtained at a time where rate of change of CRF becomes negative and remains so for remainder of the record. The initial cut-off time is obtained in the same manner, except that the search is performed in the reverse direction of time scale starting from the end of the record and continued till beginning of the record.

3.4.2 Comparison of Different Definitions

A graphical comparison of duration as per the Trifunac and Brady (1975) and McCann and Shah (1979) definitions is shown in Fig. 3.4 for

some records from the Californian earthquakes. This figure shows that duration by the McCann and Shah method is shorter than that by the definition of Trifunac and Brady (1975). On the other hand, Table 3.7 shows the average duration of records from the Loma Prieta earthquake based on three different definitions. This table indicates that the definition by McCann and Shah gives duration longer than that by the Trifunac and Brady method. This table also shows that the duration is generally higher for alluvium sites than for the rock sites.

3.4.3 Variation in Duration with Distance and with A/V Ratio

Tso et al. (1992) demonstrate that the records with high A/V ratio have shorter durations of strong shaking than those with intermediate A/V ratio, whereas the records with low A/V ratio have longer durations. They explain this in terms of epicentral distance as, "Larger the magnitude of an earthquake, the longer the duration of strong ground motion if the distance from the epicentre remains constant. If the magnitude of the earthquake is kept constant, duration increases with an increase in epicentral distance. Since the records with high A/V ratios were generated in the proximity of small or moderate earthquakes, whereas those with low A/V ratios were obtained at large distances from large or moderate earthquakes, the correlation of the A/V ratio with the duration of strong shaking can be expected."

3.5 DURATION OF STRONG SHAKING FOR THE DATA

The duration of strong shaking has been calculated for each of the198 horizontal records based on the Trifunac and Brady (1975) definition (Appendix A). The relationship between the duration and A/V

ratio for each of the events is shown in Fig. 3.5. The points for records belonging to different PGA groups (low, medium, and high) are shown with a different notation. The plots of Fig. 3.5 show no definite relationship or trend between duration and A/V or between duration and PGA group (i.e., epicentral distance), though such relationships have been reported in literature for studies based on data from other earthquakes (Tso et al. 1992).

This can also be seen in Table 3.8 which shows the mean duration of strong shaking in the three PGA groups for the six Himalayan earthquakes. For "April" and "Feb", the trend of increasing duration with decrease in PGA (i.e., increase in distance from shock-source) is quite clear. But, exactly opposite trend is observed in the event "Aug", where high PGA group records have greatest duratio of strong shaking. For events "Sept" and "Oct", the Table shows the largest duration of shaking in the medium PGA group records. However, Fig. 3.5 clearly confirms the fact that larger the earthquake magnitude, grater is duration of of strong shaking. For "sept" (M = 5.2) and "April" (M = 5.5), duration of most of records is less than 10 sec, while for events "Oct" (M = 6.6) and "Aug" (M = 7.2), duration of most of the records is more 10 sec.

Table 3.1 Summary of V/A and AD/V^2 ratios for earthquakes in California (Mohraz 1976).

Site category	Group	Mean V/A (in/s)/g	Approx. mean A/V (Sec^{-1})	AD/V^2 Mean	AD/V^2 84.1 percentile
Rock	L	27.0	14.5	6.9	11.0
	S	30.0	13.0	7.0	11.2
	V	31.0	12.6	7.6	11.8
Less than 30 ft of alluvium underlain by rock	L	37.0	10.6	5.2	7.7
	S	43.0	9.1	5.2	8.2
	V	37.0	10.6	8.5	13.3
30 - 200 ft of alluvium underlain by rock	L	33.0	11.8	5.6	7.8
	S	41.0	9.5	4.3	6.4
	V	33.0	11.8	9.1	13.7
Alluvium	L	51.0	7.7	4.3	6.0
	S	62.0	6.3	3.7	4.4
	V	51.0	7.7	5.0	7.0

L : Horizontal components with the larger peak ground acceleration
S : Horizontal components with the smaller peak ground acceleration
V : Vertical components

Table 3.2   Summary of mean V/A and AD/V^2 ratios for different source to site distances in Loma Prieta earthquake of 1989 (Mohraz 1991).

Category	Rock			Alluvium		
	V/A (in/s)/g	Approx. A/V (sec^{-1})	AD/V^2	V/A (in/s)/g	Approx. A/V (sec^{-1})	AD/V^2
Near-field (R < 20 km)	26.0	15.0	3.8	40.0	9.8	2.9
Mid-field (50 km > R > 20 km)	63.0	6.2	2.3	53.0	7.4	2.9
Far-field (R > 50 km)	54.0	7.2	2.8	48.0	8.1	2.0

R : Distance of recording station from ruptured surface

Table 3.3   Summary of the ratio of peak vertical to larger peak horizontal acceleration (Mohraz 1976).

Site category	Mean	84.1 Percentile
Rock	0.52	0.69
Less than 30 ft of alluvium underlain by rock	0.49	0.62
30 - 200 ft of alluvium underlain by rock	0.46	0.66
Alluvium	0.45	0.61

Table 3.4　Summary of A/V and AD/V^2 ratios for the six earthquake events in Himalayas.

Event	PGA Group	Horizontal components				PGA Group	Vertical component			
		A/V (sec^{-1})		AD/V^2			A/V (sec^{-1})		AD/V^2	
		m	m − σ	m	m + σ		m	m − σ	m	m + σ
April	H(10)*	21.1	14.4	2.9	4.2	H (5)	23.2	17.9	5.6	7.8
	M (4)	21.4	15.7	4.2	6.1	M (2)	14.3	13.8	3.0	3.5
	L (4)	15.7	7.2	4.2	6.7	L (2)	22.7	7.0	44.8	89.5
Sept·	H (6)	32.5	25.8	3.5	4.4	H (3)	36.0	30.1	9.2	13.6
	M (8)	31.0	20.0	5.9	10.8	M (4)	26.8	22.8	10.1	12.5
	L(10)	26.5	20.1	6.1	8.6	L (5)	22.9	13.6	6.9	9.4
May	H (0)	—	—	—	—	H (0)	—	—	—	—
	M(12)	23.7	18.3	6.5	9.9	M (6)	19.5	11.8	7.3	11.2
	L(16)	17.3	12.6	5.0	6.5	L (8)	15.2	12.5	4.8	6.5
Feb	H (2)	22.9	21.3	5.0	5.4	H (1)	28.7	—	9.2	—
	M(12)	22.6	17.4	4.7	7.0	M (6)	25.1	17.7	8.1	11.6
	L(22)	18.7	12.7	5.2	8.1	L(11)	15.2	9.2	4.6	6.2
Aug	H(28)	23.3	17.1	4.0	5.9	H(14)	25.8	18.5	6.8	9.4
	M(32)	16.7	9.8	3.6	5.6	M(16)	16.3	7.8	4.4	7.5
	L (6)	13.3	9.4	2.6	3.5	L (3)	12.8	8.9	3.2	3.4
Oct	H (8)	14.3	12.2	2.4	3.3	H (6)	15.0	10.3	2.9	3.6
	M(12)	19.1	13.0	4.1	6.8	M (4)	14.4	7.4	2.9	4.3
	L (6)	14.7	11.3	3.2	4.6	L (3)	10.7	9.0	2.9	3.2
All	(198)	20.2	12.5	4.6	8.0	(99)	19.6	10.8	5.2	8.8

*　　　: Number of records
H　　: High PGA group (PGA > 0.1 g)
M　　: Medium PGA group (0.1 > PGA > 0.05 g)
L　　: Low PGA group (PGA < 0.05 g)
m　　: Mean
m + σ : Mean-plus-one-standard-deviation

Table 3.5 Summary of variation in A/V with earthquake magnitude for the data from the six Himalayan earthquakes.

Event	Magnitude	mean A/V (sec^{-1})	mean A/V for the group
Sept	5.2	29.5	29.5
April	5.5	19.9	
May	5.7	20.0	20.0
Feb	5.8	20.2	
Oct	6.6	19.2	17.9
Aug	7.2	16.6	

Table 3.6 Summary of peak vertical to larger horizontal
acceleration   ratio for the   data used in the
present study.

Event	PGA Group	A_V/A_H		A_V/A_H of each event	
		m	m + σ	m	m + σ
April	H (5)*	0.34	0.46	0.50	0.74
	M (2)	0.57	0.76		
	L (2)	0.81	0.97		
Sept	H (3)	0.45	0.47	0.44	0.51
	M (4)	0.41	0.52		
	L (5)	0.40	0.60		
May	H (0)	—	—	0.51	0.72
	M (6)	0.39	0.52		
	L (8)	0.60	0.81		
Feb	H (1)	0.89	0.89	0.50	0.72
	M (6)	0.41	0.47		
	L(11)	0.52	0.77		
Aug	H(14)	0.44	0.55	0.47	0.61
	M(16)	0.49	0.63		
	L (3)	0.59	0.67		
Oct	H (4)	0.85	1.05	0.65	0.90
	M (6)	0.59	0.77		
	L (3)	0.53	0.80		
All	(99)			0.51	0.70

*   : Number of records
H   : High PGA group (PGA > 0.1 g)
M   : Medium PGA group (0.1 > PGA > 0.05 g)
L   : Low PGA group (PGA < 0.05 g)
m   : Mean
m + σ : Mean-plus-one-standard-deviation

Table 3.7 Average duration of strong motion (in sec) for accelerograms recorded in the Loma Prieta earthquake of 1989 (Mohraz 1991).

Category	Page et al.		Trifunac and Brady		McCann and Shah	
	Rock	Alluvium	Rock	Alluvium	Rock	Alluvium
Near-field (R < 20 km)	11.6	14.4	8.5	10.5	10.0	11.6
Mid-field (20 km > R > 50 km)	6.2	12.5	15.6	18.6	15.9	19.8
Far-field (R > 50 km)	1.9	6.7	11.6	11.5	14.7	14.8

39

Table 3.8 Summary of duration of strong shaking for the records obtained from the six Himalayan earthquakes.

Event	Magnitude of event	PGA Group	Duration (sec)	
			mean	mean
April	5.5	H(10)*	3.48	
		M (4)	6.00	5.60
		L (4)	10.55	
Sept	5.2	H (6)	6.16	
		M (8)	9.20	8.33
		L(10)	8.94	
May	5.7	H (0)	——	
		M(12)	16.27	16.28
		L(16)	17.07	
Feb	5.8	H (2)	10.51	
		M(12)	13.11	16.48
		L(22)	18.86	
Aug	7.2	H(28)	26.10	
		M(32)	22.83	23.65
		L (6)	16.62	
Oct	6.6	H (8)	11.69	
		M(12)	17.00	14.47
		L (6)	13.10	

* : Number of records
H : High PGA group (PGA > 0.1 g)
M : Medium PGA group (0.1 > PGA > 0.05 g)
L : Low PGA group (PGA < 0.05 g)
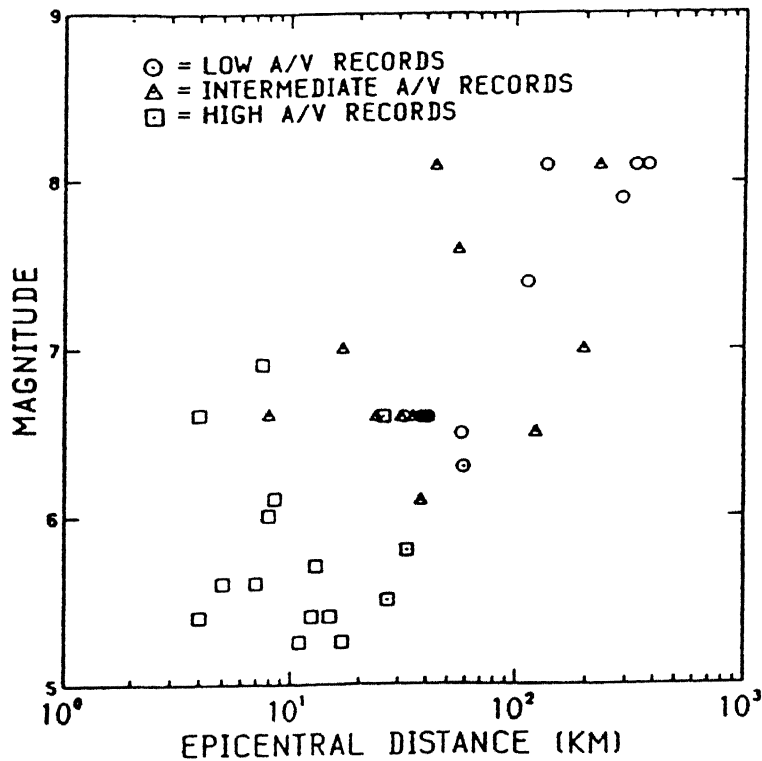
Fig. 3.1   Relationship between earthquake magnitude (M) and
            epicentral distance (R) for low, intermediate, and
            high A/V records (Tso et al. 1992).
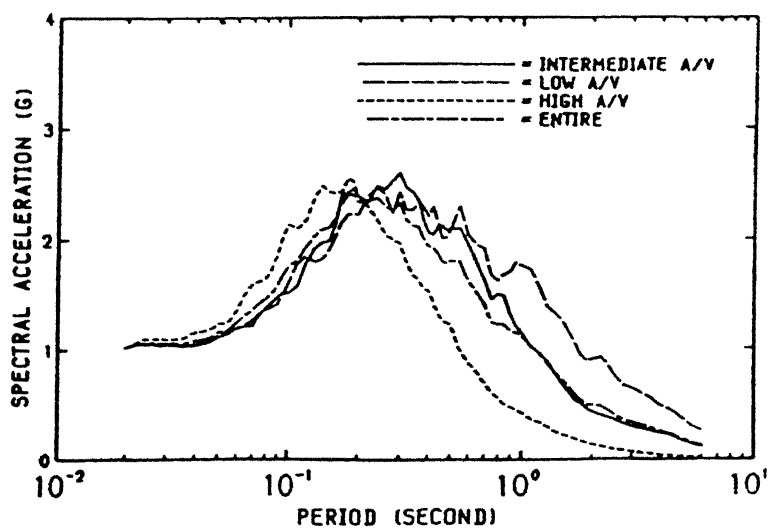
Fig. 3.2   Mean 5% damped elastic acceleration response spectra
            for the three A/V groups and whole ensemble of
            records scaled to a common PGA of   1g
            (Tso et al. 1992).
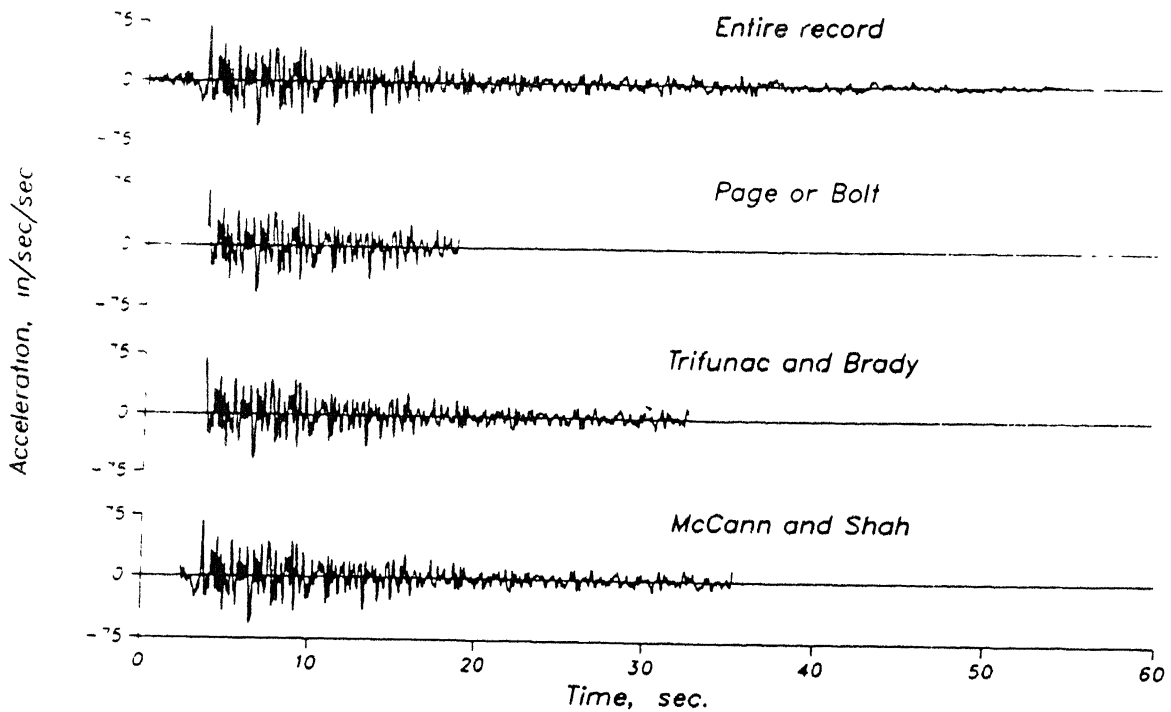
Fig. 3.3   Comparison of strong motion duration for the S69E
component of the Taft, earthquake of July 21, 1982
using different procedures
(Mohraz and Elghadamsi 1989).
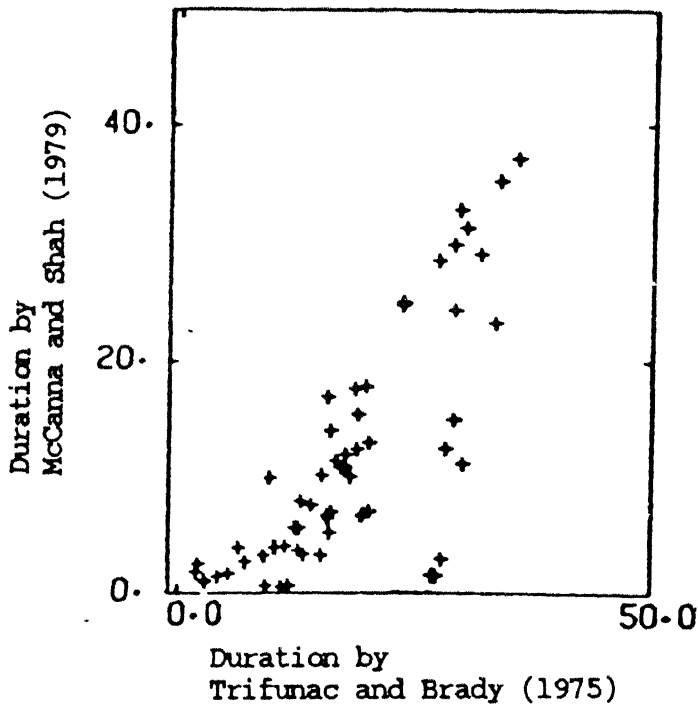
Fig. 3.4   Comparison of duration of strong shaking from
Trifunac-Brady (1975) and McCann-Shah (1979)
definitions (McCann and Shah 1979).
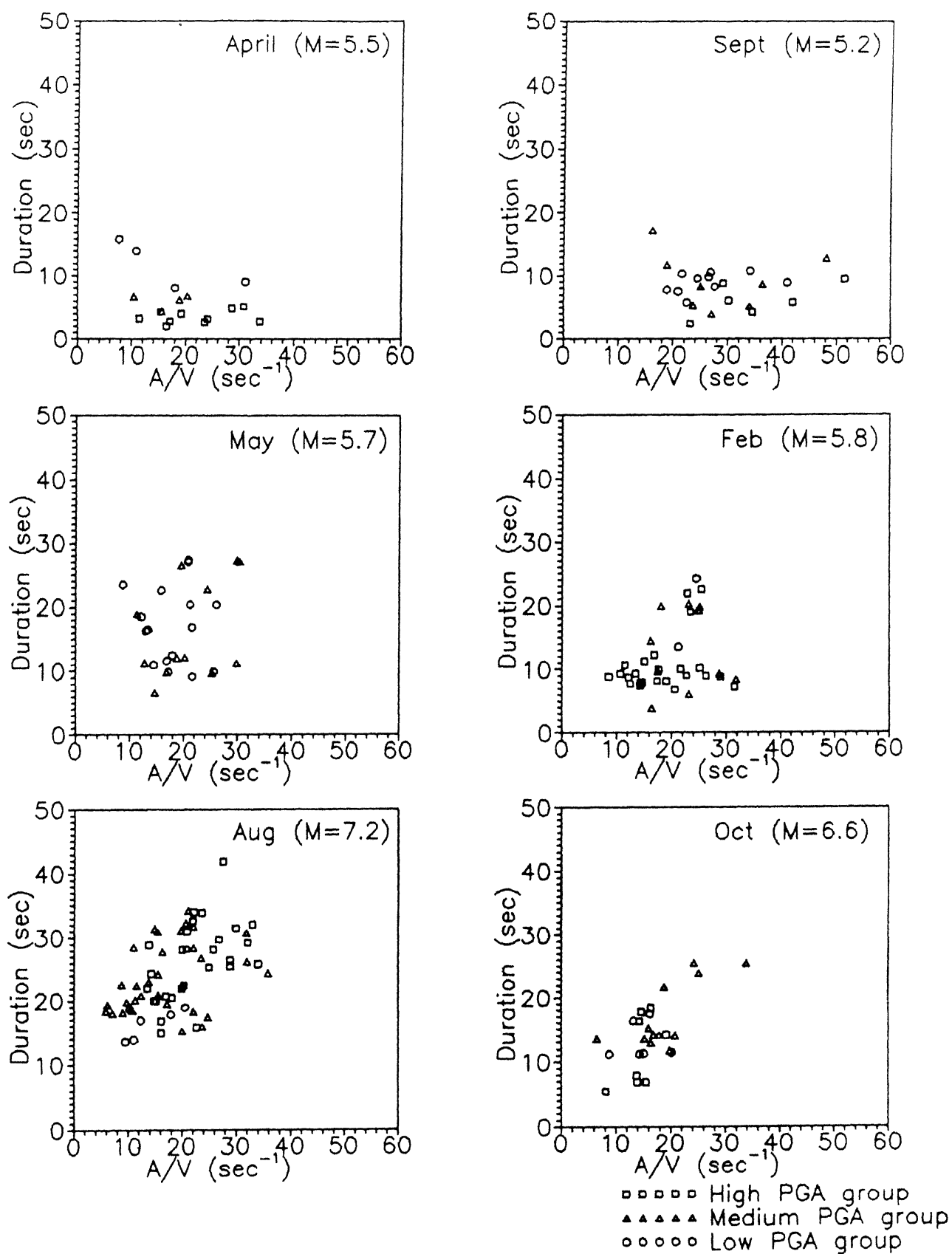
Fig. 3.5   Relationship between duration and A/V ratio for the
            six Himalayan events.

CHAPTER IV

ELASTIC RESPONSE SPECTRUM

4.1 INTRODUCTION

Response spectrum is a very useful way to characterize strong ground motion from the view point of engineering applications. Response spectrum of a ground motion is a plot showing maximum response induced by that ground motion in single degree of freedom (SDOF) systems of different natural frequency (or natural period), but for a given value of damping. The response here can be any quantity of interest such as the displacement, velocity, or acceleration. For engineering purposes, the following response quantities are most commonly plotted (Fig. 4.1):

(a) Maximum relative displacement (displacement spectrum)

$$SD(\omega,\zeta) = \left| u(t) \right|_{\substack{max \\ t}} \qquad (4.1)$$

(b) Maximum relative velocity (velocity spectrum)

$$SV(\omega,\zeta) = \left| \dot{u}(t) \right|_{\substack{max \\ t}} \qquad (4.2)$$

(c) Maximum absolute acceleration (acceleration spectrum)

$$SA(\omega,\zeta) = \left| \ddot{u}(t) + \ddot{u}_g(t) \right|_{\substack{max \\ t}} \qquad (4.3)$$

(d) Pseudo spectral velocity (pseudo-velocity spectrum)

$$PSV(\omega,\zeta) = \omega \ SD(\omega,\zeta) \qquad (4.4)$$

(e) Pseudo spectral acceleration (pseudo-acceleration spectrum)

$$PSA(\omega,\zeta) = \omega^2 \ SD(\omega,\zeta) \qquad (4.5)$$

where $u(t)$, $\dot{u}(t)$, $\ddot{u}(t)$ are relative displacement, velocity, and acceleration, respectively, at instant t for a SDOF oscillator of

natural frequency ω and damping ζ; and $\ddot{u}_g(t)$ is the ground acceleration.

A response spectrum represents the combined influence of amplitude of ground motion, frequency content, and to some extent the duration of ground shaking, on different structures (Seed and Idriss 1982). Most importantly, a response spectrum provides a most convenient way of evaluating the maximum acceleration, and thus maximum inertia force, developed in a structure subjected to the given base motion, irrespective of whether structure behaves as a SDOF system or MDOF system. Also, since a SDOF system responds mostly to the energy in the ground motion near its own natural frequency, the response spectrum characterizes the energy in ground motion.

4.1.1 Tripartite Representation of Response Spectrum

It is obvious from Eqs. (4.4) and (4.5) that SD, PSV, and PSA are directly related and provide essentially the same information; hence the corresponding response spectra can be presented on a tripartite or a four-way logarithmic plot by a single curve for each value of damping. A typical response spectrum on a tripartite-plot is shown in Fig. 4.2, which is essentially a plot of PSV versus T on log-log scale with two additional log scales at 45° to period scale for reading SD and PSA. The parameters PSA and PSV have certain characteristics that are of practical interest. The PSV is close to SV for high frequencies, and practically equal for intermediate frequencies, but different for low frequencies. PSA is practically equal to SA for damping levels encountered in most engineering applications.

4.1.2 Design Spectrum

Response spectrum, being a plot of maximum response (of a SDOF oscillator with varying natural frequency) to a given ground motion record, is a description of that particular ground motion. Hence, its use is suitable for analysis of a structure subjected to that ground motion; but it may not be suitable for the purposes of design (e.g., Anderson 1989). Furthermore, a single earthquake record has a particular frequency content which gives rise to the jagged, sawtooth appearance of peaks and valleys as shown in Fig. 4.2. When such a spectrum is used for design, structures with slightly different natural periods may reflect vastly different maximum response and hence the design parameters. To overcome this problem, the concept of smooth-shaped response spectrum has been introduced for design.

A usual method to obtain a smooth-shaped spectrum is through normalization and averaging of several response spectra obtained from records with common characteristics. Amongst the suggested normalization procedures for response spectrum, the most popular is normalization to unit peak ground acceleration; at times the normalisation is done with respect to other parameters such as peak ground velocity or displacement. Principles of statistics are then used to create a smooth-shaped spectrum. The mean or median shape of response spectra so obtained is generally used for earthquake-resistant design of normal building structures. Use of such a spectrum implies that for a given value of peak ground acceleration, there is about 50% probability that the maximum acceleration of the SDOF oscillator will be exceeded. High risk structures may be designed to higher level such as the mean-plus-one-standard-deviation shape, which implies that the probability of exceedance is only about 16%. To account for the effect

of magnitude and distance of different likely events in the vicinity of
a major project, site-specific design spectrum is sometimes obtained by
drawing an envelop of more than one spectra (e.g., Fig. 4.3).

4.1.3 The Actual Design Spectrum

The above discussion pertains to the shape of design spectrum for a
given normalised acceleration, velocity, or displacement. The actual
design spectrum is obtained by multiplying the entire spectrum shape
with the design ground motion parameter, for instance the maximum ground
acceleration (zero period acceleration, ZPA). The magnitude of this
design parameter has to be decided considering the expected ground
motion at the site, the factors of safety and load factors to be used
in design, the ductility to be provided in the structure, the damping
characteristics, and the procedure to be used for estimation of natural
period for the structure (e.g., Housner and Jennings 1982).

4.1.4 The Objective of the Study

A statistical study of the response spectrum shape has been carried
out for the records obtained from the Himalayan earthquakes, with a view
to see if there are any appreciable differences in the ground motion
characteristics of the Himalayan earthquakes vis-a-vis earthquakes
elsewhere. A comparison has also been made with the spectrum shapes
currently in design use.

4.2 REVIEW OF PAST STUDIES ON DESIGN SPECTRUM

4.2.1 Housner's Spectrum

While Biot (1941) initiated the application of response spectrum

to earthquake engineering in 1941, it was not until 1959 that Housner developed the first smooth design spectra (Housner 1959). These (Fig. 4.4) were obtained using eight strong motion records from four earthquakes recorded in California. The curves were arbitrarily scaled to 0.125g at zero period. The Indian code (IS:1893-1984) has adopted the shape given by Housner with minor modifications (Fig 4.5).

4.2.2 Newmark and Hall Spectrum

Another set of design spectra, used extensively in the nuclear power plant design in late sixties and early seventies, were suggested by Newmark and Hall (1969). They proposed a procedure for estimating site-independent design spectrum, which was based on the fact that response spectrum over certain frequency ranges is related by an amplification factor to the peak value of ground acceleration, velocity and displacement. To appreciate this, consider the response spectrum of Fig. 4.2 and compare it with the peak ground displacement, peak ground velocity, and peak ground acceleration values marked on the same plot. It is seen that at small frequencies, the maximum relative displacement is large, whereas pseudo-acceleration is very small. At large frequencies, the relative displacement is extremely small, whereas the pseudo-acceleration is relatively large. At intermediate frequencies, the pseudo-velocity is substantially larger than at either end of the spectrum. For this reason, three regions are usually identified in a response spectrum as low-frequency or displacement region, the intermediate-frequency or velocity region, and the high-frequency or acceleration region. In each region, the corresponding ground motion is amplified the most. Fig. 4.2 also shows that at small frequencies (0.05

Hz or less) the spectral displacement approaches the peak ground displacement, indicating that for very flexible systems the maximum relative displacement in a simple oscillator is equal to the ground displacement. At large frequencies (30 Hz or more), the pseudo-acceleration approaches the peak ground acceleration, indicating that for rigid systems the absolute acceleration of the mass is same as that of the ground. Newmark and Hall suggested that the three amplifications (displacement, velocity, and acceleration) are constant in their respective regions and can be determined statistically. Tables 4.1 and 4.2 give the amplification factors suggested by Newmark and Hall for horizontal ground motions for median and 84 percentile cases. Thus, in this method, first the estimated values of peak ground acceleration, velocity, and displacement for the site are plotted on a tripartite logarithmic paper; then using the amplification factors, for the desired percentage of critical damping, the peak ground motion values are amplified to give a smooth design spectrum for the site. Their spectra for "standard" earthquake with peak ground acceleration, velocity and displacement of 1.0g, 121.8 cm/sec and 91.4 cm, respectively, are shown in Fig. 4.6. It can be noted from the figure that curves for different damping values approach the peak ground acceleration at different period. Newmark and Hall observed that though the amplification factors for horizontal and vertical spectra remain unchanged, the vertical peak ground accelerations are about two-thirds of the horizontal peak ground accelerations.

4.2.3 Study by Blume and Mohraz

After San Fernando earthquake of 1971, two independent studies, one

by Blume et al. (1972) and the other by Mohraz et al. (1972), were carried out with the objective of developing recommendations for horizontal and vertical design response spectra for nuclear facilities. These studies were based on a much larger number of earthquake ground-motion records than used by the Newmark and Hall study. The results of these studies formed the basis for the guidelines contained in Nuclear Regulatory Commission (NRC) Regulatory Guide 1.6 (1973). The technique of representation was very similar to the one proposed by Newmark and Hall, except that these studies recognized that the amplifications in the three regions need not be constant always and may vary linearly. To define horizontal response spectra, the peak horizontal ground acceleration and displacement levels are first established. The peak horizontal ground displacement was considered to be proportional to the peak horizontal ground acceleration and was fixed at 91.4 cm for an acceleration of 1g (for a standard earthquake). The bounds of each of spectrum are established by five line segments, similar to the Newmark and Hall procedure. The amplification factors and the response spectra for "standard" earthquake, for horizontal ground motion, as adopted by NRC are shown in Fig. 4.7. The vertical response spectra were constructed in a manner similar to horizontal response spectra, but three differences were incorporated into the procedure: (1) the frequency control points were shifted slightly, (2) the amplification factors were different, and (3) the value of peak horizontal acceleration is used as the initial reference value. The amplification factors and the response spectra for vertical ground motion are shown in Fig. 4.8. The NRC spectra was also used extensively for seismic design of many non-nuclear facilities.

4.2.4 Spectrum for Different Soil Conditions

In 1976, two studies, one by Seed et al. (1976) and the other by Mohraz (1976), considered the influence of soil conditions on the shape of response spectrum. The study by Seed et al. used a total of 104 horizontal components of earthquake records with peak ground acceleration greater than 0.05g from 23 different earthquakes. The records were divided into four categories based on soil condition at recording station. The mean and mean-plus-one-standard-deviation spectra for the four soil types, obtained by Seed et al. are seen in Figs. 4.9 and 4.10, respectively. The figures show that for periods greater than about 0.4 sec, the amplifications for rock are substantially lower than those for soft to medium clay and for deep cohesionless soil. The AERB safety guide (S-11 1990) recommends standard response spectra for rock and soil sites based on the work of seed et al. (1976); Fig. 4.11 shows the shape recommended by AERB for rock sites.

4.2.5 Study by Mohraz

Mohraz (1976) considered a total of 162 records and divided these into four soil categories. To exclude the influence of the horizontal component of records with smaller peak ground acceleration on amplification, he divided the response spectra for each soil category into three sets: horizontal components with the larger of the two peak ground accelerations, horizontal components with the smaller of the two peak ground accelerations, and vertical components. Figure 4.12 shows the mean acceleration spectra for different soil conditions for the horizontal components with larger of the two peak ground accelerations.

t is seen that the amplification for alluvium extends over a larger :requency region than the amplifications for the other three soil :ategories. Also, for short periods, the spectral ordinates for alluvium ire lower than for the other soil types, whereas for intermediate and long periods, these are higher.

Thus, local soil conditions at the site significantly alter the frequency content in the ground motion and hence the response spectra. In the recent years, this has lead to the adoption of different design spectra for different soil conditions. Fig. 4.13 shows one such spectra adopted by UBC (1991).

Mohraz (1978) studied the influence of earthquake magnitude on acceleration amplification for alluvium. As seen in Fig. 4.14, acceleration amplifications are larger in earthquake of magnitude between 6 and 7 than for those with magnitude between 5 and 6.

Mohraz (1991) examined the influence of source-to-distance on spectral shapes for the records obtained from the Loma Prieta earthquake of 1989. The accelerograms obtained from rock and alluvium were divided into three subgroups based on distance of the recording station from the ground projection of the ruptured surface. The groups were labeled as "near-field" for records with distance less than 20 km, "mid-field" for records with distance between 20 and 50 km, and "far-field" for records with distance greater than 50 km. Fig. 4.15(a) shows the spectral shapes for the three subgroups obtained for 5% damping using horizontal components of accelerograms recorded on rock sites. The figure shows that the amplification for the near-field is substantially smaller than the amplification for mid- or far-field for periods greater than about 0.5 sec. For periods less than 0.5 sec, however, the amplification for

the near-field is greater. Fig 4.15(b) shows the results of similar exercise for records obtained from alluvium. The figure indicates that, though distance influences the spectral shapes, the influence is not as pronounced as it is for rock.

4.3 METHOD OF ANALYSIS

The data set consisted of 198 horizontal and 99 vertical component records, obtained from the six events referred to in chapter II. The ordinates of the pseudo-acceleration response spectra (PSA) are computed by the Newmark-beta numerical method of solution (e.g., Bathe and Wilson 1978). The ordinates are evaluated for a period range of 0.0075 sec to 3.0 sec at an interval of 0.0075 sec, thus generating about 400 points in this range. The computations are carried out for 0, 0.5, 2, 5, 10, and 20 percent of critical damping. Since the peak ground acceleration for various accelerograms differ, the computed responses cannot be used in statistical study without normalization. In this study, normalization of spectra by peak ground acceleration is adopted. Thus, each of the pseudo-acceleration spectra is normalized by respective PGA, giving zero period ordinates of unity.

The normalized spectra in each of the events are separated for horizontal and vertical components. These are then averaged to obtain mean and mean-plus-one-standard-deviation spectral shape for horizontal and vertical components representative for individual events. Similarly, a mean and mean-plus-one-standard-deviation spectra for horizontal and vertical component, considering all the records from 6 events is also evaluated. The average spectra are smoothened by adopting a five-point-averaging scheme. The "smooth-shapes" thus obtained are then

compared with the spectral shapes currently in use.

4.4 RESULTS

The mean pseudo-acceleration spectra for 6 events for damping values of 0, 0.5, 2, 5, 10, and 20 percent of critical damping for horizontal and vertical components, are shown in Fig. 4.16.

4.4.1 General shape

A visual comparison of spectra in the Fig. 4.16 suggests that in all the events; for a given damping value, there is a build up in acceleration amplification from unity at zero period to a peak value, which usually occurs in the period range of 0.1 to 0.3 sec. For periods longer than 0.3 sec the acceleration amplification drops down. However, for periods greater than about 2.0 sec the acceleration amplification is quite low and remains almost constant.

For low damping values (less than 5%), the spectral shape and the value of peak amplification in different events vary significantly. However, for higher damping values, the peaks of spectra in different events are nearly same and the variation in the shape is also comparatively less. For instance, in the event "Sept" (M = 5.2) the peak amplification for 0% and 5% damping are about 4.8 and 2.4, respectively, while in "Aug" (M = 7.2) the corresponding amplifications are about 9.4 and 2.6, respectively. Thus, a significant variation to the extent of 200%, is observed in zero damping spectra while the difference is insignificant for 5% damping. Though the shape of spectra differs from event to event, the peak acceleration amplification in the six events for 5, 10, and 20 percent of critical damping is nearly same and is

about 2.6, 2.0, and 1.4, respectively.

4.4.2 Variation within the Data

Spectra in the "Sept" event drops down suddenly at period of about 0.3 sec. This could be due to its low magnitude. "May" and "Feb" are of almost same magnitude, their spectral shapes are in general similar, except for some variation in maximum amplification for damping less than 5% of critical. "Aug" is of the largest magnitude, and in this earthquake most stations were at large epicentral distances (greater than 150 km). The spectra for this event show comparatively (with respect to spectra for the other earthquakes) more energy in intermediate period range (0.4-1.2 sec); this is expected because as distance from the shock-source increases, the high period waves dominate. In case of "April", though the epicentral distances involved were quite low (less than 30 km), the ordinates in intermediate period range show a substantial amplification. This is unexpected, since generally seismic waves in near-field (low epicentral distance) have high frequency content. "Oct" spectra are unique in the sense that only these show a flat top as compared to sharp tips observed in spectral shapes of the other events.

4.4.3 Variation in Shape of Spectrum with Earthquake Magnitude

Considering the large variation in amplifications for low values of damping, and the fact that in the design of ordinary buildings a damping value of 5% is usually adopted, the variation in spectral shape with earthquake magnitude has been studied for 5% damping. Fig. 4.17 shows the mean spectra for the six events for 5% damping. It is seen that

acceleration amplifications in the period range of 0.3 to 1.5 sec are highly dependent on earthquake magnitude. Larger the magnitude, greater is the amplification in this range. For instance, at natural period of 0.8 sec, the acceleration amplification is 0.3 for the event "Sept" (M = 5.2) and it is 1.0 for the event "Aug" (M = 7.2), giving a variation of as much as 500%. For periods less than 0.2 sec the variation is negligible, while it is not very significant for periods longer than 1.5 sec. This figure also suggests that one could obtain somewhat representative shapes of the response spectrum based on earthquake magnitude. Fig. 4.18 shows shapes suggested by this data for rock-sites for (a) small-magnitude earthquakes (M < 5.5), (b) moderate-size earthquakes (5.5 ≤ M ≤ 6.5), and (c) large earthquakes (M > 6.5). These have been obtained from (a) the mean shape of event "Sept" (M = 5.2), (b) average of the mean shapes of events "April" (M = 5.5), "May" (M = 5.7), and "Feb" (M = 5.8), and (c) average of the mean shapes of events "Oct" (M = 6.6) and "Aug" (M = 7.2).

The variation of acceleration amplification in the intermediate period range with earthquake magnitude can also be anticipated from the A/V ratio. As seen in table 3.5, in the low-magnitude earthquakes, the value of A/V is high, i.e., for the given value of PGA, the value of PGV is low. In the intermediate period range (the velocity region), the PGV governs the spectral ordinates, and hence, low acceleration amplification are obtained in this range.

Not many studies seem to have been done on the shape of pseudo-acceleration spectrum with earthquake magnitude. The study by Mohraz (1978) (Fig. 4.14) shows this variation but for alluvium sites. While the study by Mohraz based on data from elsewhere shows that ground

motions of large magnitude earthquakes have significantly larger values of acceleration amplification in all the three regions (acceleration, velocity, and displacement), the data of the Himalayan earthquake (Fig. 4.17) suggests that this is so only for the velocity region.

It is obvious that when choosing spectrum shape for preparing site-specific design spectrum, the earthquake magnitude should be explicitly considered, particularly in the intermediate period range; this is the period range in which a very large number of industrial structures lie. Presently, such a consideration seems to be absent in developing the design criteria for important projects in India.

4.4.4 What does Mean Spectra from Data Represent ?

Mean horizontal pseudo-acceleration spectra, derived by averaging all 198 horizontal component spectra is shown in Fig. 4.20. Comparison of shape of mean spectra from all horizontal records with spectral shapes from "Oct" (M = 6.6) and "Feb" (M = 5.8), shown in Fig. 4.21, indicates that mean shape (from all horizontal records) lies in between the mean spectra for two events, suggesting that mean spectral shape from all records is a representative of earthquake of magnitude of about 6.2 for moderate distances (80-130 km). Incidentally, the average of magnitudes of events studied is 6.0.

4.5 VARIATION IN SPECTRAL SHAPES WITH DISTANCE

To study the variation in response spectrum shape with epicentral distance, mean response spectra for high, medium and low horizontal PGA groups are plotted for different events in Fig. 4.19. The shapes for events "Sept", "May", and "Oct" do not show significant variation with

distance even though the peaks in the acceleration region vary somewhat. For "April", the ordinates at large values of natural period are higher for the low PGA group, but in this event epicentral distance for all the stations lie within 30 km. For event "Feb", the shape for high PGA group is significantly different from that for the other two groups, but in this case only two records (i.e., one station) falls in the high PGA group and therefore this comparison may not be very general. In the intermediate period range, the events "Feb" and "Aug" show significant variation for different PGA groups; the high PGA group (low epicentral distance) has much lower values of acceleration amplification in this period range as is also expected.

Thus, in general, the Himalayan data does not show a significant variation in the spectral shape with epicentral distance; this is in contrast with the data from elsewhere. For instance, compare the variation for rock sites from the Loma Prieta earthquake (Fig. 4.15) with the event "Oct" (Fig. 4.19). While the Loma Prieta earthquake shows a very significant variation even within the epicentral distance of 80 km, the data of "Oct" pertaining to the epicentral distances of 25-150 km shows not much variation. Only for event "Aug", where large epicentral distances (100-320 km) are involved, there is significant difference in spectral shape with distance, that too only in the velocity region.

On the whole, it could be concluded that the Himalayan data shows somewhat insignificant variation in spectral shape with epicentral distance, except in the intermediate period range for the very large distances (say more than about 150 km). This is in line with the observation made in Chapter III that A/V ratio for the Himalayan

earthquake does not vary as significantly with distance as the data from elsewhere would suggest. Therefore, it is obvious that the geological features in the Himalayas are such that the attenuation is not significantly different for waves of different frequencies.

An examination of mean spectral shapes in the three PGA groups together with mean A/V of the corresponding group (Table 3.4) reveals that spectra with high A/V value have least amplification in moderate period range, whereas for spectra in low A/V group just the opposite is true. This again demonstrates that A/V is a good indicator of frequency content of ground motion.

4.6 MEAN-PLUS-ONE-STANDARD-DEVIATION SPECTRUM

While the mean spectrum shape is often recommended for design of buildings, important facilities such as nuclear power plants are usually designed on the basis of mean-plus-one-standard-deviation shape. This ensures that the variation in spectra ordinates for a given value of PGA is accounted for in an adequately conservative manner. In the case of Himalayan data, where many parameters such as local soil conditions, epicentral distance, and earthquake magnitude are not very reliably known, the mean-plus-one-standard-deviation shape has the added significance such a shape based on all the data accounts for variation in these factors.

Fig. 4.22 shows the mean-plus-one-standard-deviation spectra for the six events. In general, shape of mean-plus-one-standard-deviation spectra is very similar to shape of mean spectra (Fig. 4.16). Similar to mean spectra for the three range of earthquake magnitude (Fig. 4.21), mean-plus-one-standard-deviation spectra are also obtained. Fig. 4.23

shows the average representative shapes of the spectra for large magnitude (M > 6.5), moderate magnitude (5.5 ≤ M ≤ 6.5) and low magnitude (M < 5.5) earthquakes. Fig. 4.23 reveals that the amplification in intermediate period range is highly dependent on earthquake magnitude. As magnitude increases, the spectral ordinates also increases and the increase could be as high as 500%.

Figure 4.24 shows the mean-plus-one-standard-deviation spectra evaluated considering all the horizontal component records; these are the shapes that may be adopted for major projects in the Himalayas.

Figure 4.25 shows the coefficient of variation (COV) of response spectra for 0, 5, and 20 percent damping, considering all the horizontal component records. The figure suggests that COV decreases with increase in damping. Also, COV is highly dependent on the natural period. The value of COV for 5% damping is as low as 0.17 at period of 0.1 sec and increases to a value of around 0.8 at the period 1.2 sec. This is because the scaling of spectra has been performed with respect to the PGA.

4.7 COMPARISON OF SPECTRAL SHAPES

The design spectrum adopted by IS:1893-1984 is compared with the the mean horizontal spectral shape for 5% damping in the six Himalayan earthquakes (Fig. 4.26). It is readily apparent from the figure that irrespective of magnitude of earthquake, the IS code spectra underestimates the acceleration amplification in period range of 0.1 to 0.35 sec while overestimates in the period range greater than 0.35 sec. The mean spectra of event "Aug" (M = 7.2) is closest to IS spectra for periods greater than 0.5 sec. In this event, records were obtained from

large epicentral distances (100-320 km); this suggests that for long period range, the IS spectra actually represents large-magnitude, far-field spectra. IS code spectrum shape in the low-period range needs to be revised upwards in light of this data. As will also be seen in the next chapter, this is the period range in which ductility is somewhat less effective in reducing the seismic force on a structure.

4.7.1 Mean Spectrum with the IS code and UBC (1991) Spectrum

A comparison of the mean spectral shape based on all 198 records with the design spectra of IS:1893-1984 and UBC-1991 (rock site) has been shown in Fig. 4.27. The shape given in UBC-1991 appears quite conservative as compared to the Himalayan data. Note however that UBC-1991 does not specify a value of damping for this spectrum shape; it is assumed here to be 5%.

4.7.2 Mean-Plus-One-Standard-Deviation Spectra with the AERB Spectra

Fig. 4.28 shows comparison of mean-plus-one-standard-deviation spectral shapes from the data with the "standard spectra" suggested by AERB for rock sites. It is seen that except for zero damping, the AERB spectra match very well with the mean-plus-one-standard-deviation spectra obtained from the data.

4.8 STUDY ON AMPLIFICATION FACTORS

Representation of spectra in the characteristics trapezoidal form as done in the previous works by Newmark and Hall (1969), Mohraz et al. (1972), Blume et al.(1972), and Mohraz (1976) has also been attempted in the present study. For this the ordinates of PSV, PSA, and SD spectra

are evaluated using Newmark-beta method (Bathe and Wilson 1978). The ordinates were computed for a set of 200 periods, distributed between 0.003 sec to about 30.0 sec. The intervals of periods are chosen such that they get uniformly distributed on a log scale.

From the log-log plots of mean and mean-plus-one-standard-deviation normalised PSA, PSV, and SD spectra in each of the events, the most amplified region is identified. The period limits between which these amplifications occur are recognised as amplification region of that spectra. For instance, the most amplified region in a PSA spectra is recognised as acceleration region. The spectrum in the most amplified region is then represented by a straight line, which in most cases is a good approximation. This representation is illustrated in Figs. 4.29 and 4.30, which show mean PSA and PSV spectra, respectively, for "Oct" event. Also shown in those figures are the straight line representation of the spectra in the acceleration and velocity regions, respectively.

Figure 4.30 also suggests that spectra in the displacement region (which is mostly between 3 to 10 sec) cannot be represented as a straight line as has been done in the previous studies. In fact the shape of spectra in this region is unexpected. Further investigations are necessary for the representation of spectra in this region. Hence, in the present study amplification factors only for the acceleration and velocity regions are evaluated; this is sufficient for most of the engineering structures.

The spectra in acceleration region are obtained as straight lines parallel to period axis, that is, constant amplification (constant with respect to period) of peak ground acceleration is obtained. However, in

inclined straight lines (e.g., Fig. 4.30), indicating that in this period range the amplification of PGV is linearly varying (on log-log plots) and it decreases as period increases. For each of the events considered, the mean acceleration and velocity amplification factors are presented in Table 4.3 and Table 4.4. For velocity region, the spectra being linearly varying, amplification factors at the ends of the velocity region are presented. The Tables also indicate the period limits of the acceleration and velocity region as seen for these events.

Table 4.3 reveals that for low damping values (less than 5%) the acceleration amplification factor varies for the six events, however for higher damping values this factor is quite consistent for the events considered. Also, the period limits defining the acceleration region do not vary significantly for different events. Generally, acceleration region of the Himalayan data is between 0.12 sec to 0.26 sec. Table 4.4 indicates large variation in amplification factors in the period range defining the velocity region. Though the lower period end of velocity region is somewhat consistent in the six events, the higher period end varies significantly. This also gives rise to large variation in amplification factor at the higher period end of velocity region. The velocity region for the Himalayan data lies between 0.26 to 2.6 sec.

Acceleration and velocity amplification factors evaluated considering all the horizontal component records, are compared with the amplification factors reported in previous studies by Newmark and Hall (1969), Mohraz (1976) and those recommended in NRC guide 1.6 (1973). The comparisons for 5% damping are shown in Figs. 4.31 and 4.32. The comparison is also summarized in Tables 4.5 to 4.8 for 2, 5 ,10, and 20

percent damping.

Figure 4.31 for mean acceleration and velocity amplification factors, clearly reveals that mean acceleration amplification obtained from the Indian data is higher than that for data from earthquakes elsewhere. On the other hand, mean amplification in the velocity region is lower than those obtained by Newmark-Hall and Mohraz. Also the velocity amplification factor reduces sharply with period in the Himalayan ground motions. However, mean-plus-one-standard-deviation acceleration amplification from Indian data is comparable (Fig. 4.32) with those obtained by Newmark-Hall, Mohraz and the one recommended by NRC guide. This means that the standard deviation in acceleration amplification in the acceleration region is much lower for the Himalayan data than for data from elsewhere.

4.9 SPECTRUM INTENSITY

Peak ground acceleration is the most commonly used ground motion parameter in design. However, it has come under much criticism for its lack of correlation with observed structural performance. Hence, many other parameters have been proposed to measure the intensity of earthquake ground shaking. One such parameter is spectrum intensity, proposed by Housner (1959). Spectrum intensity (SI) is defined as the area under a pseudo-velocity spectrum curve between the periods 0.1 to 2.5 sec, i.e.

$$SI\ (\beta) = \int_{0.1}^{2.5} S_V\ (T,\beta)\ dT \qquad (4.6)$$

Where S_V is PSV and β the percentage of critical damping.

Tso et al. (1992) studied the correlation between A/V ratio and spectral intensity, with β being 5%. They observed that mean spectral intensity evaluated from PSV curves normalized to a common PGA of 1.0g for low A/V (A/V less than 7.9 sec^{-1}) group of records is over four times higher than that for the high A/V group (A/V greater than 11.8 sec^{-1}). Further, they show that SI correlates well with peak ground velocity (V), irrespective of A/V ratio (Fig. 4.33). They have obtained an empirical relationship between SI and V as

$$SI = 3.3V \qquad\qquad (4.7)$$

For the data set used in this study, a similar correlation between SI and V is obtained. Spectrum intensity for 5% damping, for all the horizontal component records used in the study are presented in Appendix A for ready reference. Fig. 4.34 shows the plots of SI versus peak ground velocity, for the six earthquakes; also shown in the figure are the best-fit linear (in the form $y = m\,x$) relationships. Empirical relationships for each of the six events are presented below

$$
\begin{aligned}
SI &= 2.65V \quad \text{(For "April", M = 5.5)} \\
SI &= 2.19V \quad \text{(For "Sept", M = 5.2)} \\
SI &= 3.36V \quad \text{(For "May", M = 5.7)} \\
SI &= 3.00V \quad \text{(For "Feb" M = 5.8)} \qquad (4.8) \\
SI &= 3.56V \quad \text{(For "Aug", M = 7.2)} \\
SI &= 3.98V \quad \text{(For "Oct", M = 6.6)} \\
SI &= 3.55V \quad \text{(For All records)}
\end{aligned}
$$

The relationships indicate that, in general, slope of straight line correlating SI with V increases with increase in magnitude of earthquake. However, no definite relationship in slope and earthquake magnitude can be concluded from this study.

Table 4.1 Spectrum amplification factors for horizonta
elastic response (Newmark and Hall 1969).

Damping,	One Sigma (84.1%)			Median (50%)		
% Critical	A	V	D	A	V	D
0.5	5.10	3.84	3.04	3.68	2.59	2.01
1	4.38	3.38	2.73	3.21	2.31	1.82
2	3.66	2.92	2.42	2.74	2.03	1.63
3	3.24	2.64	2.24	2.46	1.86	1.52
5	2.71	2.30	2.01	2.12	1.65	1.39
7	2.36	2.08	1.85	1.89	1.51	1.29
10	1.99	1.84	1.69	1.64	1.37	1.20
20	1.26	1.37	1.38	1.17	1.08	1.01

A : Acceleration
V : Velocity
D : Displacement

Table 4.2 Equations for Spectrum Amplification Factors
for Horizontal Motion (Newmark and Hall 1969)

Quantity	Cumulative Probability, %	Equation
Acceleration Velocity Displacement	84.1	$4.38-1.04 \ln(\beta)$ $3.38-0.67 \ln(\beta)$ $2.73-0.45 \ln(\beta)$
Acceleration Velocity Displacement	50.0	$3.21-0.68 \ln(\beta)$ $2.31-0.41 \ln(\beta)$ $1.82-0.27 \ln(\beta)$

β : Fraction of critical damping

Table 4.3   Summary of mean acceleration amplification   factors
for the six Himalayan earthquakes.

Event	period limits (sec)	Percentage of critical damping			
		0.5	2.0	5.0	10.0
April	0.13-0.24	4.2	3.3	2.6	2.1
Sept	0.12-0.21	4.1	3.3	2.6	2.1
May	0.12-0.27	5.8	3.9	2.8	2.0
Feb	0.11-0.24	4.7	3.7	2.6	2.0
Aug	0.11-0.27	5.4	3.6	2.5	1.9
Oct	0.14-0.29	5.4	3.8	2.7	2.1
All records	0.12-0.26	5.0	3.5	2.6	2.0

Table 4.4   Summary of mean velocity amplification factors   for
the six Himalayan earthquakes.

Event	period limits (sec)	Percentage of critical damping			
		0.5	2.0	5.0	10.0
April	0.24-0.90	2.8-2.8	2.3-2.3	1.8-1.8	1.4-1.4
Sept	0.21-0.30	3.6-3.6	2.7-2.7	2.3-2.3	1.6-1.6
May	0.27-2.10	3.6-2.0	2.7-1.6	1.9-1.4	1.5-1.0
Feb	0.24-2.00	2.9-1.9	2.2-1.6	1.6-1.4	1.3-1.0
Aug	0.27-1.20	3.9-3.6	2.7-2.7	2.0-2.0	1.5-1.5
Oct	0.29-1.28	3.8-2.6	2.9-2.1	2.1-1.7	1.6-1.3
All records	0.26-2.6	3.6-1.7	2.6-1.3	2.0-1.1	1.4-0.9

Table 4.5 Comparitive summary of mean acceleration amplification
factors.

Percent of critical damping	Present study	Newmark & Hall (1969)	Mohraz (1976) for rock sites
	Period, 0.12-0.26 sec	Period, 0.12-0.50 sec	Period, 0.12-0.33 sec
2	3.5	2.74	2.57
5	2.6	2.12	1.98
10	2.0	1.64	1.56
20	1.5	1.17	1.22

Table 4.6 Comparitive summary of mean velocity amplification
factors.

Percent of critical damping	Present study	Newmark & Hall (1969)	Mohraz (1976) for rock sites
	Period, 0.26-2.60 sec	Period, 0.50-3.33 sec	Period, 0.33-3.33 sec
2	2.6-1.3	2.03	1.57
5	2.0-1.1	1.65	1.28
10	1.4-0.9	1.37	1.04
20	1.1-0.9	1.17	0.81

Table 4.7 Comparitive summary of mean-plus-one-standard-deviation acceleration amplification factors.

Percent of critical damping	Present study	Newmark & Hall (1969)	Mohraz (1976) for rock sites	NRC
	Period, 0.12-0.28 sec	Period, 0.12-0.50 sec	Period, 0.12-0.33 sec	Period, 0.11-0.40 sec
2	4.6	3.66	3.80	3.54-4.25
5	2.9	2.71	2.82	2.61-3.13
10	2.4	1.99	2.11	2.27-2.72
20	1.7	1.26	1.54	1.90-2.28

Table 4.8 Comparitive summary of mean-plus-one-standard-deviation velocity amplification factors.

Percent of critical damping	Present study	Newmark & Hall (1969)	Mohraz (1976) for rock sites
	Period, 0.28-2.54 sec	Period, 0.50-3.33 sec	Period, 0.33-3.33 sec
2	3.6-1.9	2.92	2.44
5	2.6-1.6	2.30	1.90
10	1.9-1.1	1.84	1.48
20	1.4-0.9	1.37	1.11
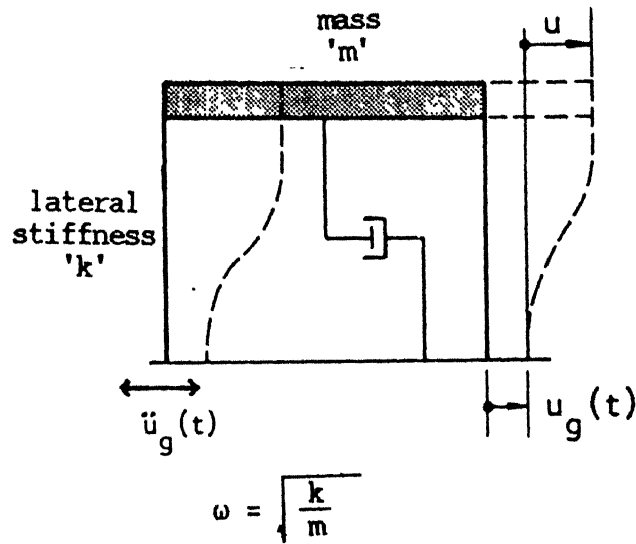
Fig. 4.1   SDOF System, subjected to earthquake ground motion.
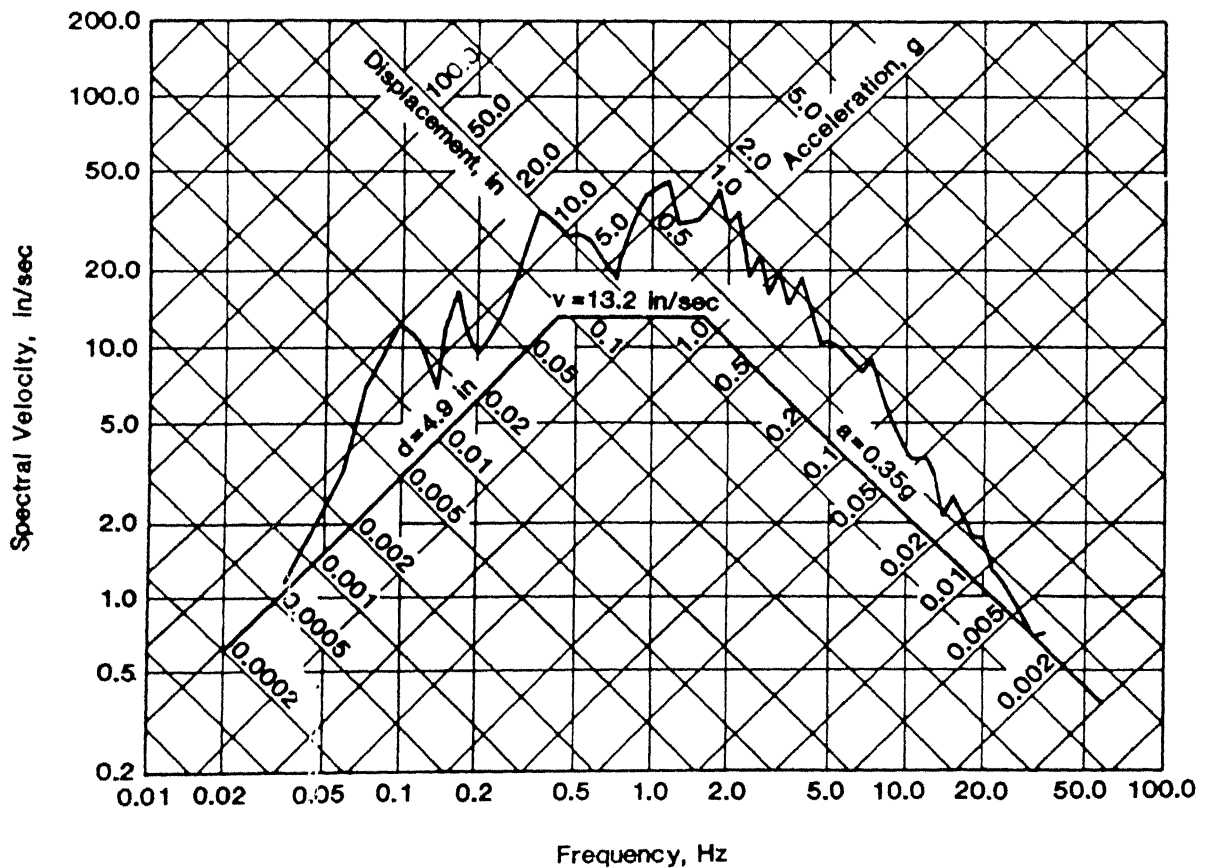
Fig. 4.2   A typical response spectrum with a tripartite plot.
Also, marked are the values of peak ground
acceleration, peak ground velocity, and peak ground
displacement (Gupta 1990).
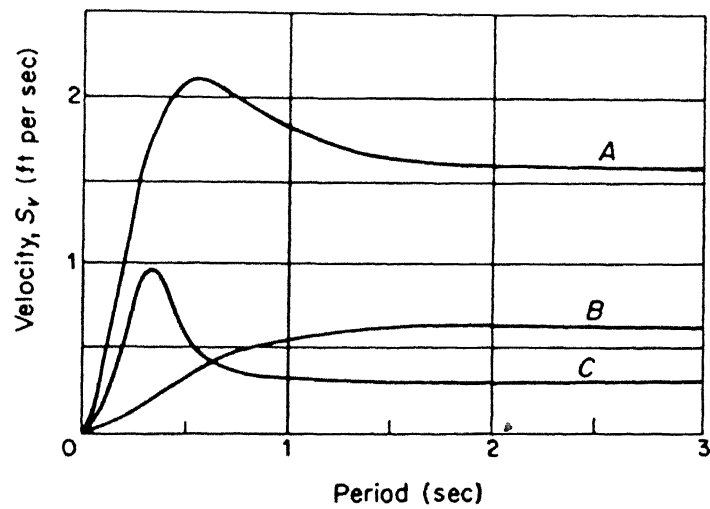
Fig. 4.3   Idealized   undamped   velocity   spectrum   curves
illustrating the effect of magnitude and distance.
curve A, 25 miles from centre of large earthquake;
curve B, 70 miles from centre of large shock; curve
C, 8 miles from centre of small (M=5.3) shock
(Housner 1970).
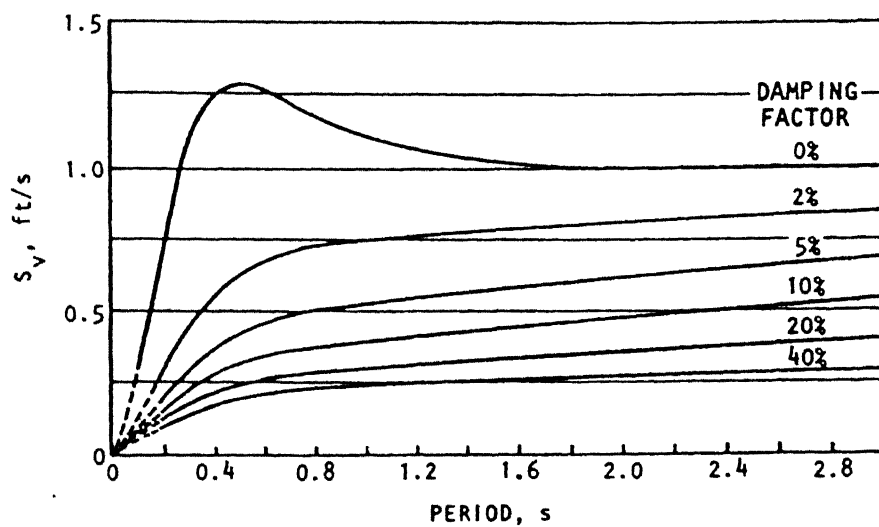
VELOCITY SPECTRUM CURVES
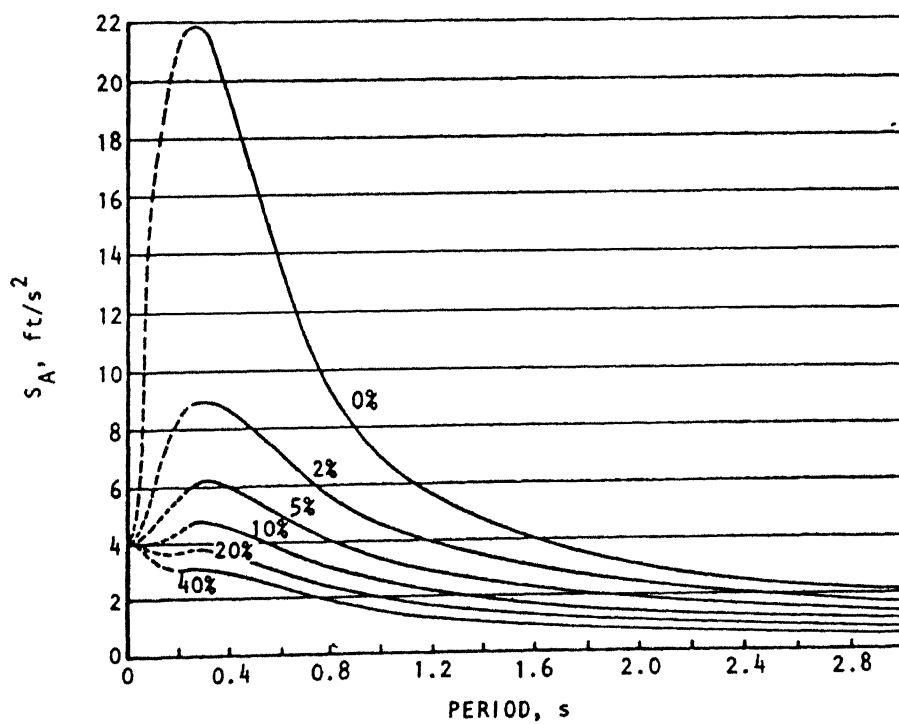
ACCELERATION SPECTRUM CURVES

Fig. 4.4   Smooth design spectrum curves developed by Housner (1959).
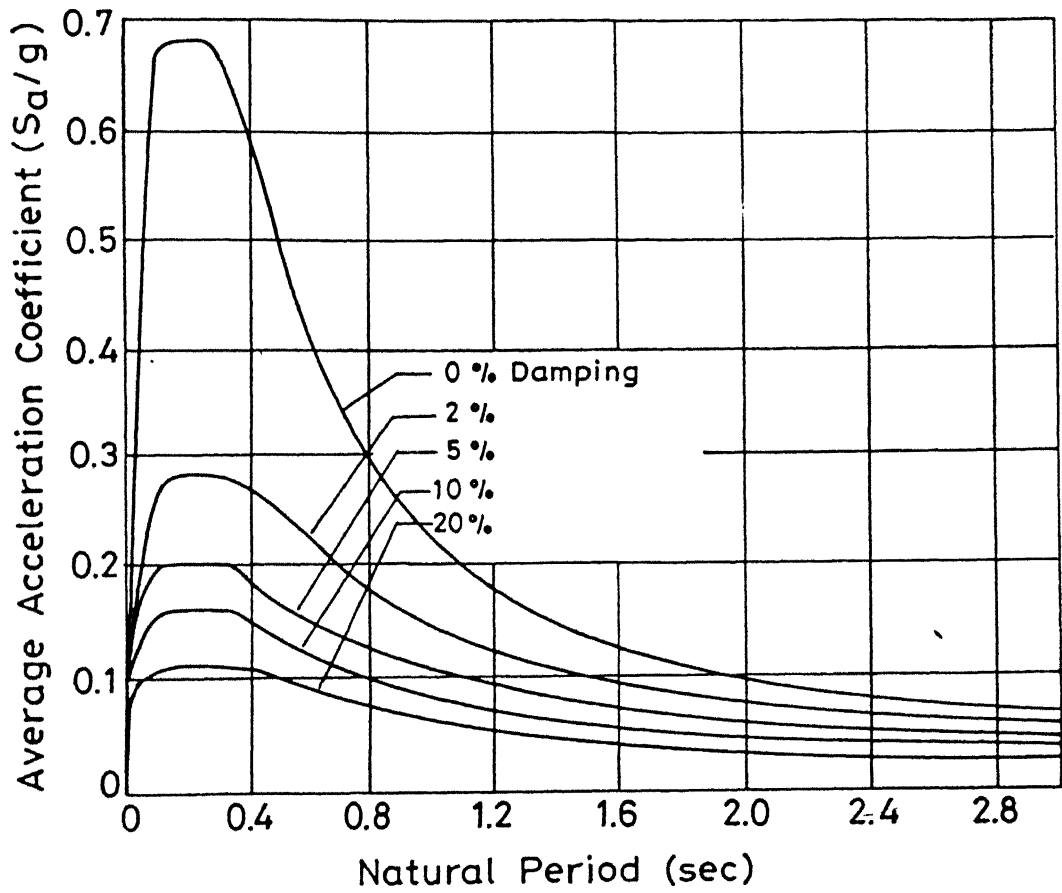
Fig. 4.5   Average   acceleration   spectra S_a/g versus   T
(IS:1893-1984).
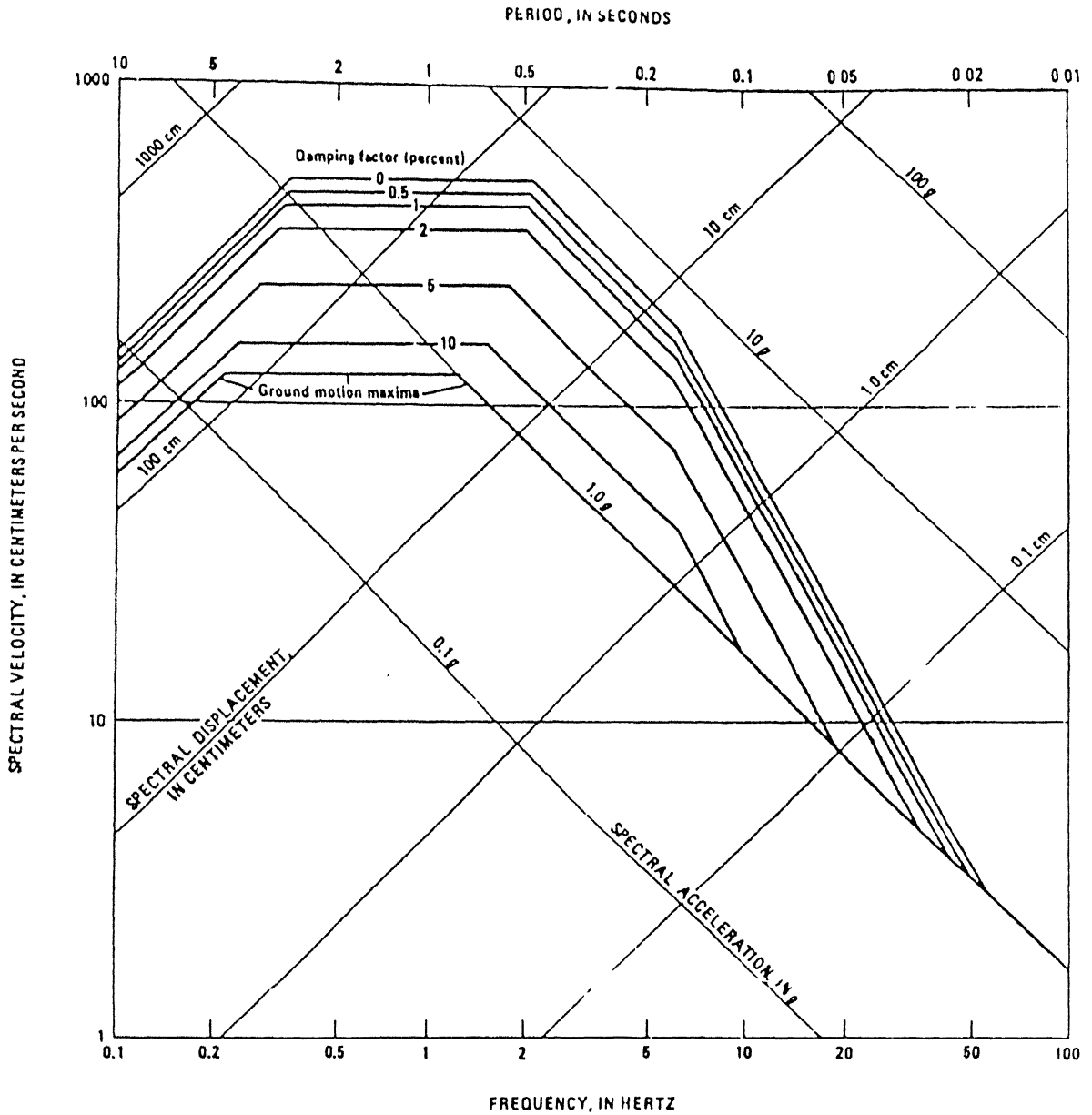
Fig. 4.6   "Standard" site independent horizontal response spectra modified from Newmark and Hall 1969 (Hays 1980).
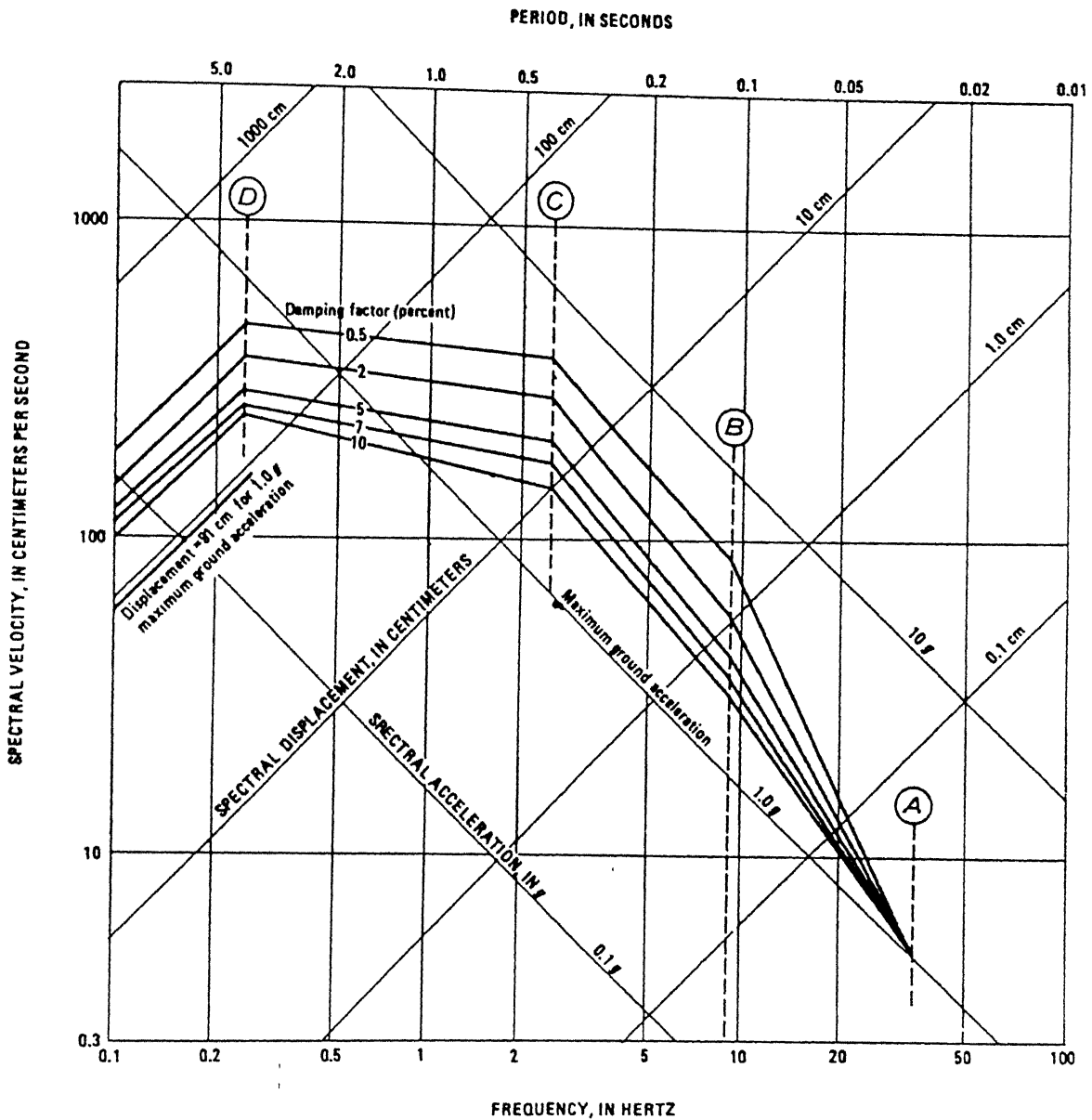
% of critical damping	Acceleration			Displacement
	A(33 Hz)	B(9 Hz)	C(2.5 Hz)	D(0.25 Hz)
0.5	1.0	4.96	5.95	3.20
2.0	1.0	3.54	4.25	2.50
5.0	1.0	2.61	3.13	2.05
7.0	1.0	2.27	2.72	1.88
10.0	1.0	1.90	2.28	1.70

Fig. 4.7   Horizontal design spectra and relative values of spectrum amplification factors for control points, adopted by NRC regulatory guide 1.6 (1973) (Hays

PERIOD, IN SECONDS

FREQUENCY, IN HERTZ
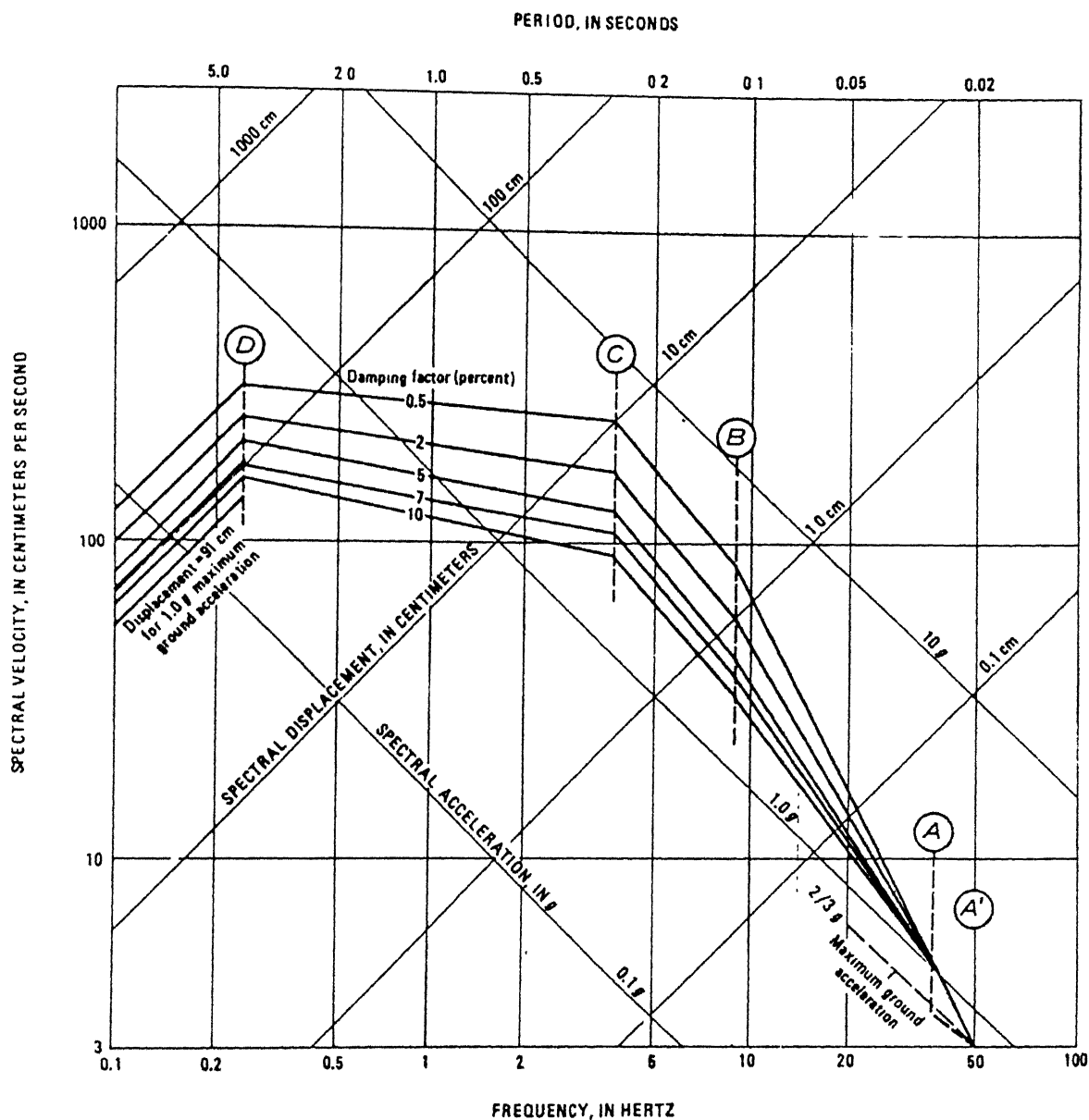
% of critical damping	Acceleration				Displacement
	A'(50 Hz)	A(33 Hz)	B(9 Hz)	C(3.5 Hz)	D(0.25 Hz)
0.5	0.67	1.0	4.96	5.67	2.17
2.0	0.67	1.0	3.54	4.05	1.67
5.0	0.67	1.0	2.61	2.98	1.37
7.0	0.67	1.0	2.27	2.59	1.25
10.0	0.67	1.0	1.90	2.17	1.13

Fig. 4.8   Vertical design spectra and relative values of spectrum amplification factors for control points, adopted by NRC regulatory guide 1.6 (1973) (Hays 1980).
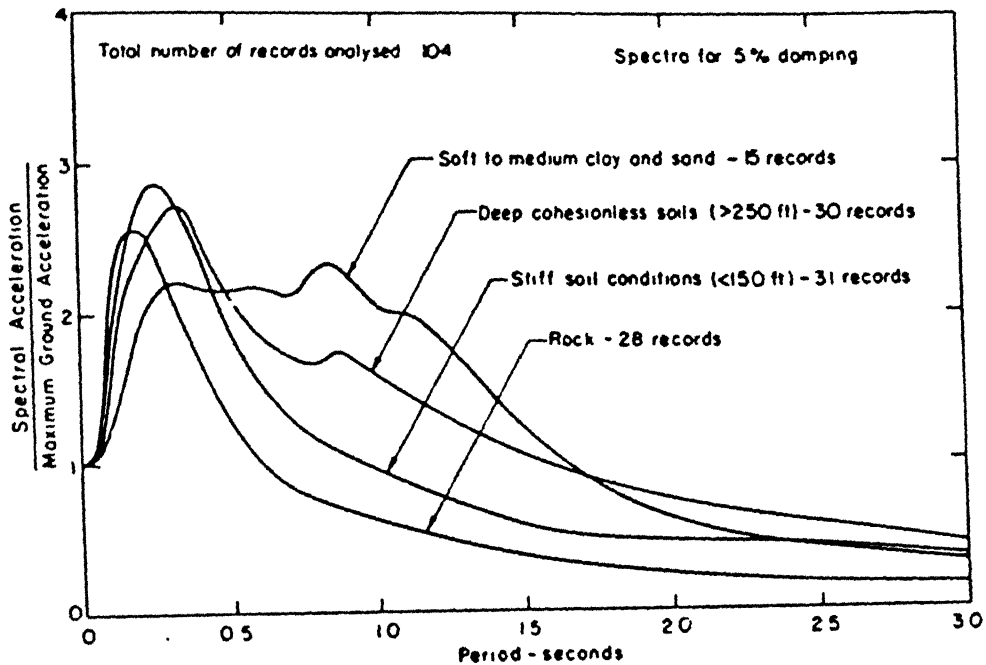
Fig. 4.9   Average acceleration spectra for different site conditions (Seed et al. 1976).
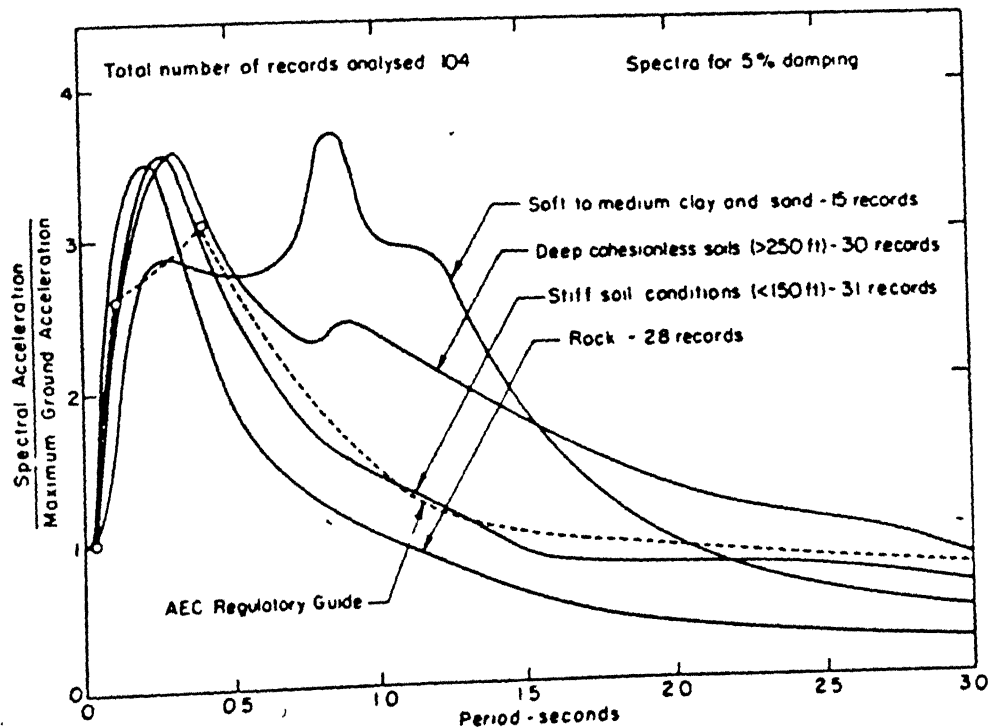
Fig. 4.10   Mean-plus-one-standard-deviation spectra for different site conditions (Seed et al. 1976).
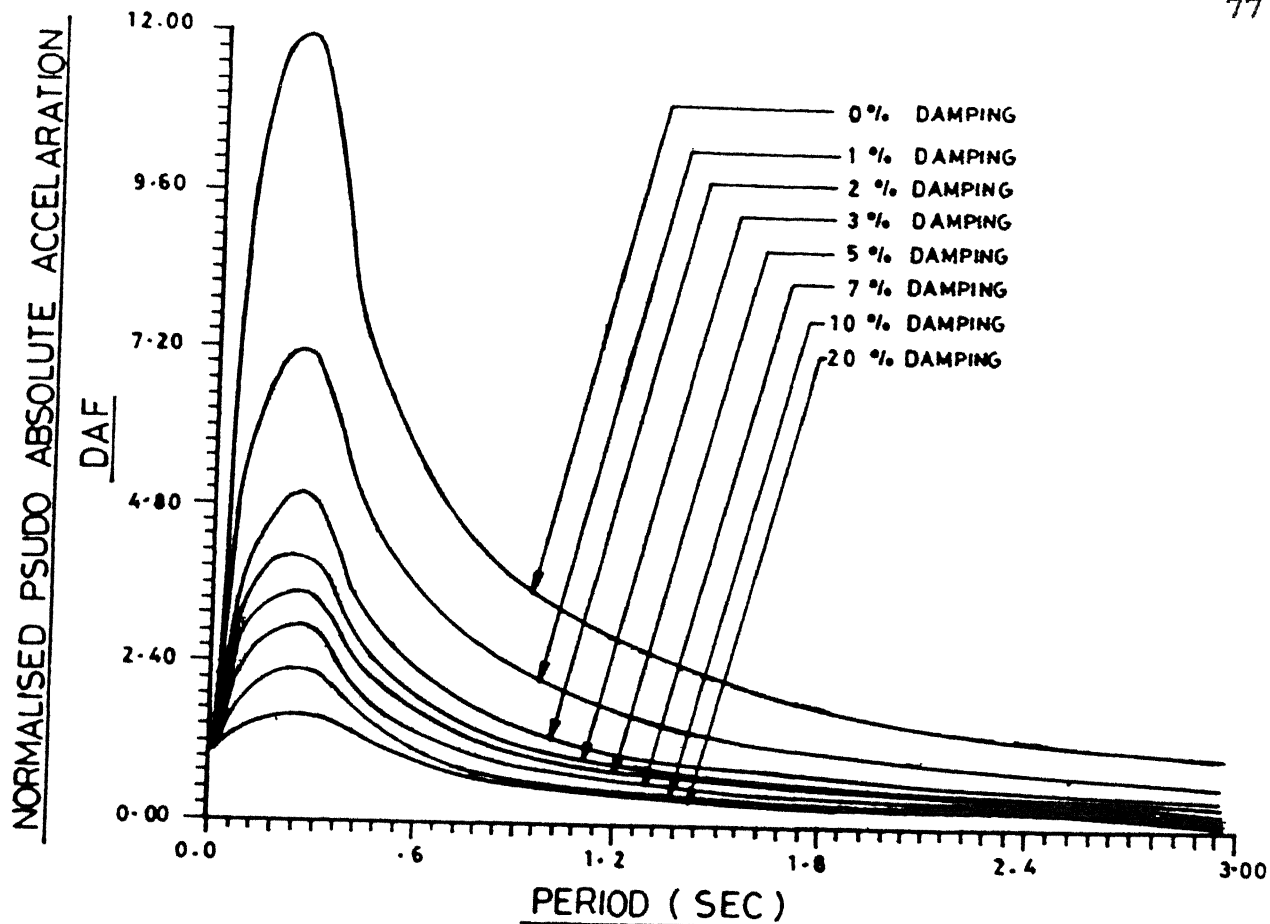
Fig. 4.11　　AERB "standard" spectra for rock sites.
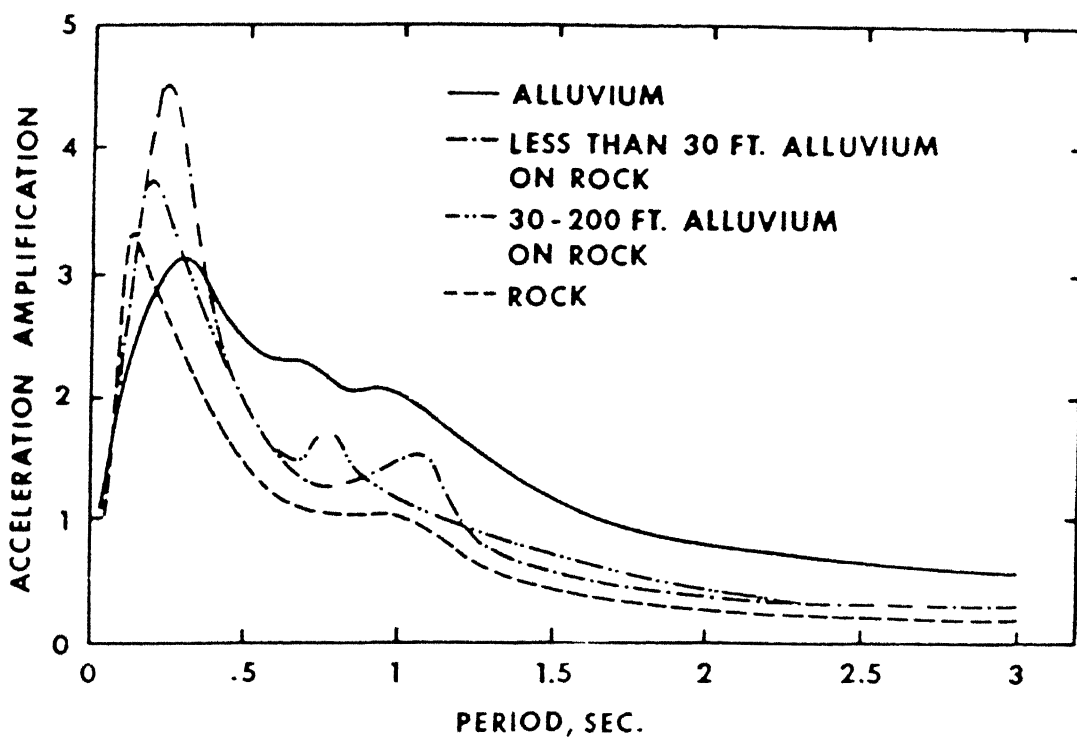
Fig. 4.12　　Average acceleration amplification for 2 percent damping (Mohraz 1976).
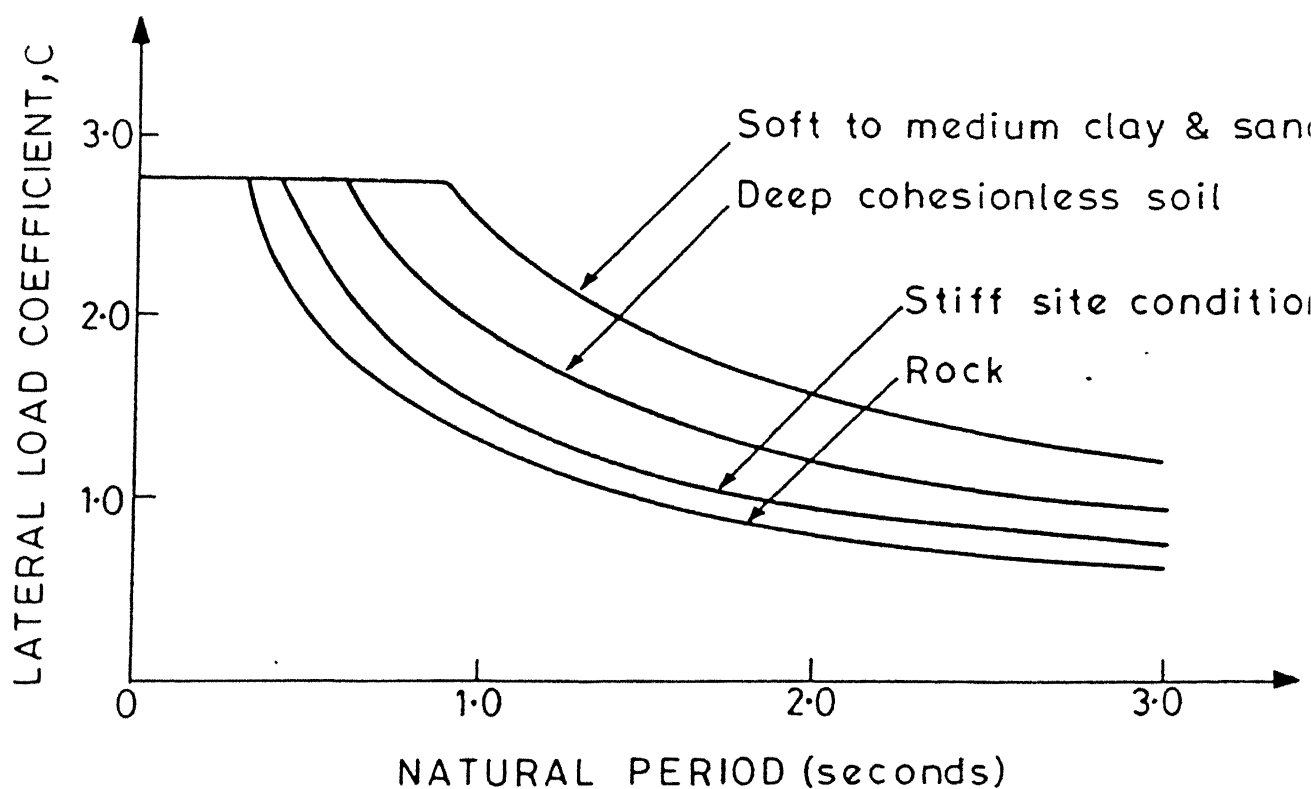
Fig. 4.13   Shape of design spectra for different soil conditions
(UBC 1991).
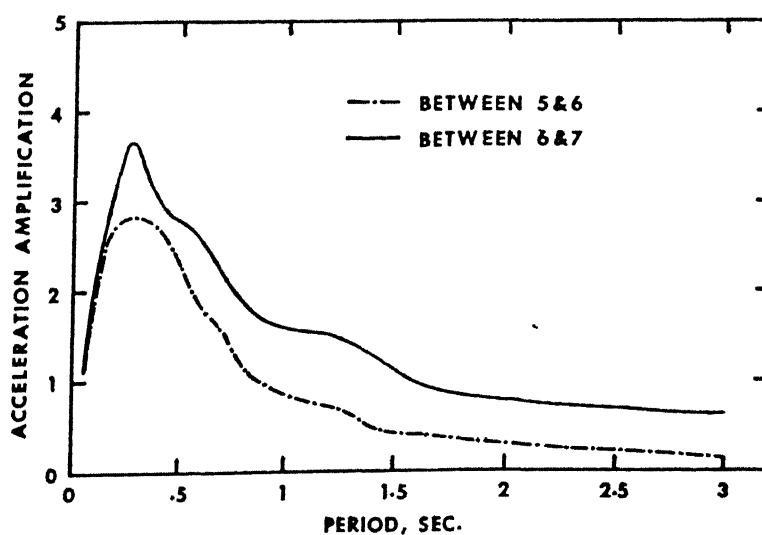
Fig. 4.14   Effect of earthquake magnitude on spectral shapes
(Mohraz 1978).
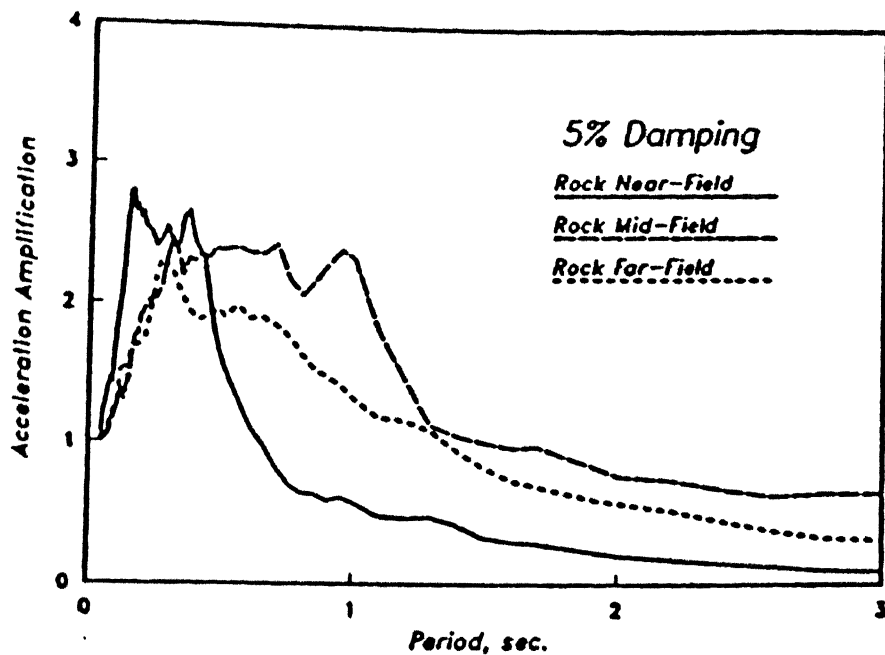
(a)
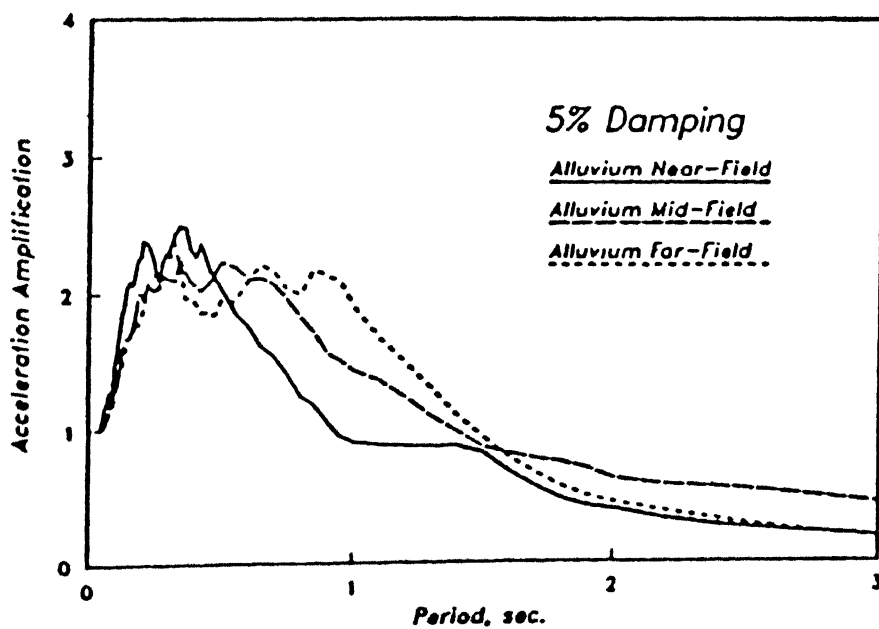
(b)

Fig. 4.15   Average acceleration amplification for different distances, (a) for rock sites, (b) for alluvium.

Feb (M=5.8)

Aug (M=7.2)

Oct (M=6.6)
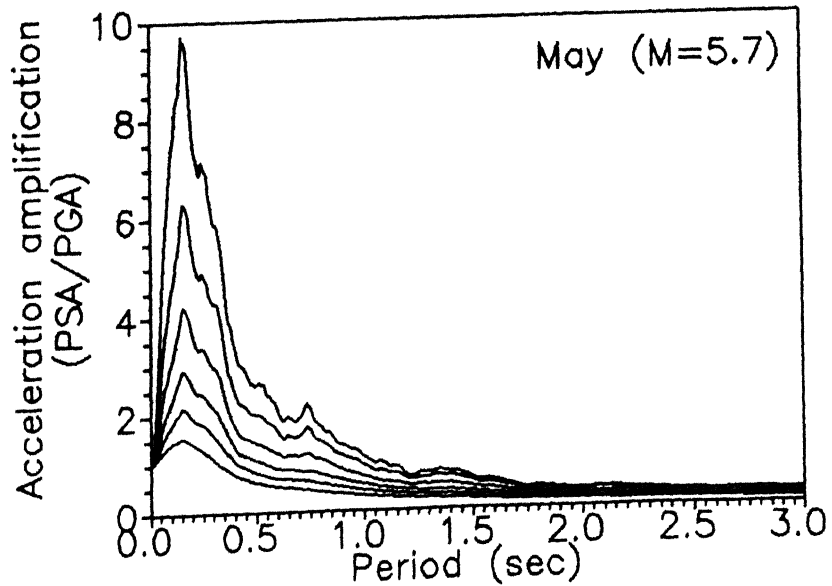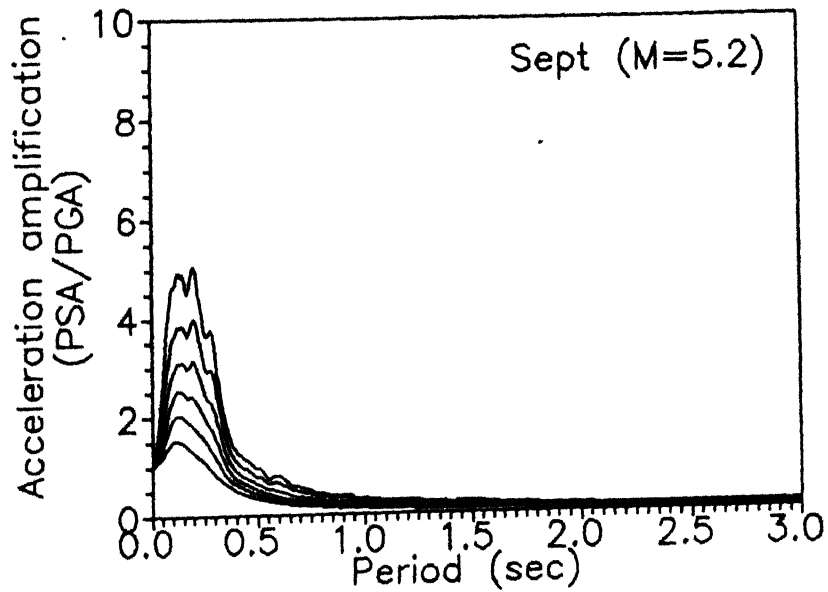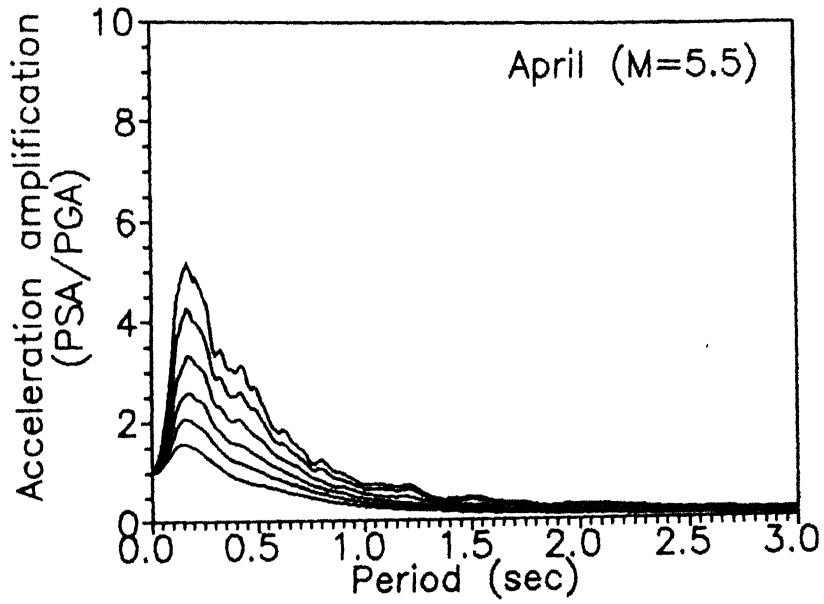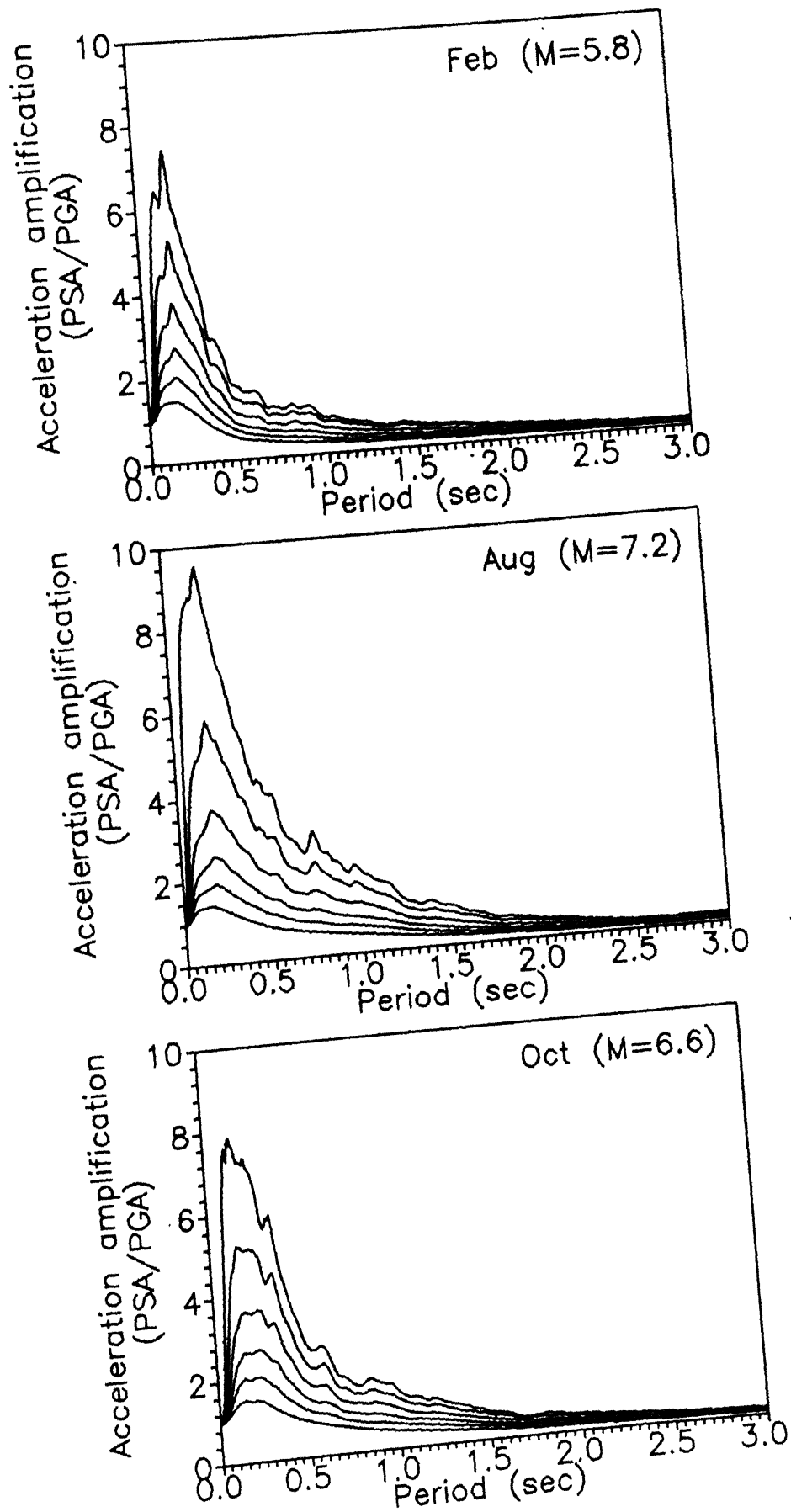
Fig. 4.16   Mean horizontal acceleration spectra for 0, 0.5, 2, 5, 10, 20% damping for the six Himalayan earthquakes.
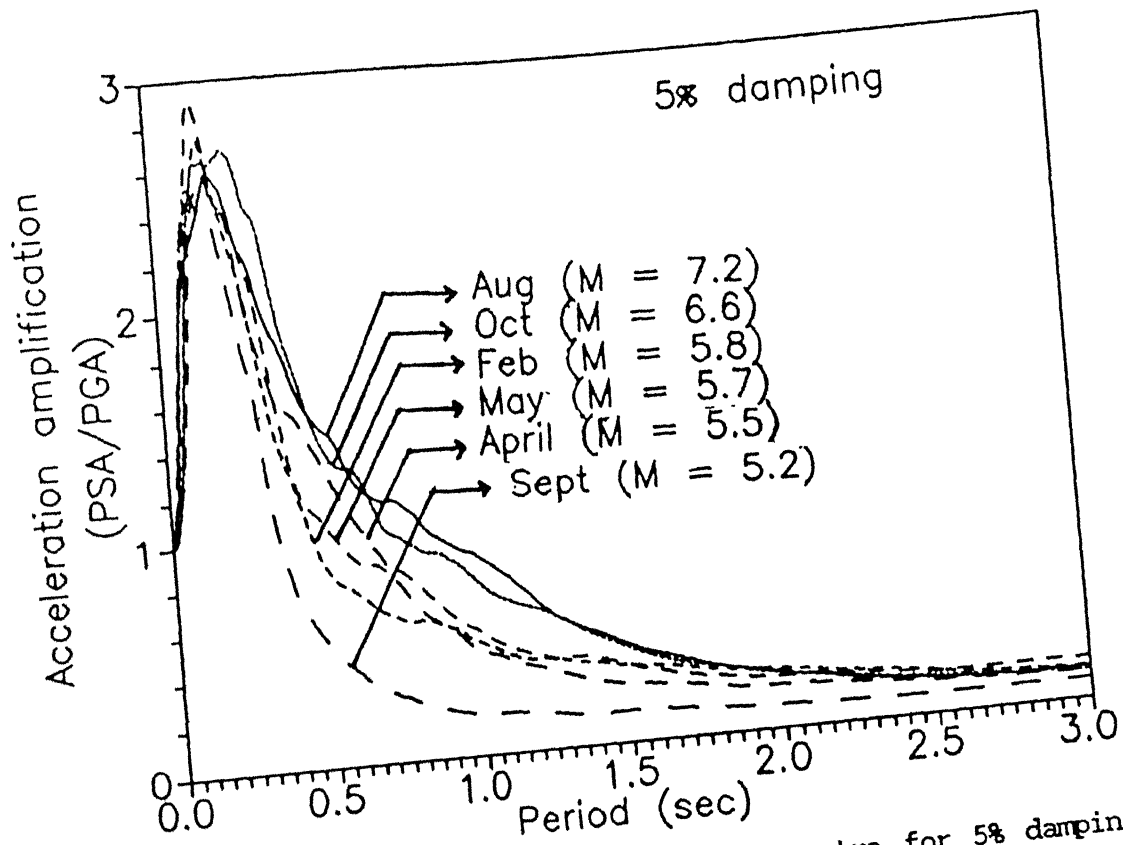
Fig. 4.17   Mean horizontal acceleration spectra for 5% damping for the six Himalayan earthquakes.
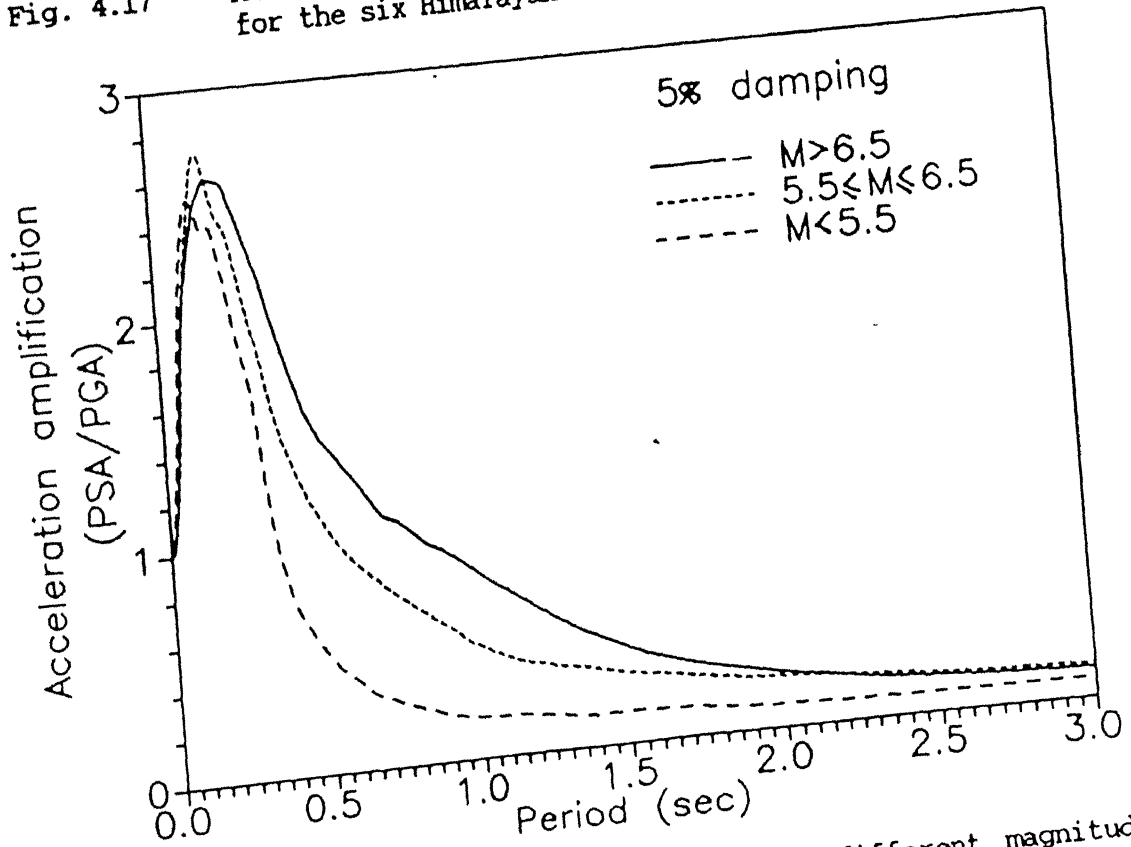
Fig. 4.18   Mean spectral shapes for three different magnitude (M) range.
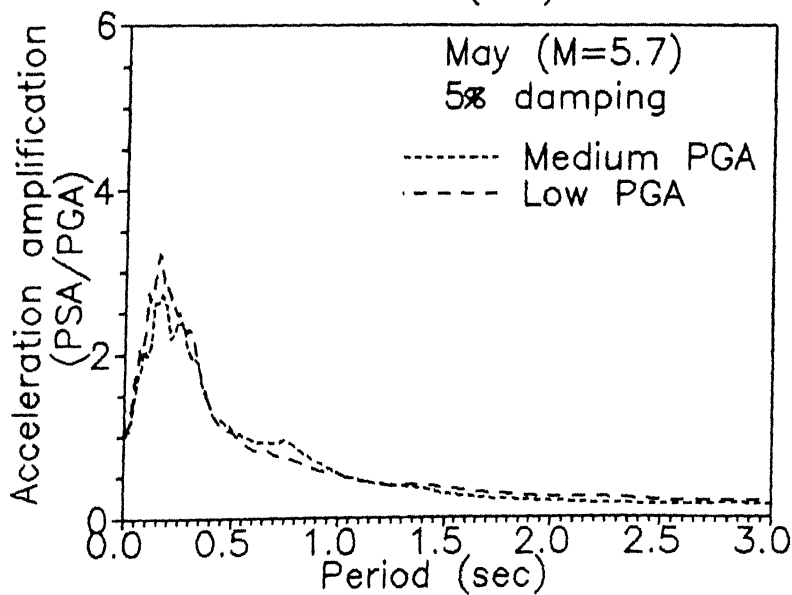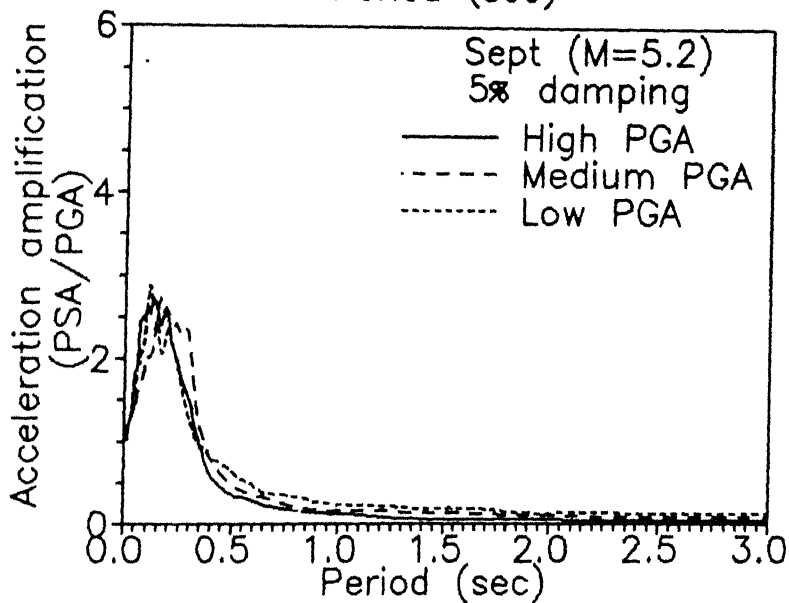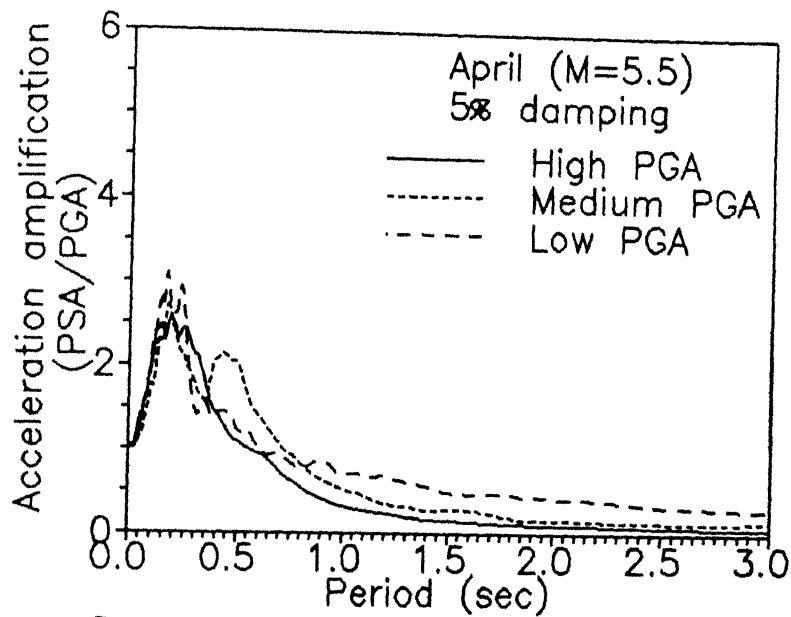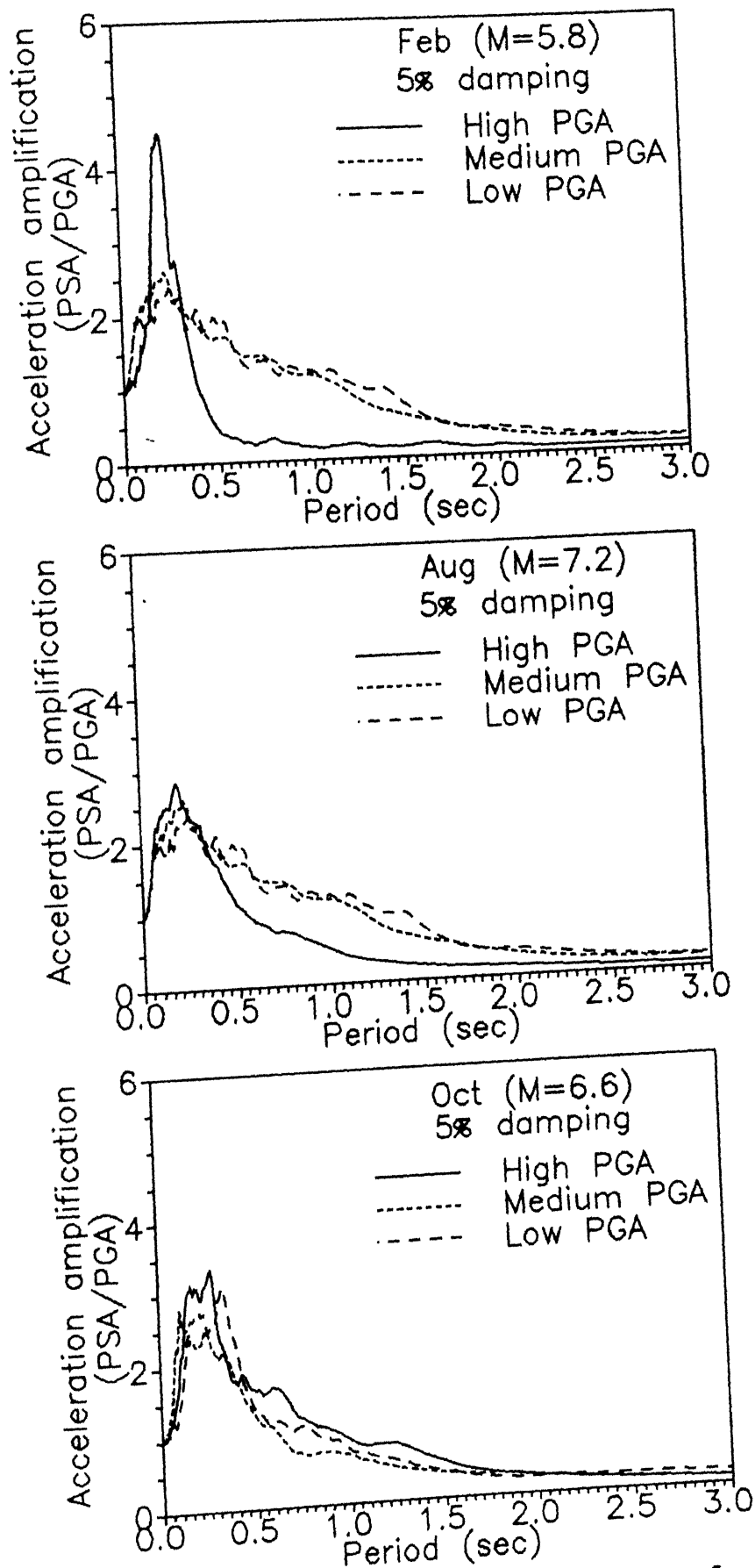
Fig. 4.19   Mean horizontal acceleration spectra for 5% damping in the three PGA groups, for the six Himalayan earthquakes.
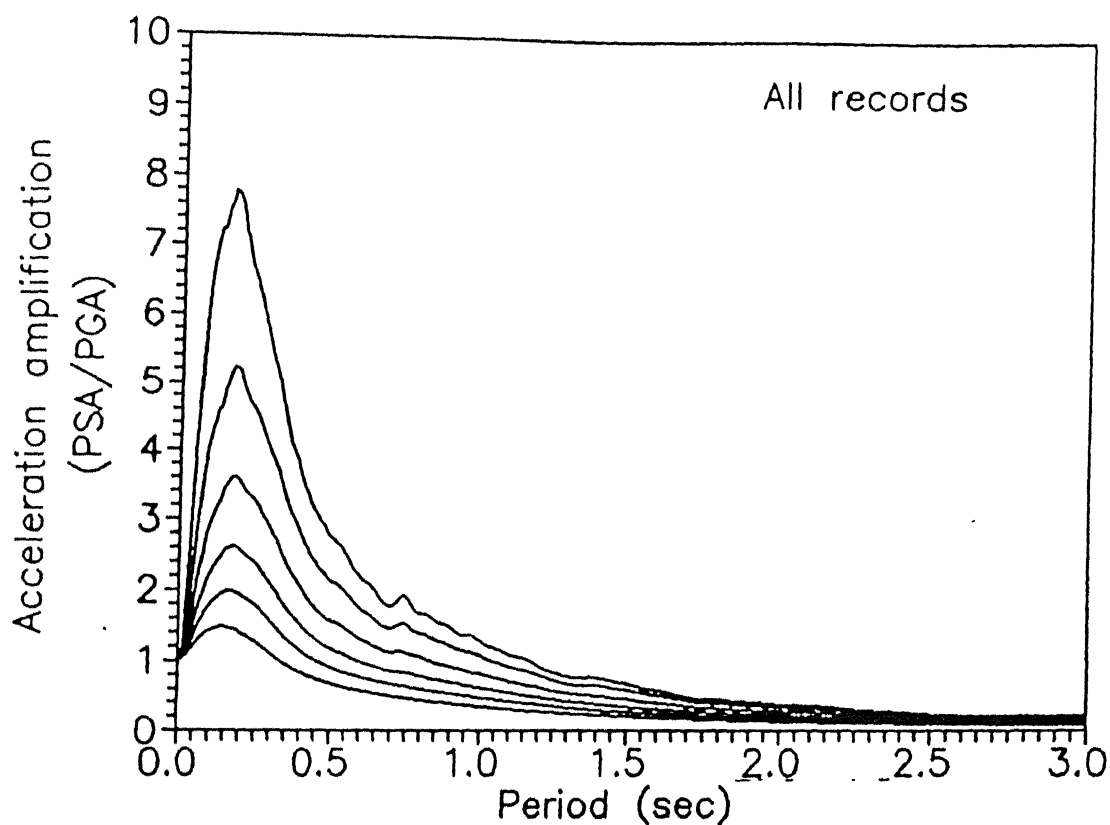
Fig. 4.20   Mean horizontal spectra considering all records for 0, 0.5, 2, 5, 10, and 20% damping.
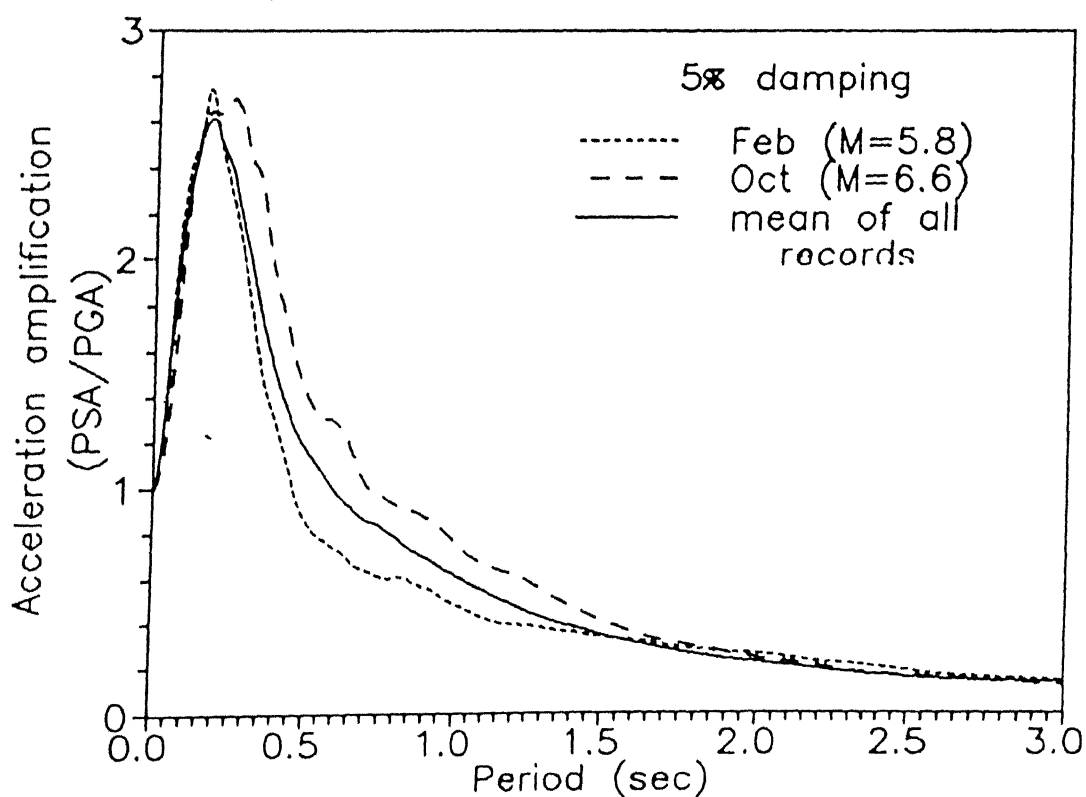
Fig. 4.21   Comparison of mean spectral shape with the shape obtained in the events "Feb" and "Oct".

April (M=5.5)

Sept (M=5.2)

May (M=5.7)
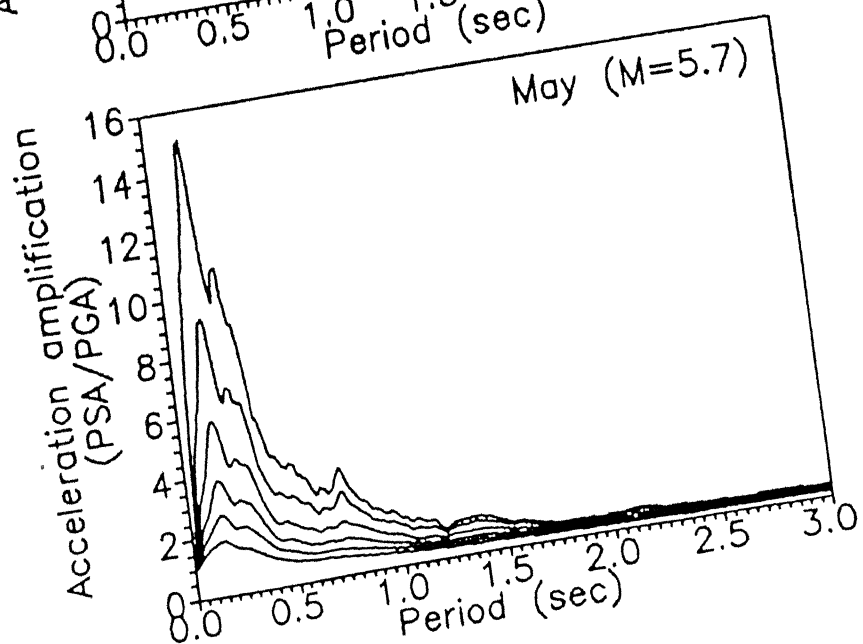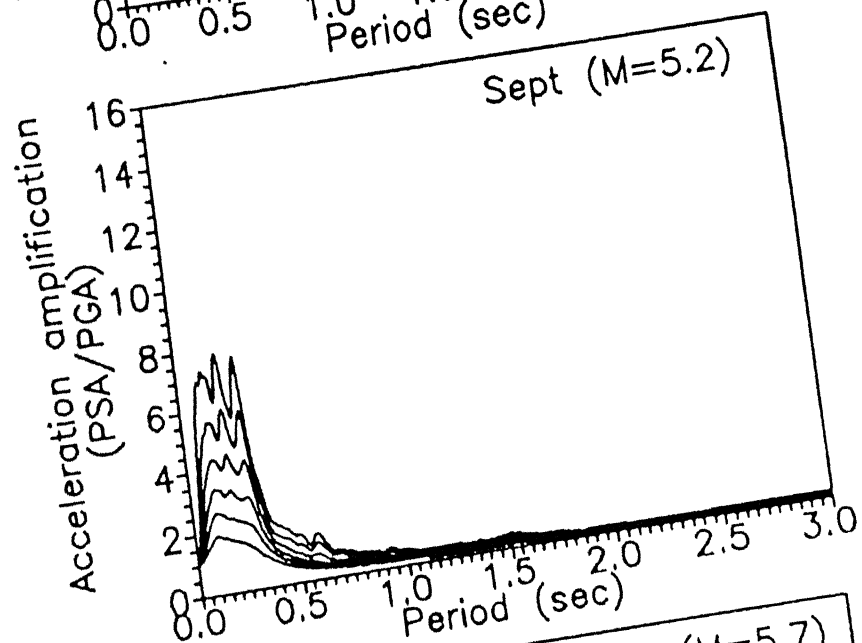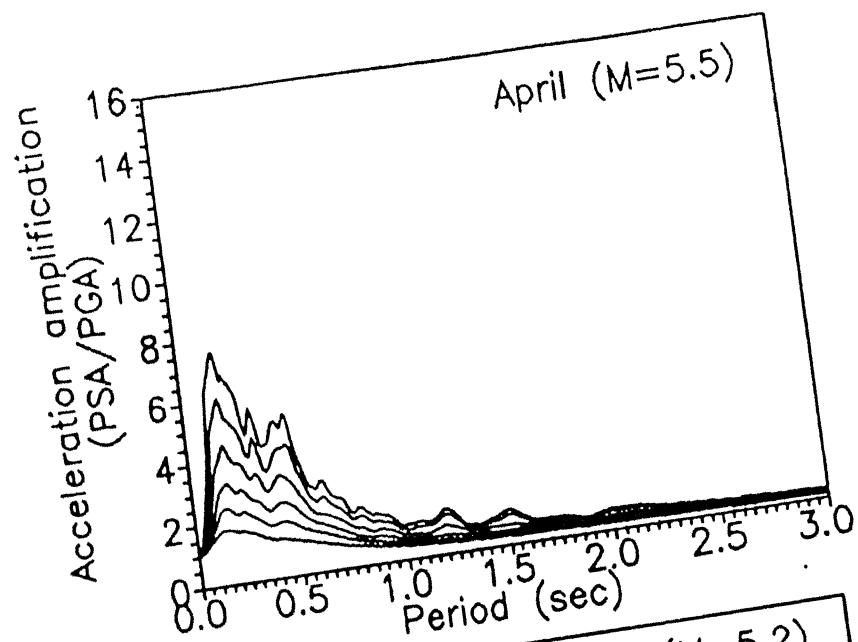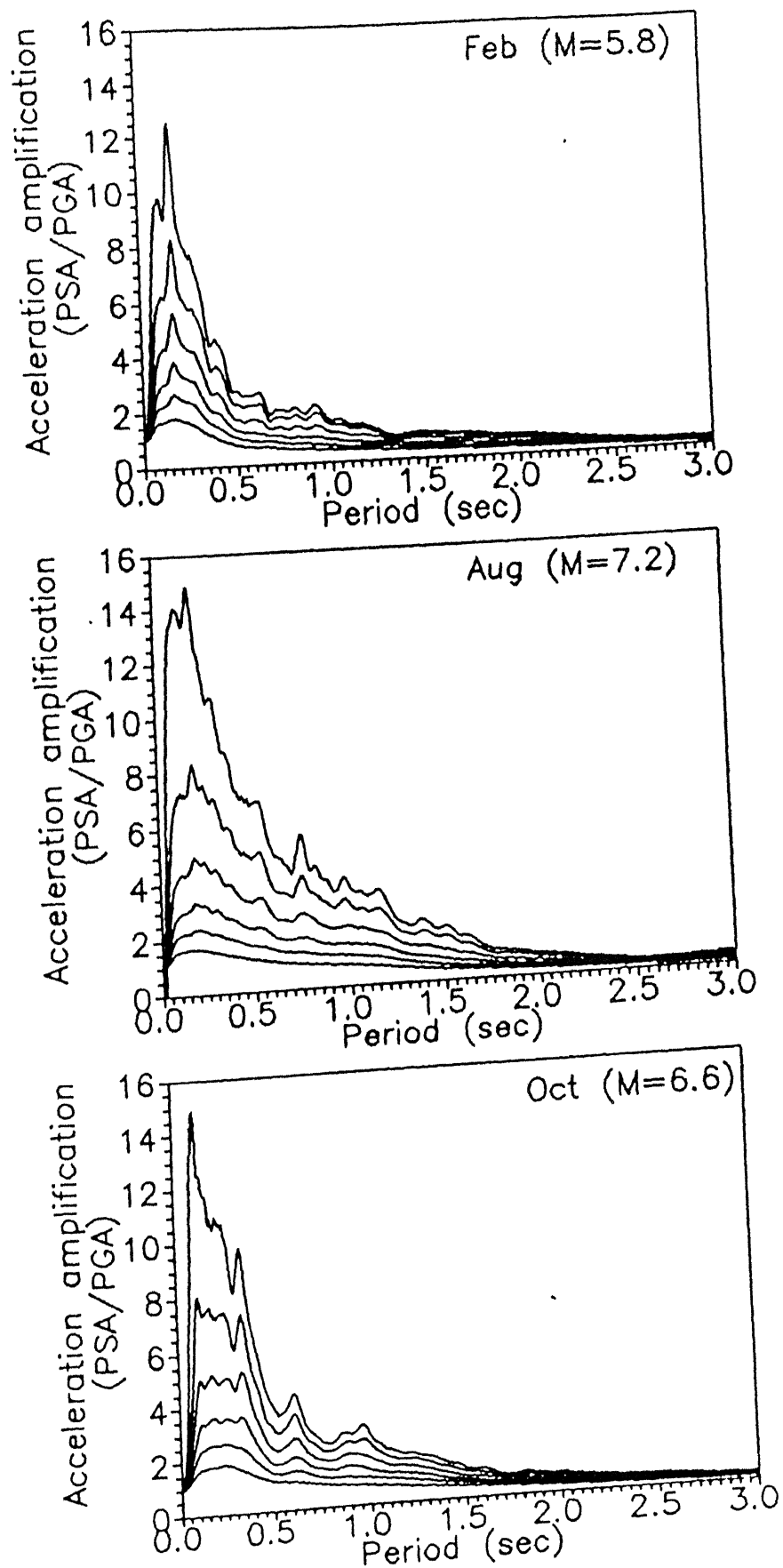
Fig. 4.22   Mean-plus-one-standard-deviation   horizontal spectra
for 0, 0.5, 2, 5, 10, and 20% damping for the six
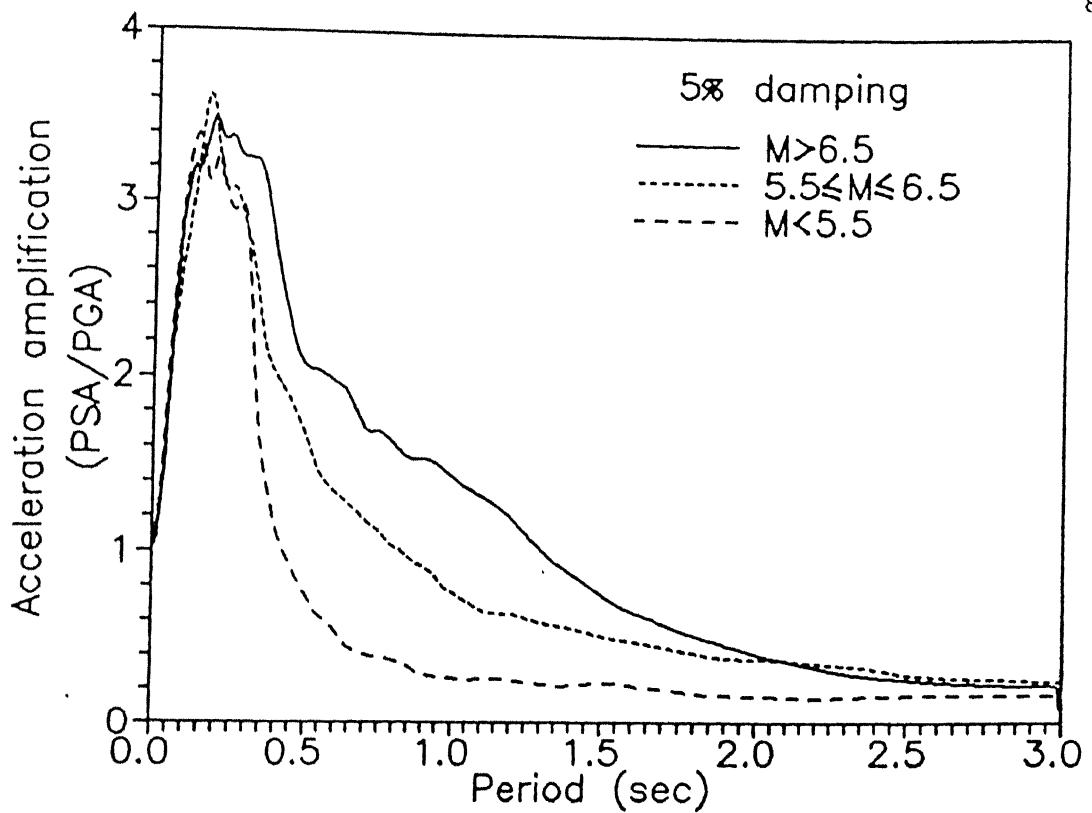
Fig. 4.23   Mean-plus-one-standard-deviation spectra for the three earthquake magnitude (M) range.
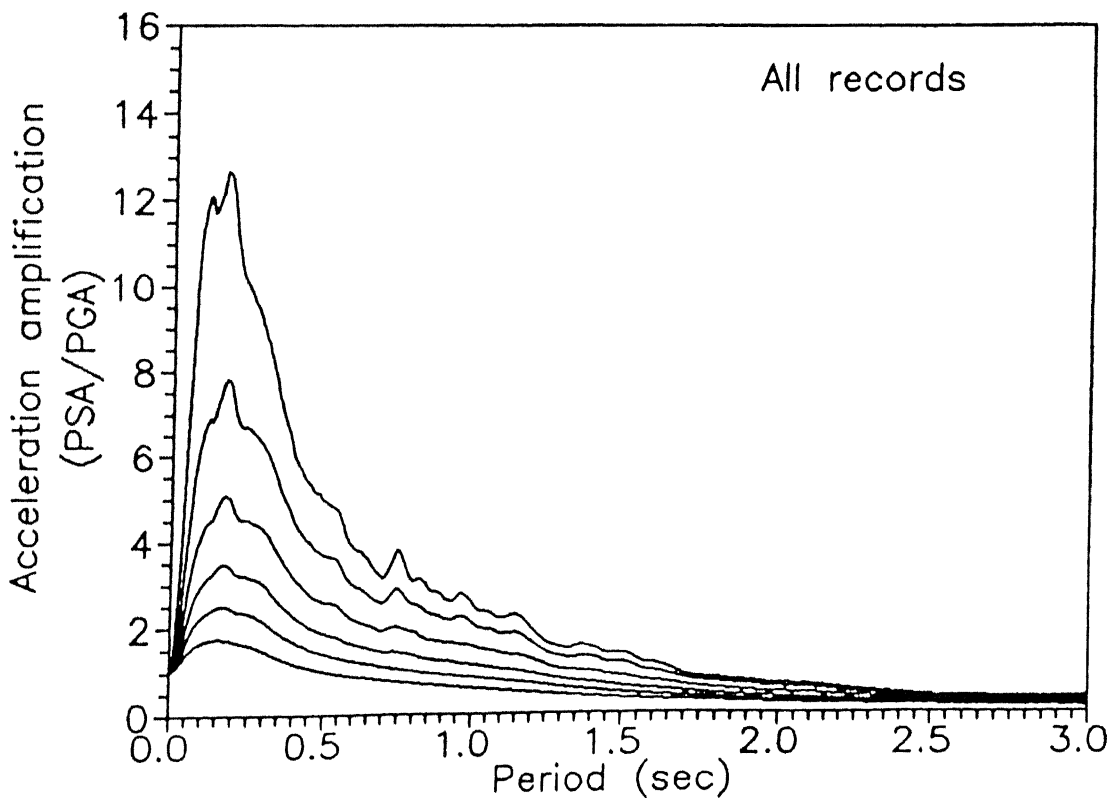
Fig. 4.24   Mean-plus-one-standard-deviation horizontal spectra considering all records together for 0, 0.5, 2, 5, 10, and 20% damping.
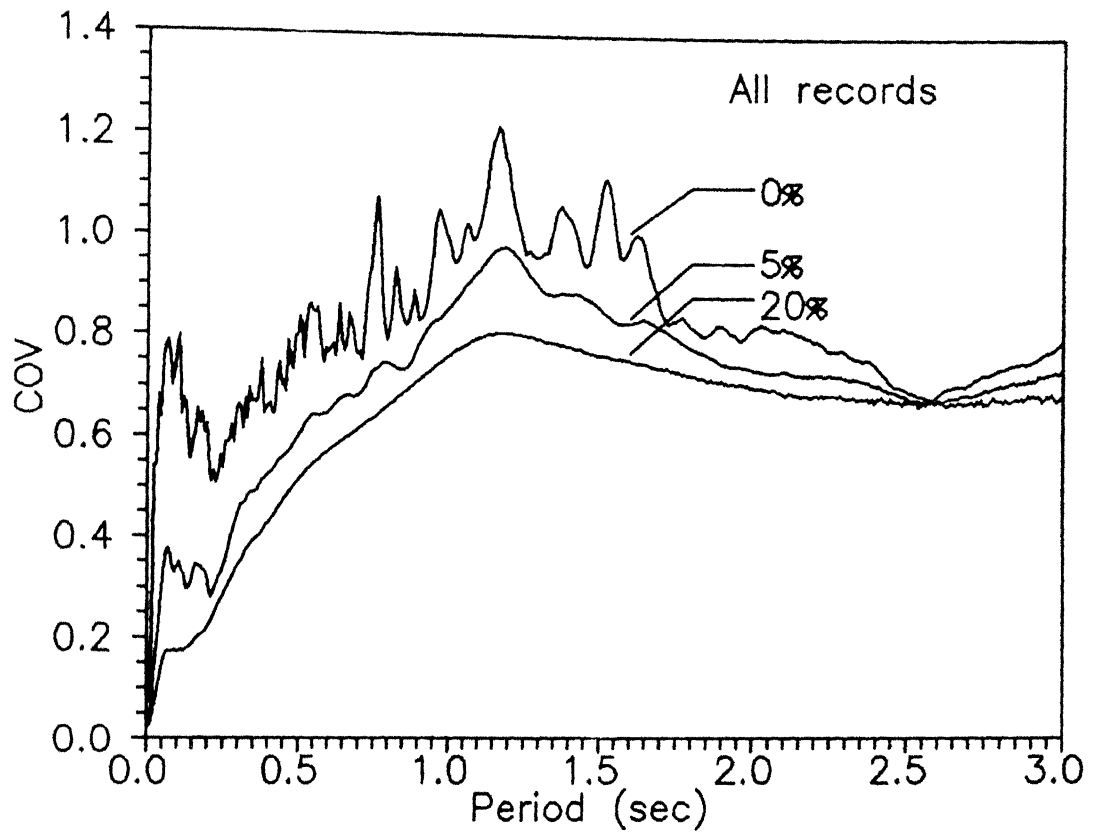
Fig. 4.25   COV of acceleration spectra for 0, 5, and 20% damping considering all horizontal records together.
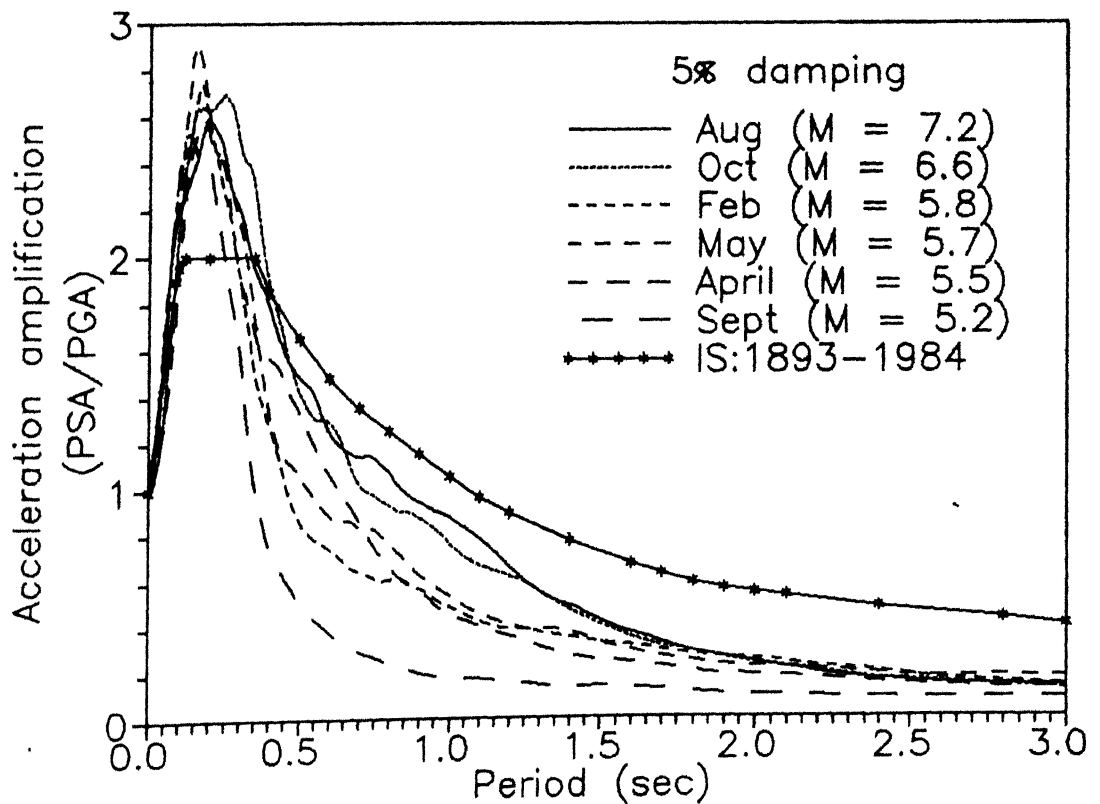
Fig. 4.26   Comparison of IS:1893-1984 spectra with mean spectra from six Himalayan earthquakes.
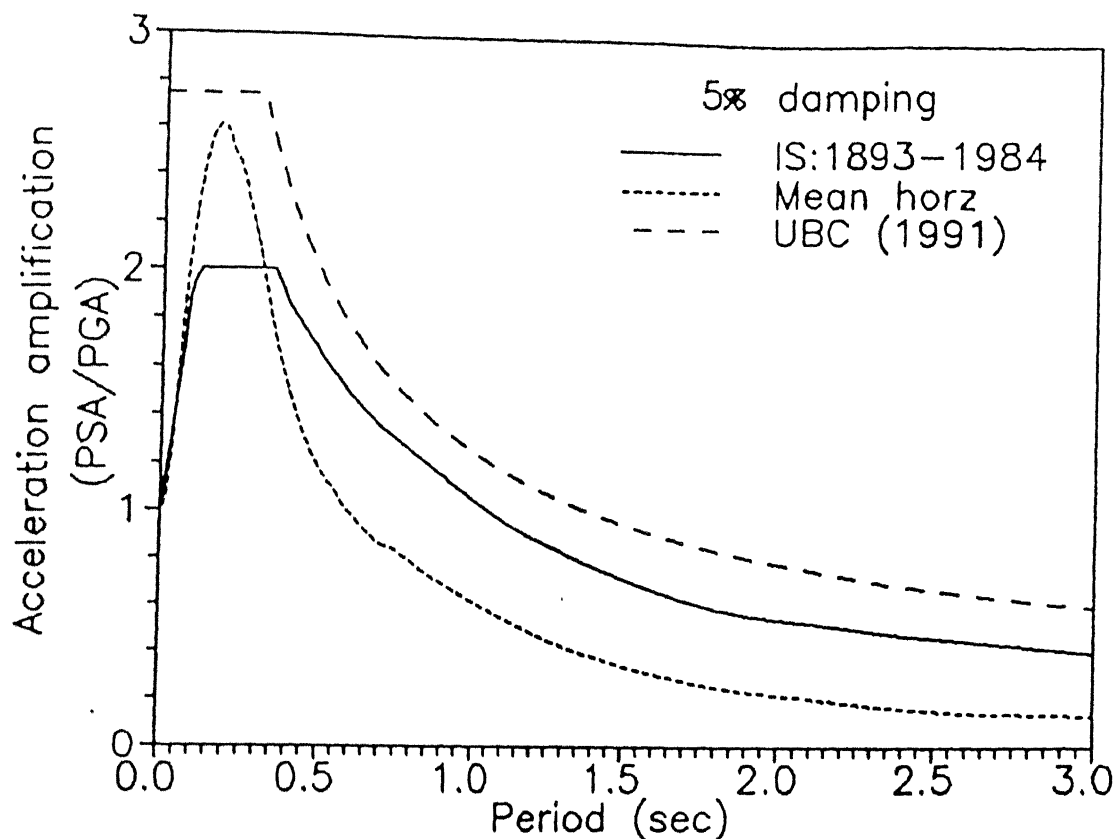
Fig. 4.27   Comparison of 5% damping spectral shapes obtained from data with that of IS:1893-1984 and UBC (1991).
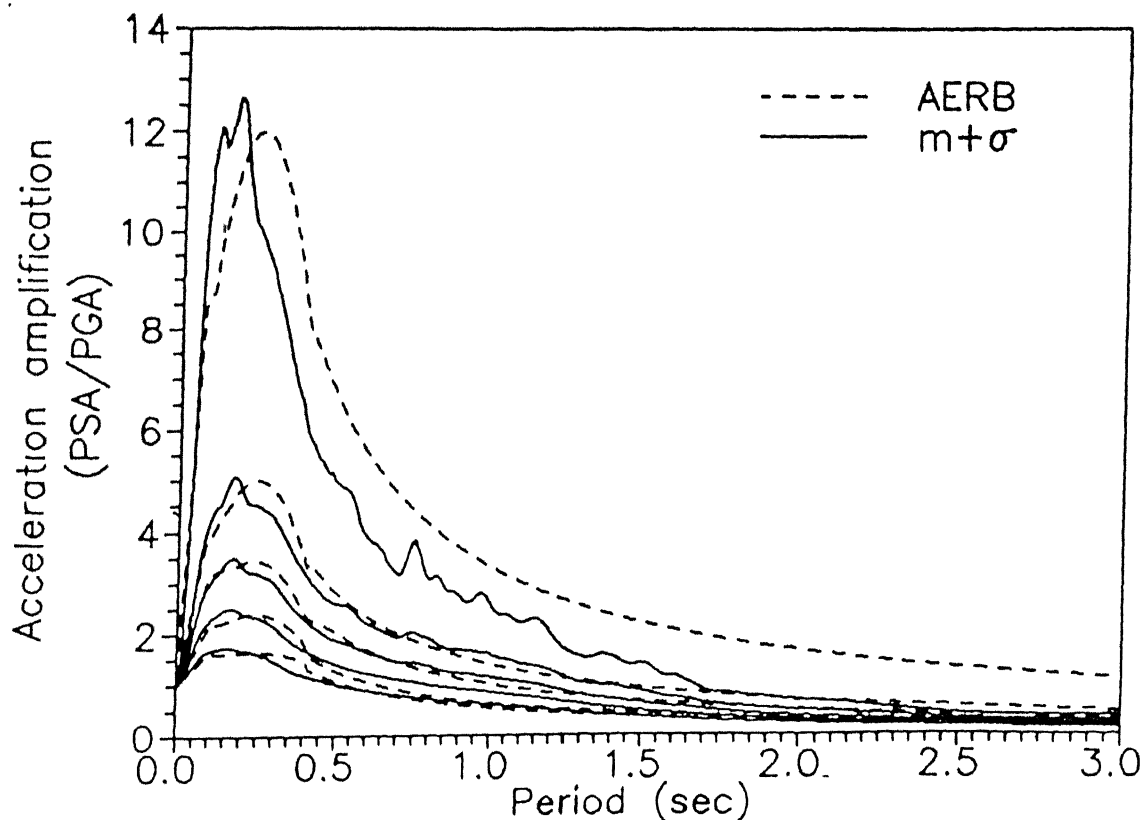
Fig. 4.28   Comparison of mean-plus-one-standard-deviation (m +σ) spectra from the Himalayan earthquakes data with "standard spectra" for rock sites recommended by AERB (0, 2, 5, 10, and 20% damping).
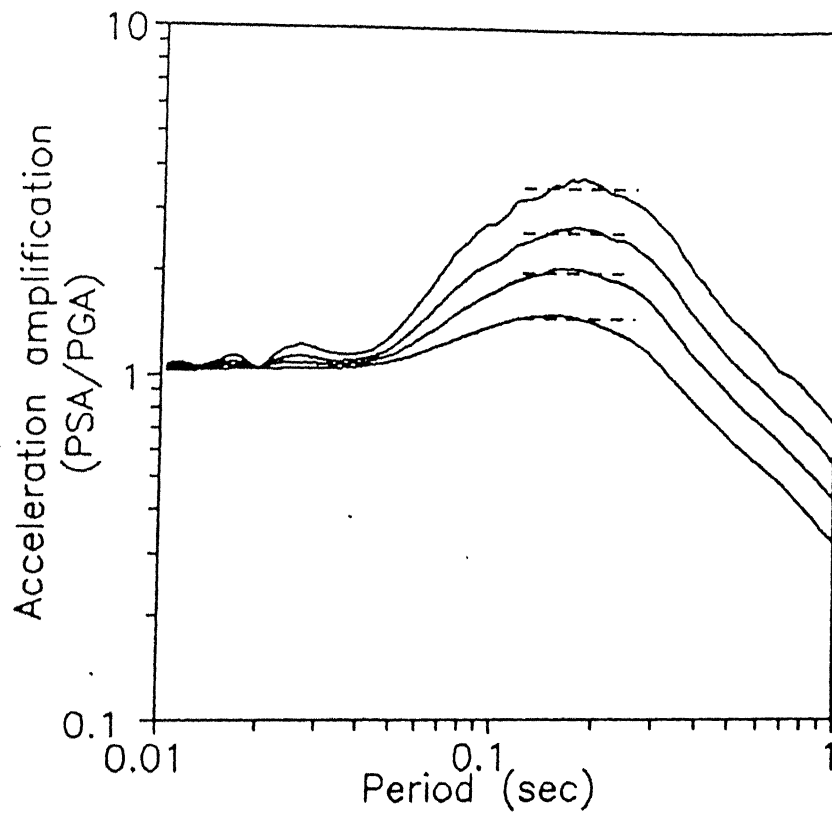
Fig. 4.29   PSA spectra for 0, 2, 5, 10, and 20% damping, indicating straight line representation in acceleration region.
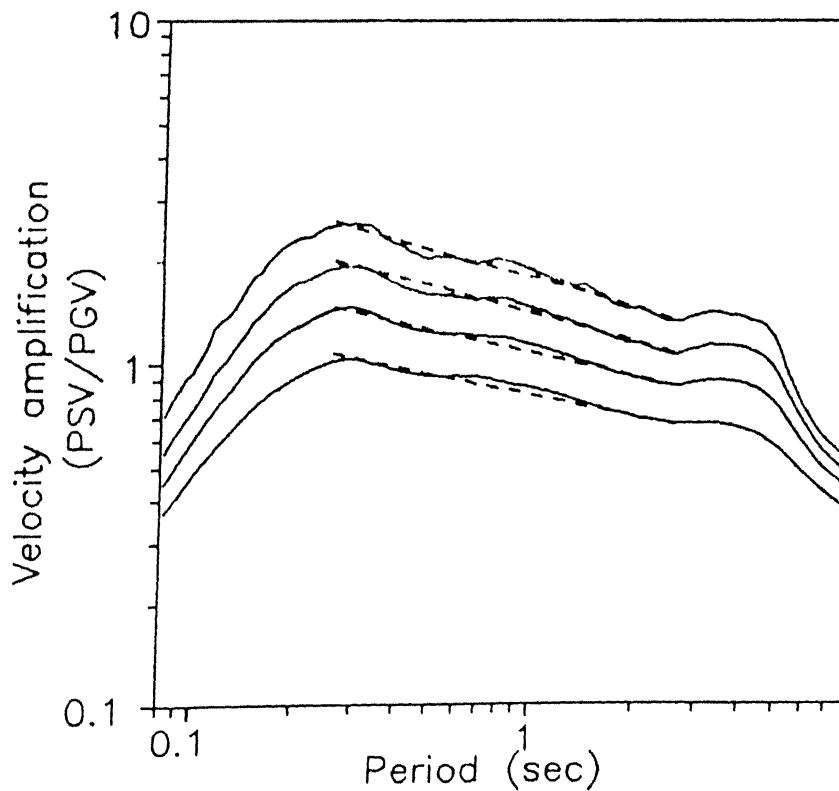
Fig. 4.30   PSV spectra for 0, 2, 5, 10, and 20% damping, indicating straight line representation in velocity region.
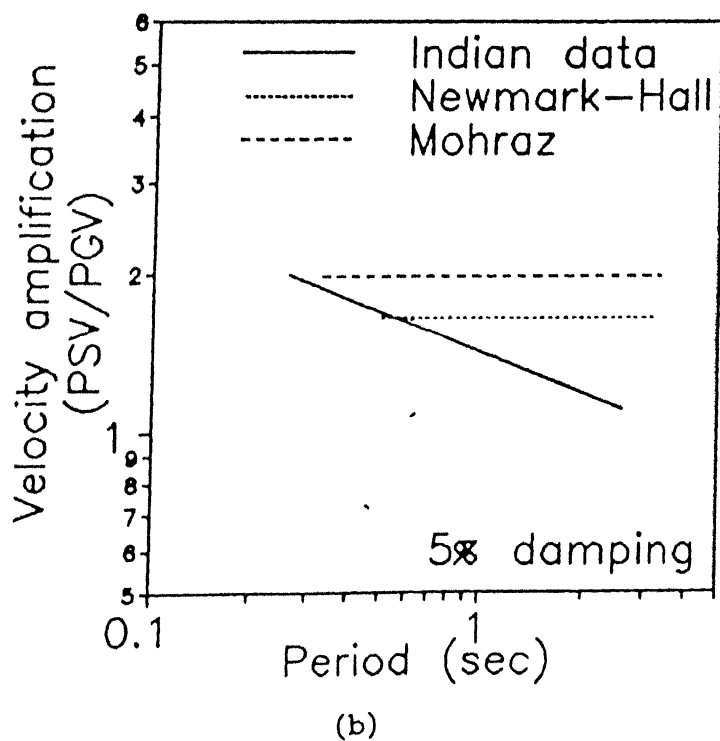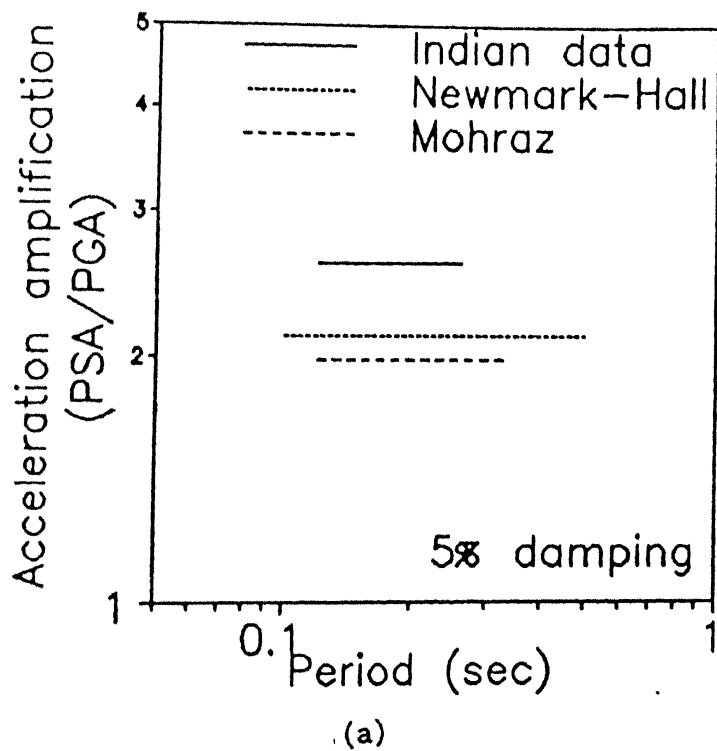
Fig. 4.31   Comparison   of   mean   amplification   factors   (a)
            acceleration   amplification   and   (b)   velocity
            amplification.
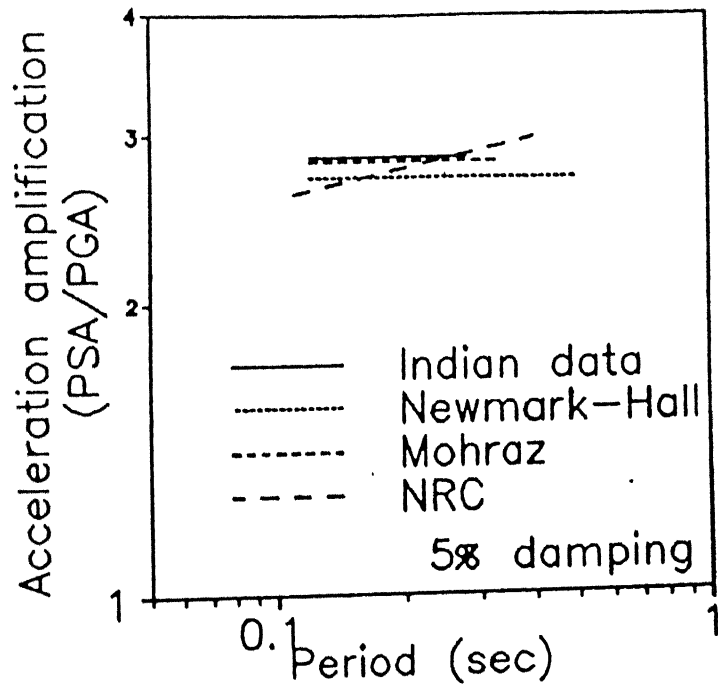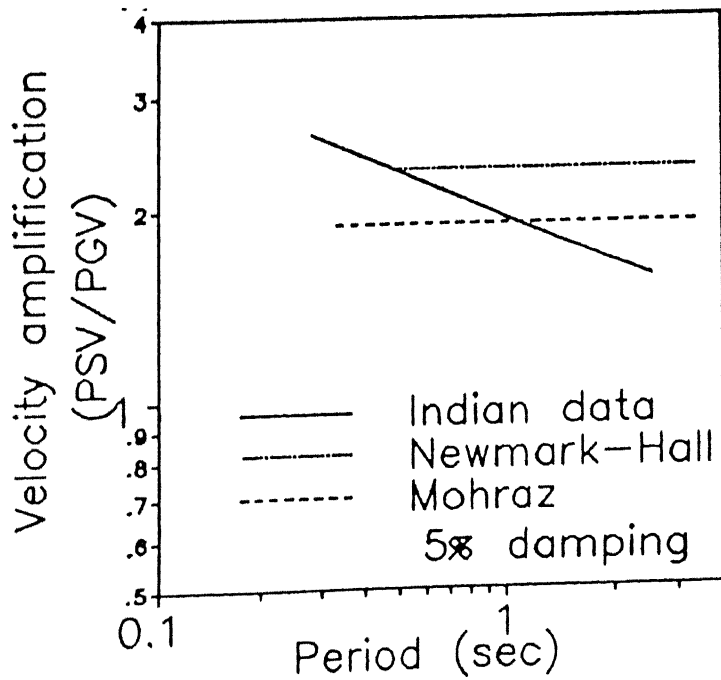
Fig. 4.32   Comparison   of   mean-plus-one-standard-deviation
amplification factors (a) acceleration amplification
and (b) velocity amplification.
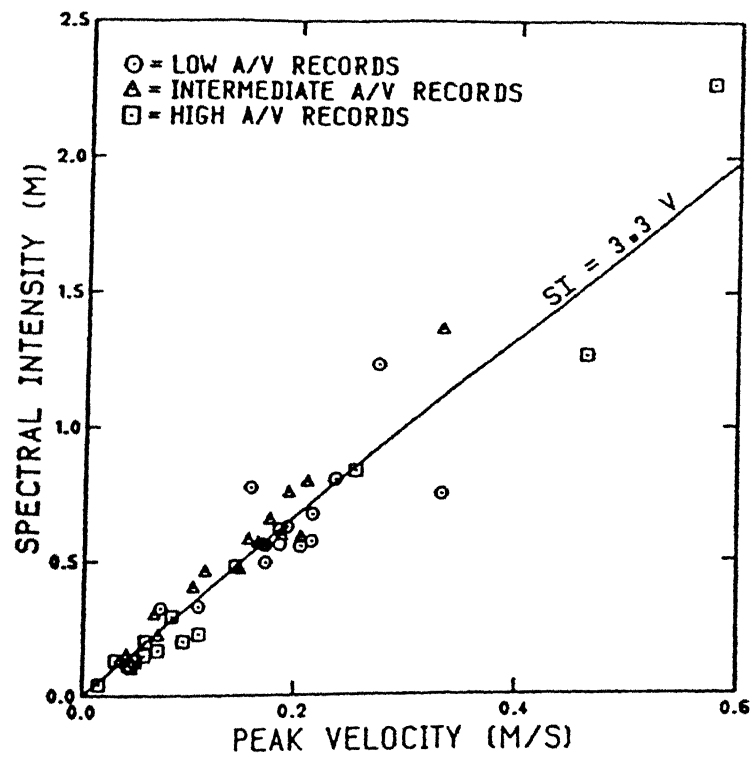
Fig. 4.33   Correlation between spectrum intensity and PGV for three groups of records having low, intermediate, and high A/V ratios.
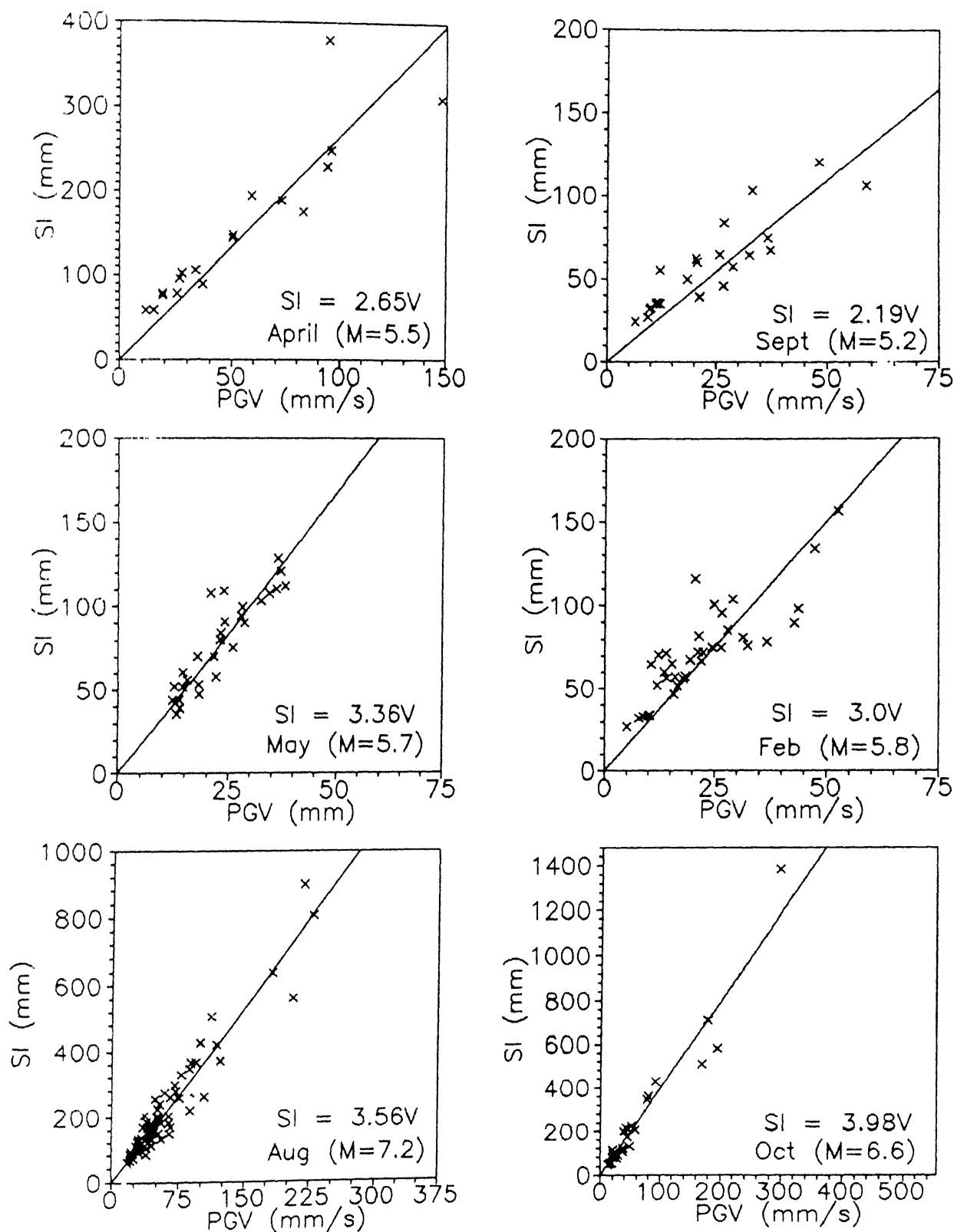
Fig. 4.34   Correlation between spectrum intensity (SI) and PGV
for the six Himalayan earthquakes.

CHAPTER V
DUCTILITY REDUCTION FACTOR

5.1 INTRODUCTION

Elastic response spectrum is obtained by assuming that the structure behaves linearly elastic even during severe earthquake ground motion. However, it will be impractical, or at least uneconomical, to design a structure to remain elastic during severe earthquake ground motion of rare occurence. Hence, the seismic design specifications for structures must incorporate the inelastic response appropriately. It is well understood and recognized that when inelastic deformations are permitted in design by providing adequate ductility, the structure can be designed for a much lower seismic force than otherwise.

The codes, particularly in the earlier years, provided for seismic design spectrum which was much lower than the elastic spectrum for the expected severe ground motion of rare occurence. Such an approach implicitly assumed the inelastic response of structure. However, the current trend of seismic code development is to prescribe a realistic level of elastic design spectrum corresponding to severe ground motion. Force obtained by this spectrum is then reduced by a "response reduction factor" (R). IS:1893-1984 still has the first approach; many recent codes (ATC-1978, UBC-1991, NEHRP-1991, etc.) have adopted the later approach. The response reduction factor primarily consists of two factors. One factor is to reduce the elastic demand force to the level of maximum yield strength of the structure; this reduction basically depends on ductility of the structure and hence on its energy dissipation capacity. This factor is called the ductility reduction

factor, R_μ. The other factor, called overstrength, is due to the overstrength inherently introduced in the code-designed structures and is defined as the ratio between the maximum lateral strength of the structure and the code prescribed unfactored design base shear force.

Fig. 5.1 shows idealized linearly elastic-perfectly plastic (EPP) global response of a building in terms of base-shear coeffecient versus roof displacement relationship during severe ground shaking. Also shown in the figure is the response of building, if it remains elastic. The maximum base shear that develops in the structure, if it were to remain elastic, is $C_{eu}W$; where W is the total weight of building. During nonlinear response, the maximum roof displacement of the structure is Δ_{max}. If the global ductility demand μ, defined as

$$\mu = \frac{\Delta_{max}}{\Delta_Y} \tag{5.1}$$

can be achieved through appropriate design and detailing of structure, then such a building needs to be designed only for maximum yield strength of C_YW, where $C_Y = \dfrac{C_{eu}}{R_\mu}$. Hence, R_μ plays an important role in evaluating the design force on a structure.

Ductility reduction factor (DRF, R_μ) depends on natural period and damping of the structure, its ductility, its load-displacement behaviour, and on the ground motion characteristics. In the present study, the structure has been assumed as a SDOF elastic-perfectly plastic (EPP) system. The value of DRF has been taken as the ratio of maximum elastic response (PSA) to the maximum inelastic response (PSA) with ductility μ for a SDOF EPP oscillator with 5% damping, i.e.,

$$R_\mu(T,\mu) = \frac{PSA \ (T, \ \zeta \ = \ 5\%)_{\mu=1}}{PSA \ (T, \ \zeta \ = \ 5\%, \ \mu)} \tag{5.2}$$

In this chapter, the value of DRF has been studied for the Himalayan ground motion records, and compared with studies available in the literature for ground motions recorded elsewhere.

5.2 REVIEW OF THE PAST STUDIES

The first attempt to relate R_μ with μ was made by Newmark and Hall (1973, 1982) for SDOF systems with EPP force-deformation model. Based on analytical studies, they concluded that:

- In structures of natural period less than 0.1 sec, ductility does not help in reducing the response. Hence, for such structures, no ductility reduction factor should be used.

- For moderate period structures, corresponding to acceleration region of elastic response spectrum (T = 0.1 to 0.5 sec), the energy absorbed by an inelastic structure at its maximum displacement approximates that absorbed by an elastic system. This results in the ductility reduction factor as (Fig.5.2a)

$$R_\mu = (2\mu - 1)^{1/2} \tag{5.3}$$

- For relatively long period structures, corresponding to velocity region (T = 0.5 to 3 sec) and displacement region (T = 3 to 10 sec) of elastic response spectrum, the maximum displacement of elastic and inelastic systems is nearly equal. This gives the value of ductility reduction factor as (Fig.5.2b)

$$R_\mu = \mu \tag{5.4}$$

Figure 5.3 shows the DRF spectra proposed by Newmark and Hall (1973).

Riddell and Newmark (1979, 1980) conducted a statistical analysis of the response of SDOF systems with elasto-plastic, bilinear, and stiffness degrading load-deformation model. For EPP, SDOF systems they obtained empirical formulae for R_μ depending on ductility (μ) and viscous damping ratio (ζ) for different period ranges. They observed that:

- The ordinates of the mean inelastic spectra do not vary significantly when various nonlinear models are used; differences occur mainly for intermediate frequencies and large ductility, and are practically negligible at the low and high frequency ends of the spectrum.

- Use of the elasto-plastic idealization provides, in almost every case, a conservative estimate of the average response to a number of earthquake motions.

- It is particularly significant that, on the average, the stiffness degradation phenomenon is not as critical as one might expect a priori.

Using ten "standard" ground motions from five different seismic events, Mahin and Bertero (1981) have computed displacement ductility demands for EPP SDOF systems designed using Newmark-Hall inelastic design response spectra with 5% damping. They concluded that displacement ductility demand on the average is less than the values specified by Newmark-Hall method. However, Newmark-Hall method becomes less conservative as the values of the specified ductility and viscous damping are increased.

Briseghella et al. (1982) have proposed a relation between μ and R_μ as a function of period based on a study of SDOF systems, for Takeda

model of load-deformation relationship. They have used artificial time histories compatible with the power spectral density of a recorded motion during the 1976 Friuli earthquake.

For EPP load-deformation relationship, Lai and Biggs (1980) have investigated the sources of variability of inelastic response spectra, due to strong motion duration, ductility, and damping. From time history analyses, they concluded that the inelastic response spectra are not significantly dependent on strong ground motion duration. However, they added that this conclusion is valid only when the strong ground motion with varying durations are compatible with the same prescribed elastic response spectrum. They also found that the Newmark-Hall procedure for predicting the inelastic response of a 5% damped EPP system is unconservative, on the other hand for 2% damping the Newmark-Hall approach predicts a conservative inelastic response. Fig. 5.3 shows the DRF spectra proposed by them.

Pal et al. (1987) have developed yield displacement spectra, constant strength spectra, constant displacement spectra, reduction factor spectra, inelastic acceleration spectra, and inelastic yield displacement spectra for three artificial and two actual earthquake time-histories using EPP, bilinear, and stiffness degrading models. They concluded that the design seismic loads for strong motion earthquake can be reduced below those required for elastic analysis by a factor of about 1.1 to 15 depending upon the time period of the structure and the desired displacement ductility. Further, the reduction factors due to stiffness degrading model are only slightly higher than those for EPP models. This can be seen in Fig. 5.5.

Miyama et al. (1988) have calculated the inelastic response of

SDOF systems for bilinear, and "origin" oriented models of load-deformation relationship. The study is based on artificial earthquake ground motions of which the target spectrum is elastic response spectrum. They have expressed R_μ as function of ductility factor, natural frequency of system, and shape of the elastic response spectra.

Riddell et al. (1989) studied non-linear behaviour of EPP SDOF system, particularly for short period range, using 53 ground motion records, and concluded that reduction factor tends to a value very close to unity for very small periods and to a constant value larger than one for periods over 0.4 sec. The idealized bilinear relation between R_μ and T for different values of ductility is shown in Fig. 5.5.

Using bilinear load-deformation relationship, Miranda (1992) has reported a statistical study on SDOF systems from 124 ground motion records from different types of site. The study shows that local site conditions significantly affect the value of R_μ. Fig. 5.7 shows the variation of ductility reduction factor with time-period for rock sites and for soft soil sites. Notice that while the plot for rock sites is R_μ versus T, for soft soil the plot is R_μ versus T/T_g. Here T_g is the predominant period of the site defined as the period corresponding to the maximum spectral velocity.

Vidic et al. (1992) state that peaks in the DRF-spectrum correspond to peaks in the elastic acceleration spectrum and that, for this reason, smooth DRF-spectra are applicable in combination with smooth elastic design spectra. Based on the response of an oscillator with Q-hysteretic model with 5% damping, they show the influence of ground motions (Fig. 5.8).

Thus, several studies (eg., Riddell et al. 1989, Vidic et al. 1992) conclude that the value of R_μ

(a) in the short period range depends on T and μ; it increases linearly with T, starting with μ = 1 and going upto $R_\mu = \mu$, and

(b) in the medium and long period range, depends on μ but is independent of T; its value is around μ.

5.3 METHOD OF ANALYSIS

DRF spectra for all the horizontal component records were obtained for SDOF, EPP systems using Newmark-beta method. The displacement ductility value chosen was 2, 3, 5, and 10. The computations were carried out for 41 values of natural periods (0.001, 0.055, 0.01, 0.02, ..., 0.09, 0.1, 0.2, ..., 3.0). Mean, mean-minus-one-standard-deviation, and coeffecient of variation (COV) of ductility reduction factors for individual events and for the average of six events have been evaluated.

5.4 RESULTS

Mean DRF spectra in the six events for displacement ductility of 2, 3, 5, and 10 are shown in Fig. 5.9. It is seen that, irrespective of the value of ductility, for very small periods, DRF is close to unity. However, for periods upto 0.2-0.3 sec, the spectral values build up and later remain fairly constant upto period of about 2.7 sec. A slight increase in DRF value is observed in the period range 2.7 to 3.0 sec.

5.4.1 Mean DRF Spectra

The mean DRF spectra for different events are compared in Fig. 5.10 for the four values of ductility. It is seen that for low ductility (less than 5) spectral shapes are quite consistent for different events with only nominal variations. However, for higher value of ductility the variation in mean DRF spectrum tends to increase. This is in line with the observation by Riddell et al. (1989), that "the inelastic response of SDOF systems with large inelastic incursions are more affected by the characteristics of accelerograms than those with small inelastic incursions".

The mean DRF spectra in "Sept" achieve an unusual peak at natural period of around 0.2 sec to 0.3 sec. However, beyond 0.4 sec the mean DRF spectra of this event are lower than thosefor all the other events. Notice that while the mean elastic spectra of this earthquake (Fig. 4.16) shows a sharp drop at natural period of around 0.4 sec, the elastic response spectra of this earthquake do not show large amplifications in the period range of 0.2 sec to 0.4 sec. Hence, the DRF spectra of this event do not reflect the elastic response spectrum characteristics; this is in contrast with the observations of Vidic et al. (1992). The DRF spectra are the highest for event "April" as compared to other events. Interestingly, the amplification factors in the acceleration and velocity regions of elastic spectra for this event are the lowest.

5.4.2 COV and Mean-Minus-One-Standard-Deviation Spectra

The coeffecient of variation in ordinates of DRF spectra, for different ductility, for the six events is shown in Fig. 5.11. The spectra is shown for period range of 0.1 to 3.0 sec. It is very clear

that the COV is higher for large value of ductility and vise versa. Also, irrespective of event, COV remains mostly between 0.2 to 0.4, for ductility value between 10 to 2. These observations can be clearly seen in Fig. 5.12, which shows the average of COV spectra from each event. This has impotant implications for design of important structures where the DRF to be used is more like mean-minus-one-standard-deviation than the mean value. Such a consideration is not being made in the profession at present.

Fig. 5.13 shows the of mean-minus-one-standard-deviation spectra in the six events. In general, shape of mean-minus-one-standard-deviation spectra is same as that of mean DRF spectra.

5.4.3 Idealisation of Mean and Mean-Minus-One-Standard-Deviation Spectra

Fig. 5.14 and Fig. 5.15 show the mean and mean-minus-one-standard-deviation spectra obtained by averaging the corresponding spectra obtained in the six events. These shapes are idealised as bilinear curves and are shown in the same figure. Similar shapes were obtained by Riddell et al. (1989) (Fig. 5.6). The relation between DRF and period for idealised shapes of mean and mean-minus-one-standard-deviation spectra can be expressed as;

$$R_\mu = 1.0 + \frac{R_\mu^* - 1}{0.2} T \qquad \text{for} \quad 0 \leq T < 0.2 \text{ sec}$$

$$R_\mu = R_\mu^* \qquad \text{for } 0.2 \leq T < 3.0 \text{ sec}$$

(5.6)

The values of R^* for ductility 2, 3, 5, and 10 are given in Table 5.1. It can be seen from Fig. 5.9, that for longer periods (T > 2.7 sec), for high ductility ($\mu \geq 5$), a slightly higher ductility reduction factorthan

that indicated by idealised shape is affordable. Thus, idealized shape in this period range is conservative.

5.5 COMPARISON OF RESULTS

Fig. 5.16 shows the idealized DRF spectra obtained from the data in comparison with the DRF spectra proposed by, Newmark and Hall (1973), Lai and Biggs (1980) and Riddell et al. (1989) studies. The figure clearly indicates that, the variation in different methods exists mostly in the period range of 0.2 to about 0.6 sec. The spectra proposed by Lai-Biggs is most conservative. The Newmark-Hall spectra matches quite well with the proposed spectra for, periods longer than 0.6 sec. But, for shorter periods the Newmark-Hall spectra is quite lower than the obtained spectra. The proposed idealised shape of DRf spectra is similar to the shape proposed by Riddell et al. (1989). However, there are some differences in the period from which R_μ becomes constant. For higher ductility ($5 \leq \mu \leq 10$), Riddell et al. suggests this period as 0.4 sec as against 0.2 sec proposed from the data. Due to this difference the slope of initial linear portion of the two bilinear curves vary.

Table 5.1 R_{μ}^{*} for mean and mean-minus-one-standard-deviation DRF spectra.

Ductility	For mean spectra	For m-σ spectra
2	2.2	1.7
3	3.2	2.2
5	4.8	3.2
10	8.7	5.2

m-σ : mean-minus-one-standard-deviation

Base Shear Coefficient
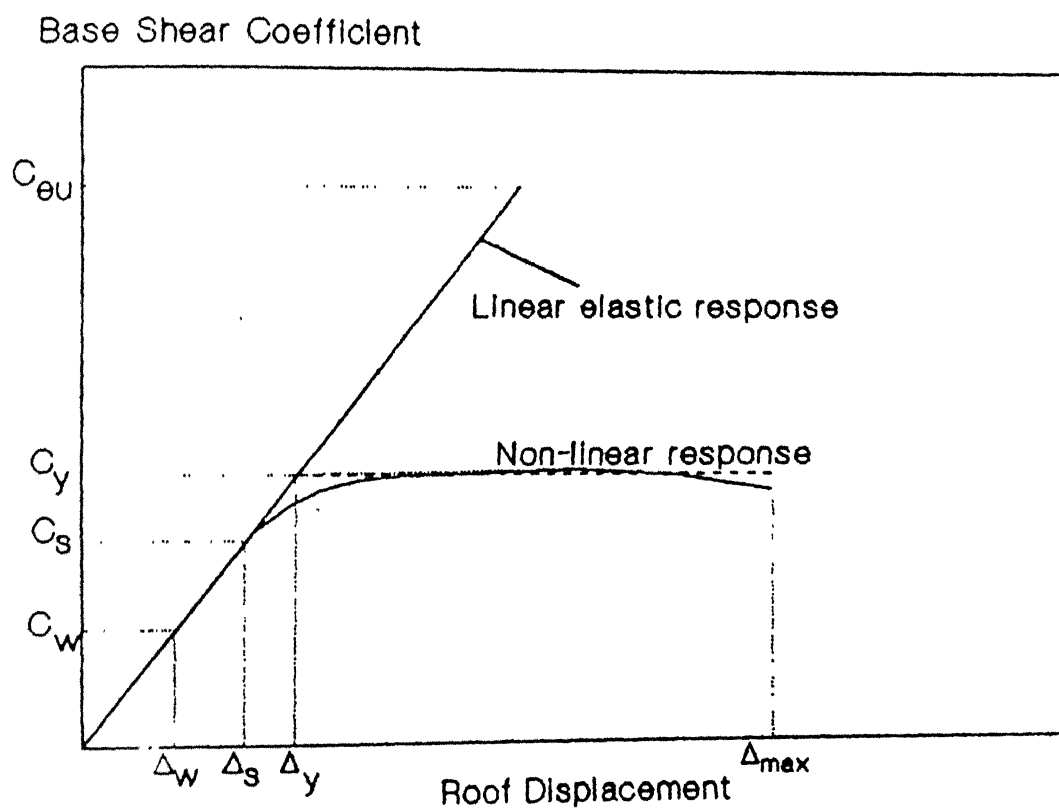
Fig. 5.1   Typical global structural response idealized as linearly elastic-perfectly plastic curve.

(a)

Lateral Inertia Load (vertical axis)

Lateral Deflection (horizontal axis)
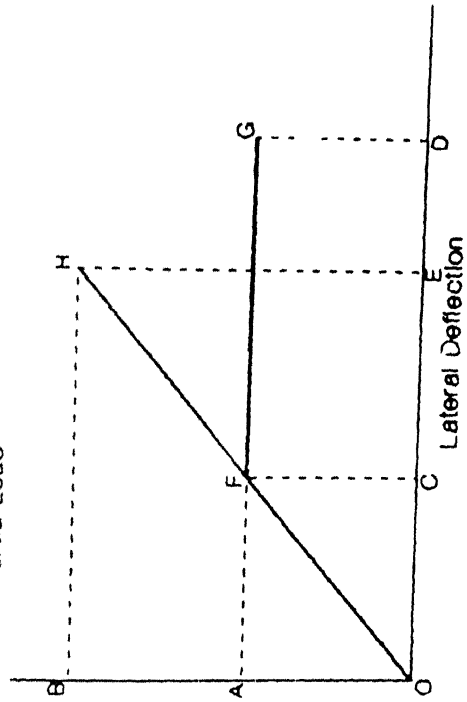
$R_\mu = \dfrac{OB}{OA}$; $\mu_s = \dfrac{OD}{OC}$

area (OHE) = area (OFGDO)

→ $R_\mu = (2\,\mu_s - 1)^{0.5}$

(b)

Lateral Inertia Load (vertical axis)

Lateral Deflection (horizontal axis)

$R_\mu = \dfrac{OB}{OA}$; $\mu_s = \dfrac{OD}{OC}$

→ $R_\mu = \mu_s$
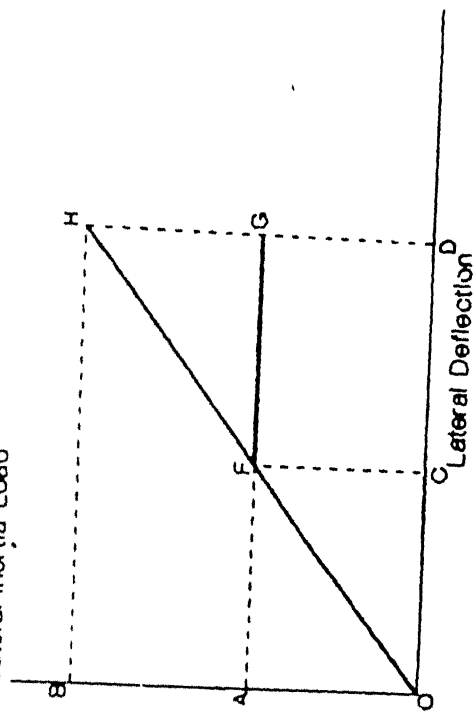
Fig. 5.2   Response of elastic and elasto-plastic structures.
(a) Equal maximum potential energy response.
(b) Equal maximum deflection response.
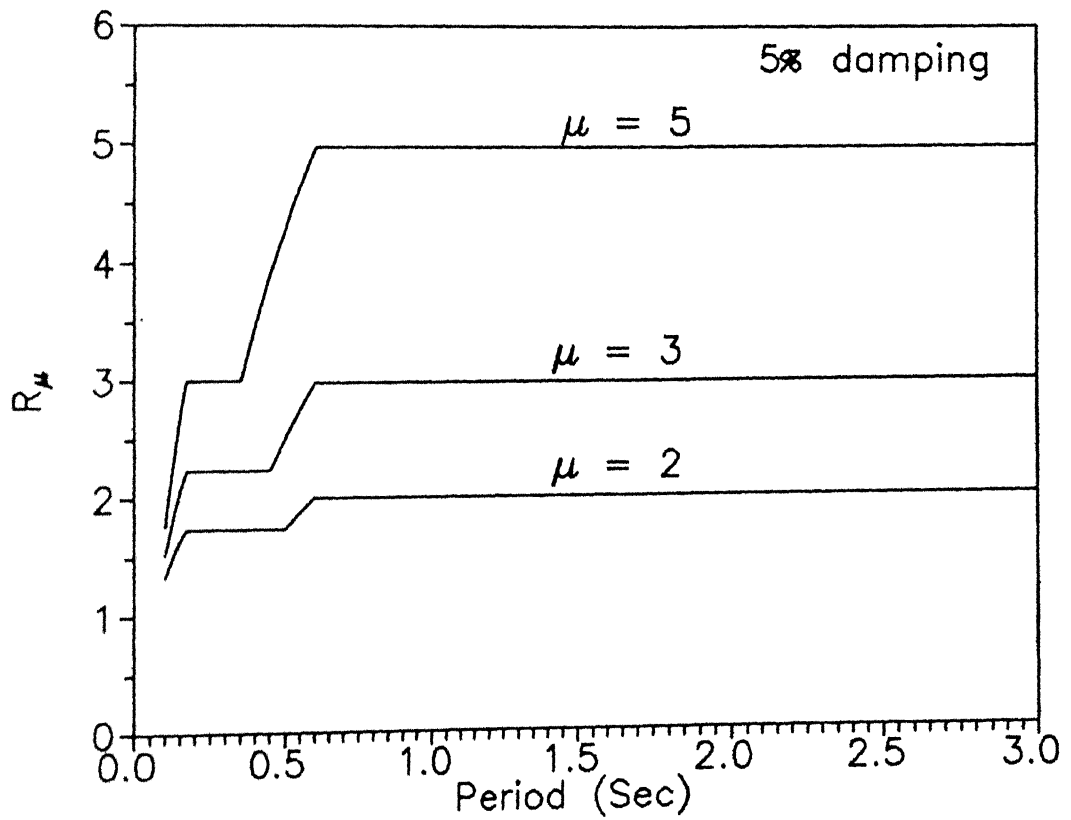
Fig. 5.3   Ductility reduction factor spectra (Newmark and Hall 1973).
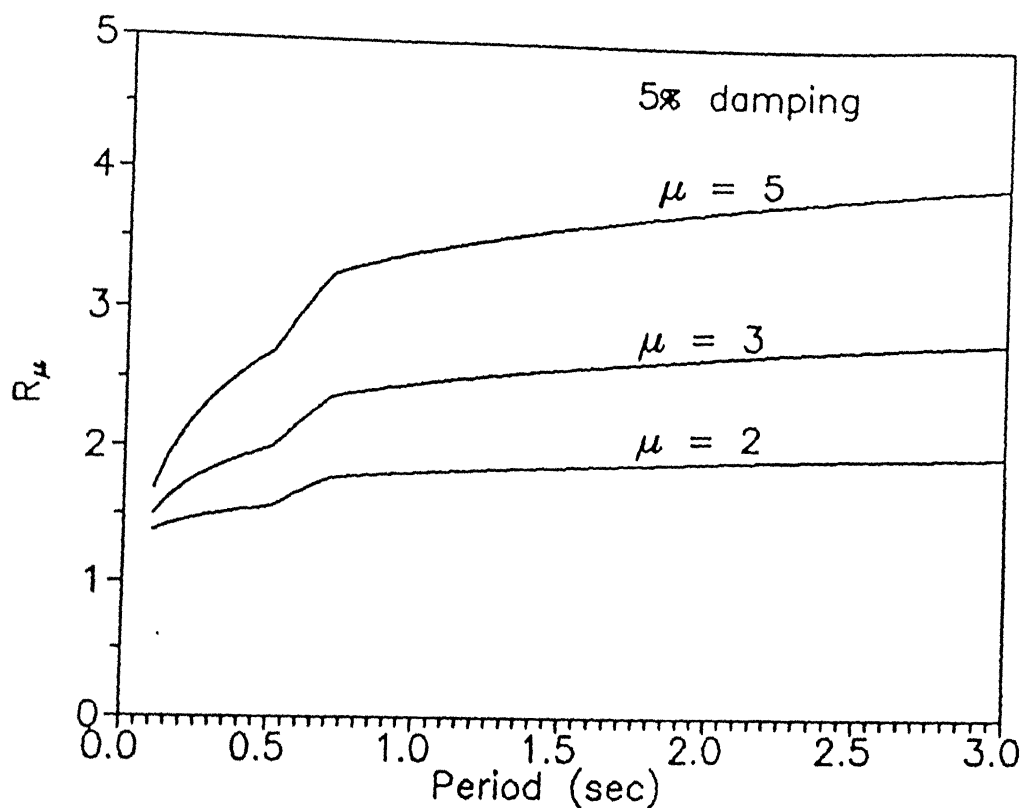
Fig. 5.4   Ductility reduction factor spectra (Lai and Biggs 1980).
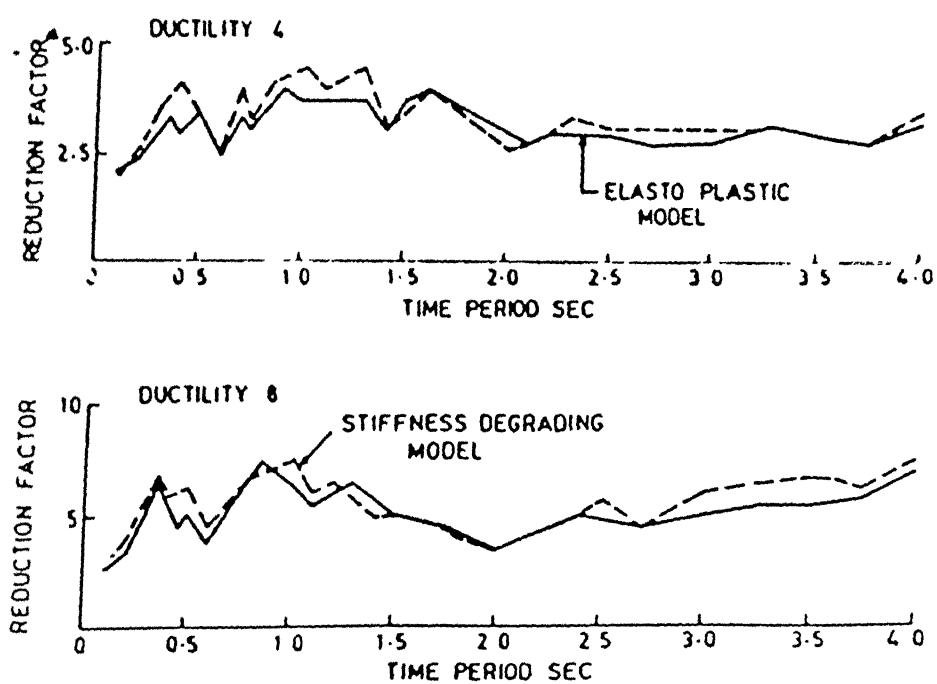
Fig. 5.5   Comparison of ductility reduction factor spectra for elasto-plastic and stiffness degrading models (Pal et al. 1987).
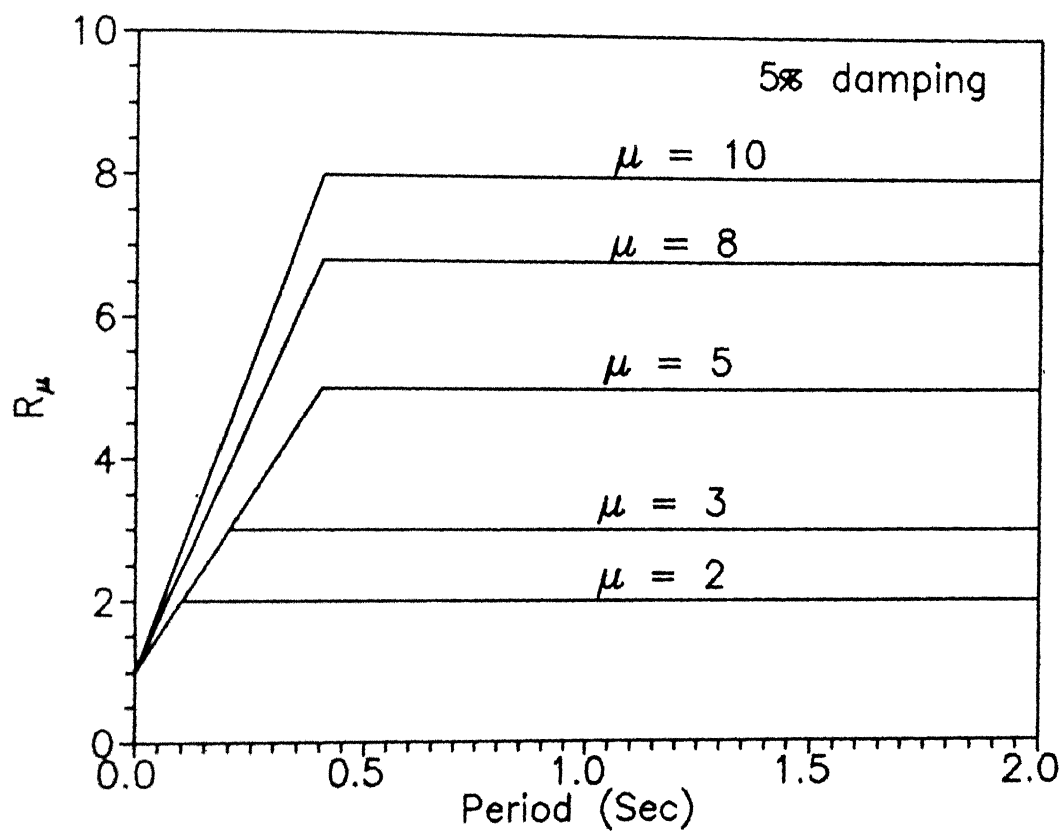
$$R_\mu = 1 + \frac{R_\mu^* - 1}{T^*} T \quad \text{for} \quad 0 < T < T^*$$

$$R_\mu = R_\mu^* \quad \text{for} \quad T \geq T^*$$

μ_s	R_μ^*	T^*
2	2.0	0.1
3	3.0	0.2
4	4.0	0.3
5	5.0	0.4
6	5.6	0.4
7	6.2	0.4
8	6.8	0.4
9	7.4	0.4
10	8.0	0.4

Fig. 5.6   Ductility reduction factor spectra (Riddell et al. 1989).
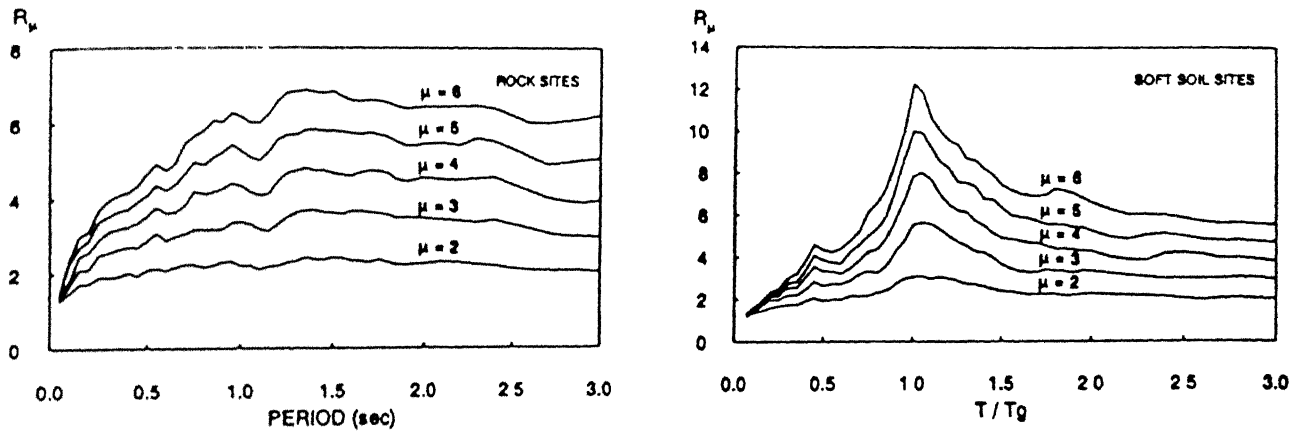
Fig. 5.7   Mean of strength reductions due to non-linear behaviour for rock sites and for soft soil sites (Miranda 1992).
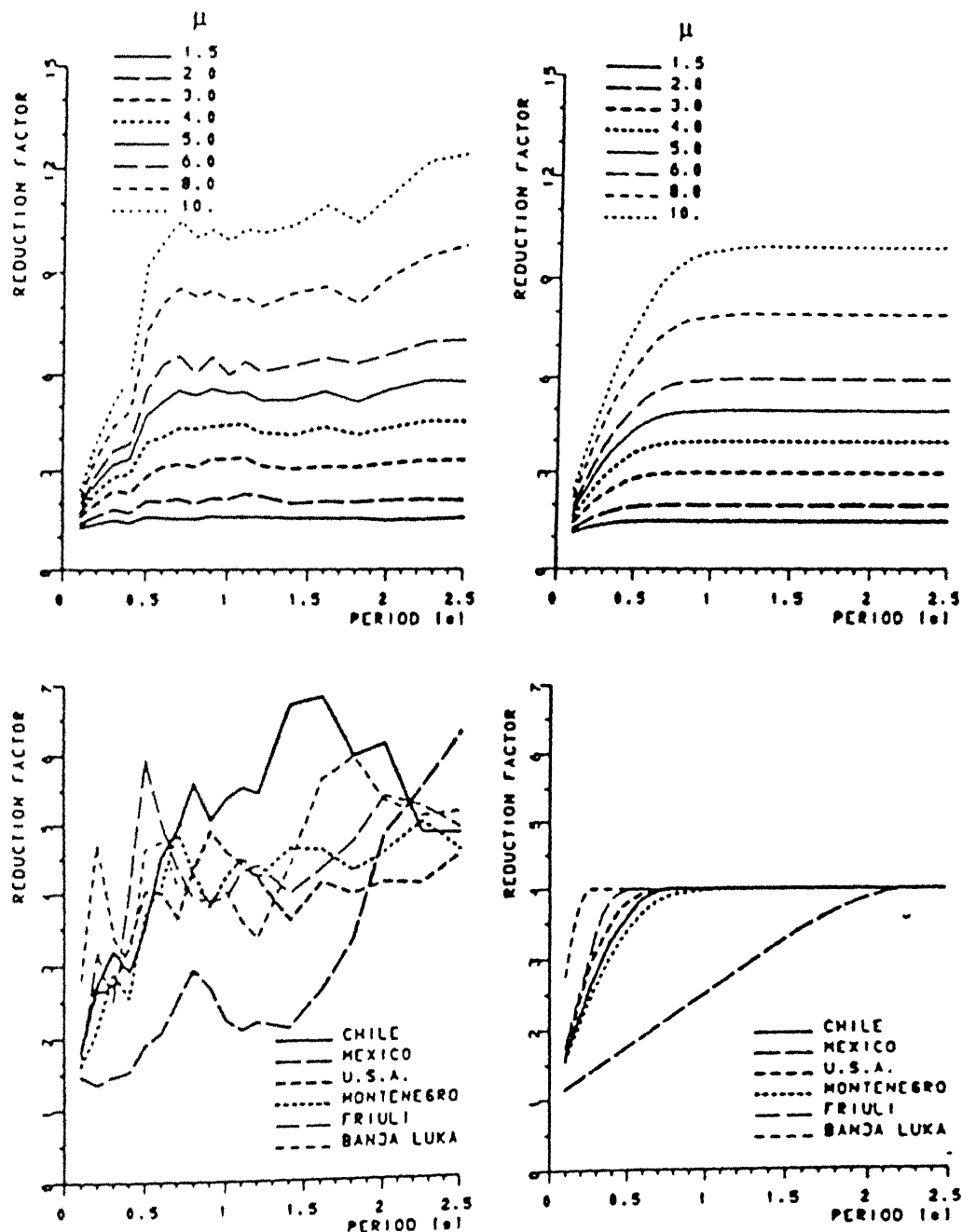
Fig. 5.8   DRF spectra.
(a) "Exact" (left hand side), "approximate" (right hand side).
(b) The influence of ductility for the group of standard records, $\mu=4$ (Vidic et al. 1992).
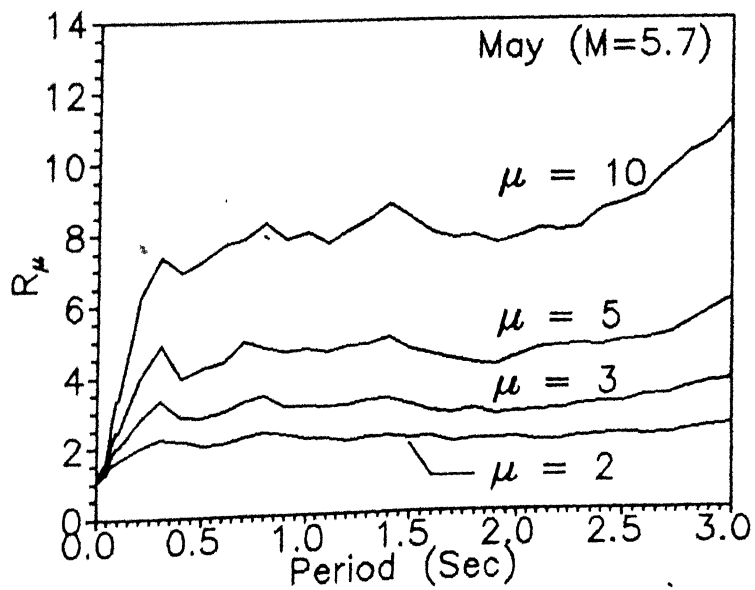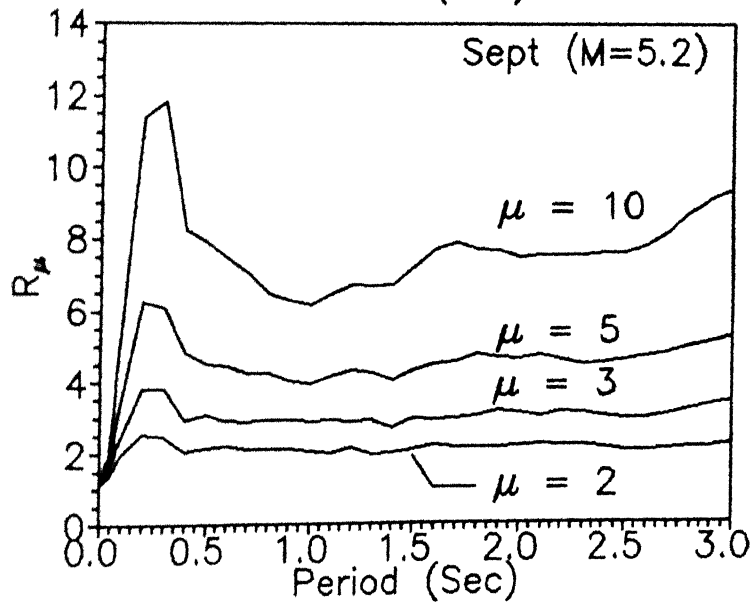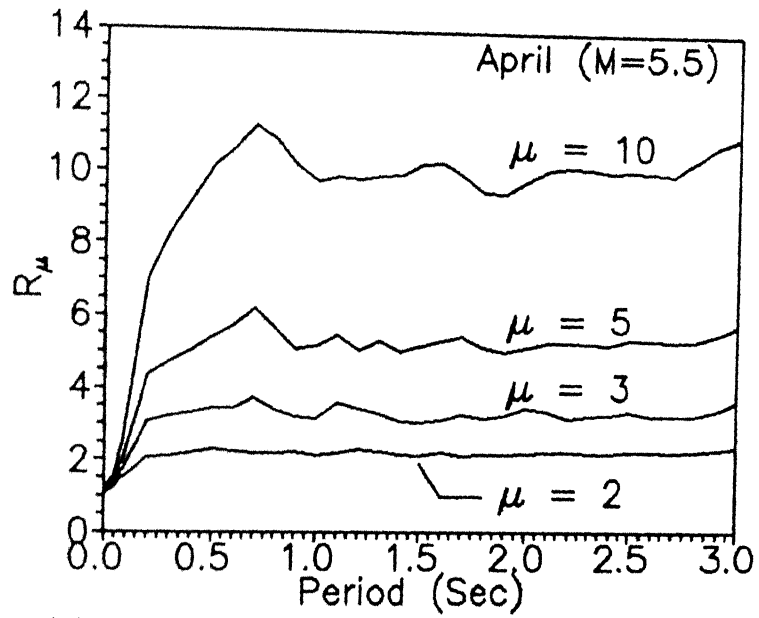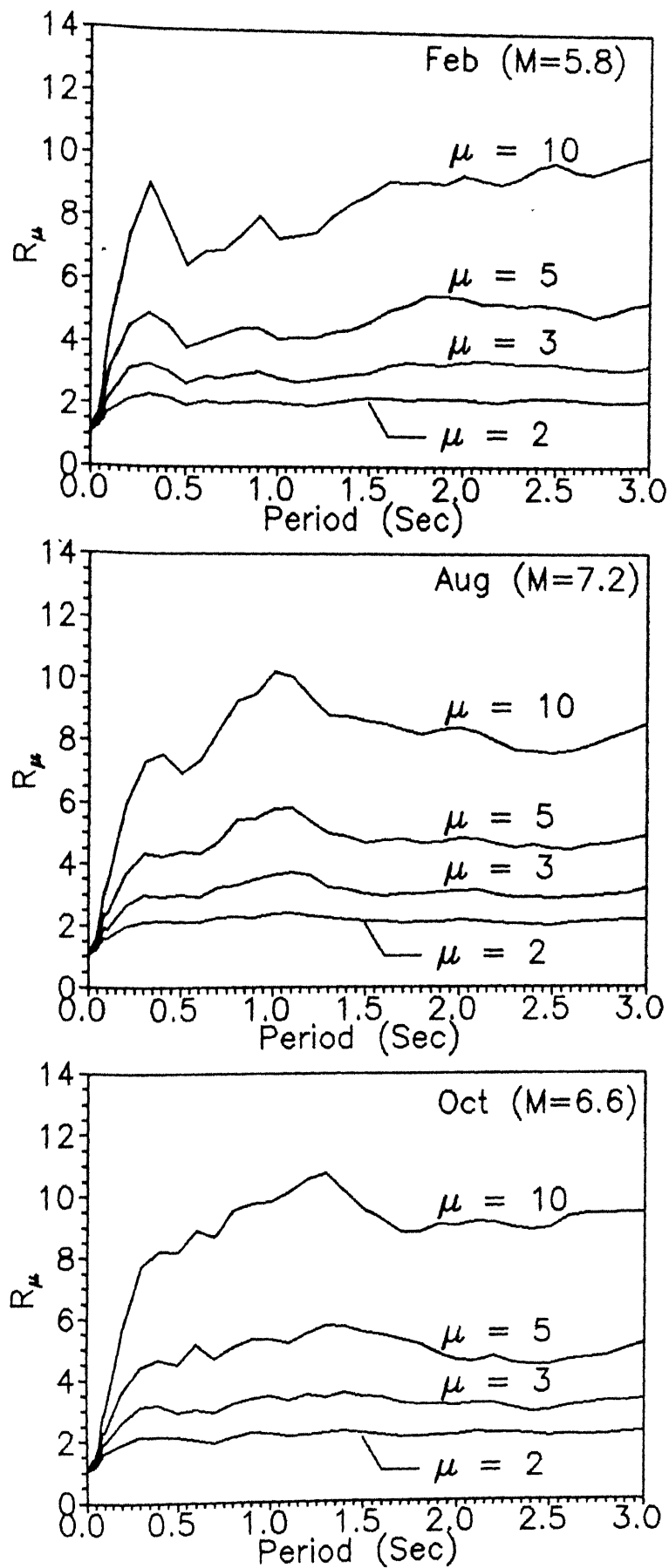
Fig. 5.9   Mean DRF spectra for 5% damping for ductility 2, 3, 5, and 10 for the six Himalayan earthquakes.
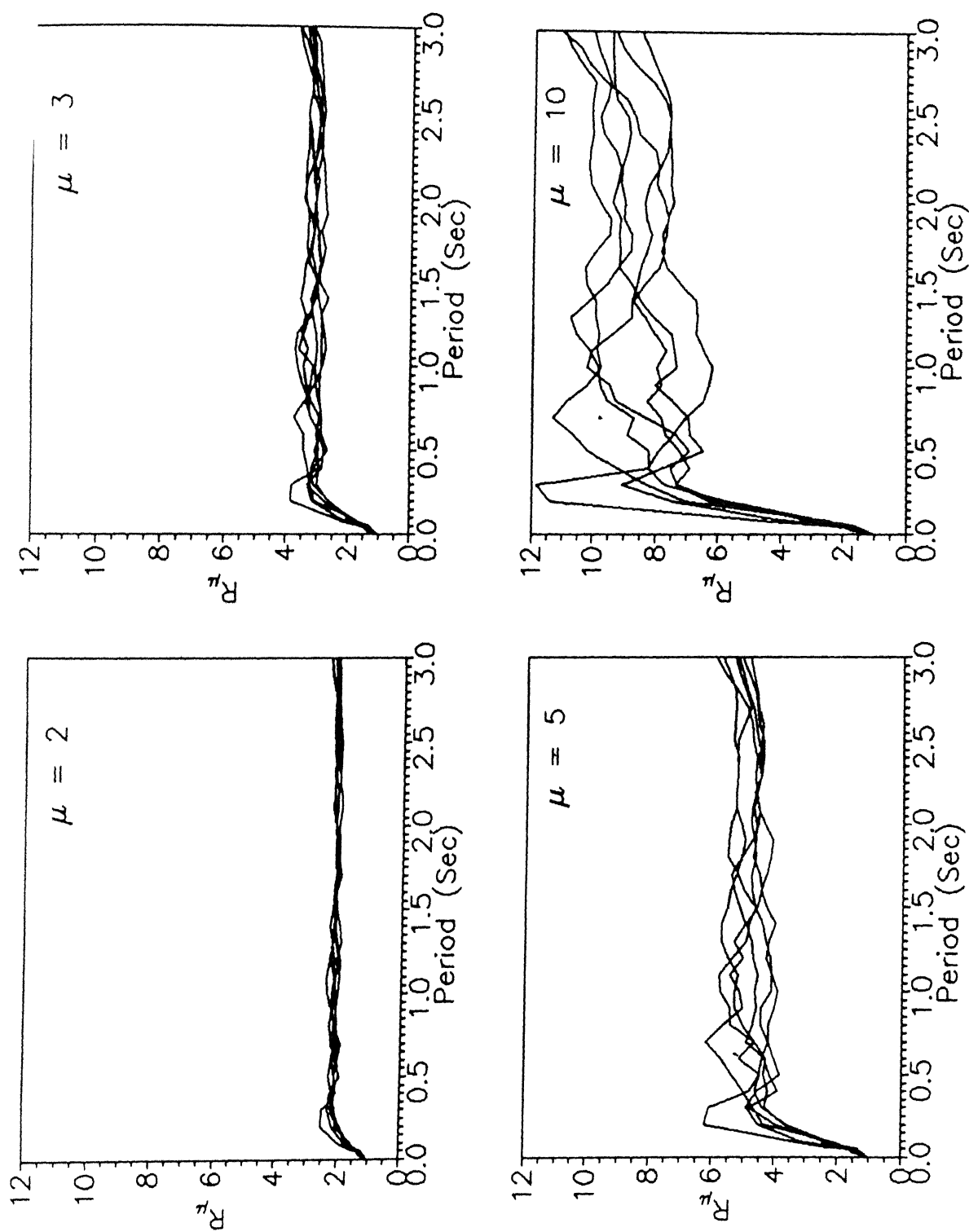
Fig. 5.10 Comparison of R_μ for each ductility for the six
Himalayan earthquakes.

April (M=5.5)

Sept (M=5.2)

May (M=5.7)
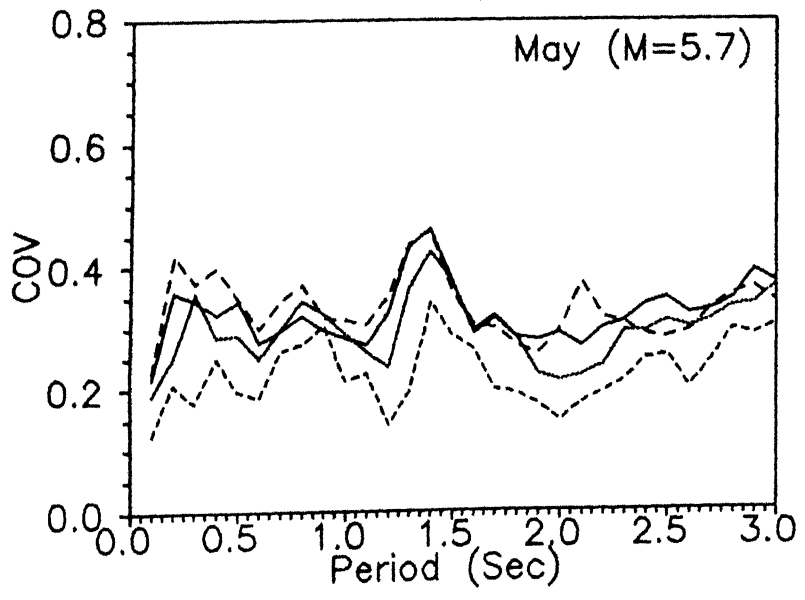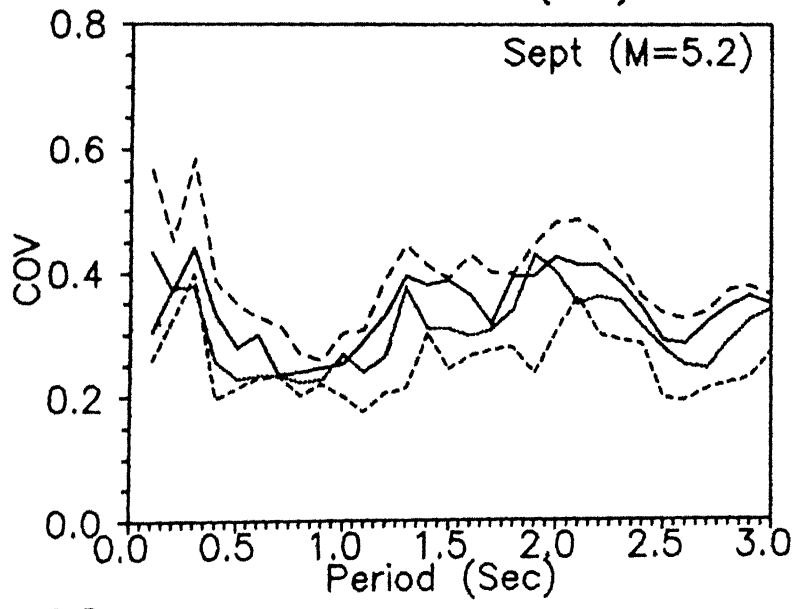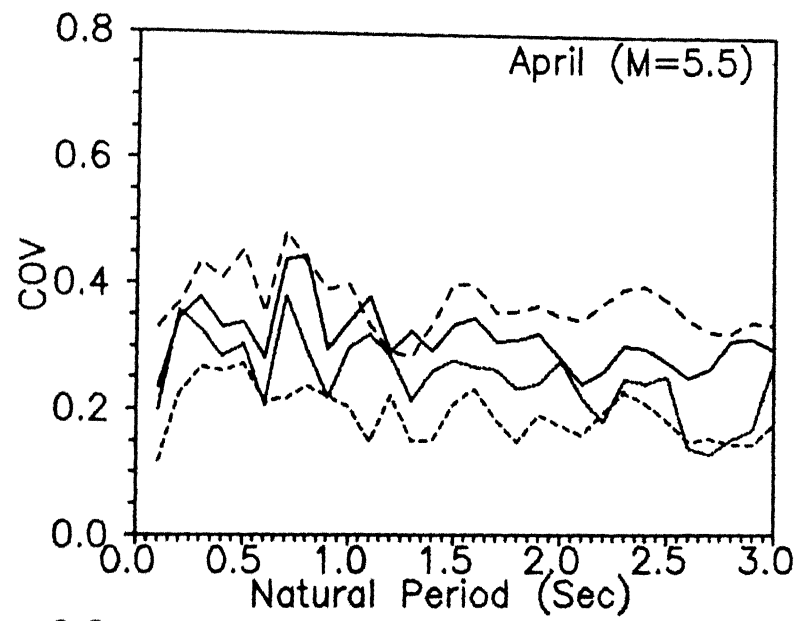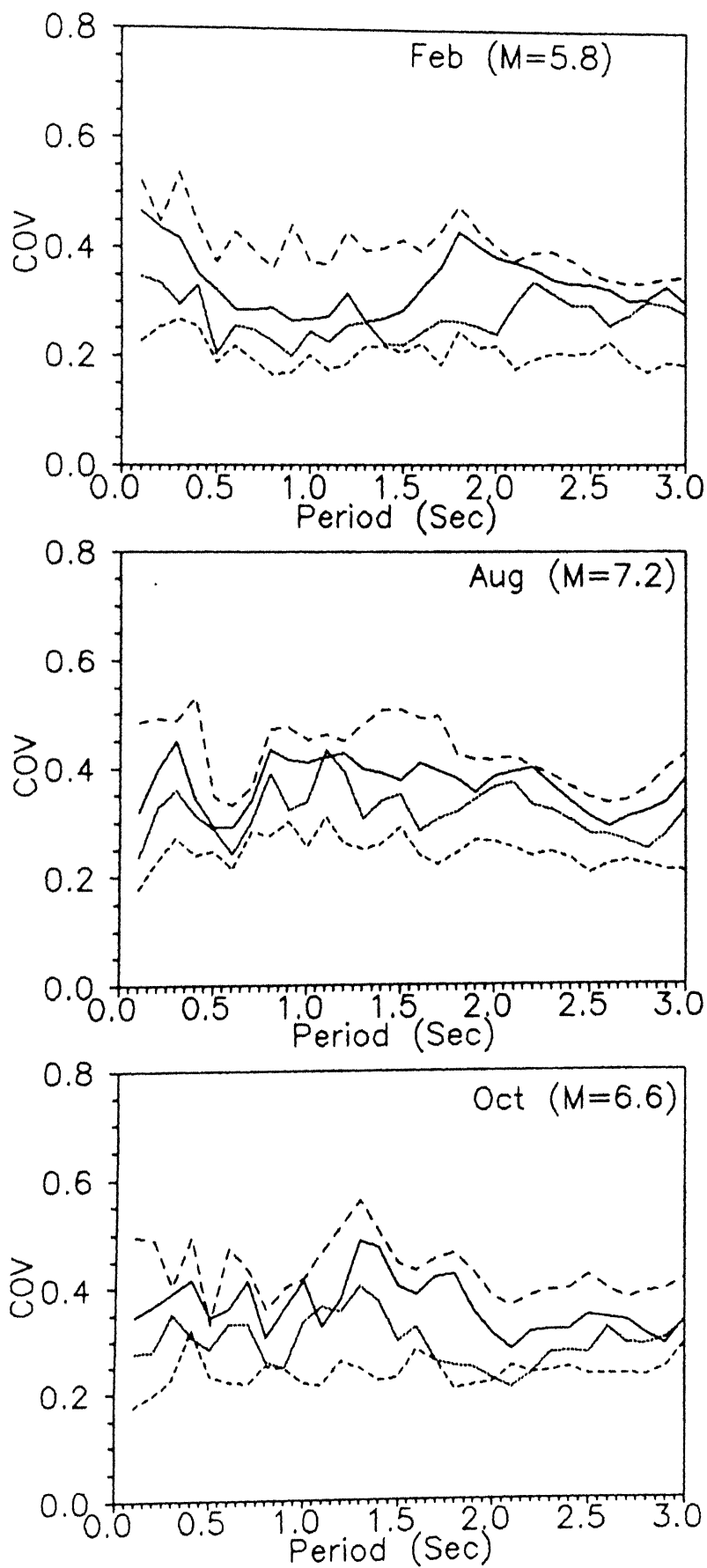
Fig. 5.11   COV of DRF spectra for the six Himalayan earthquakes.

$(\text{-----}\ \mu=10,\ \text{———}\ \mu=5,\ \text{———·——}\ \mu=3,\ \text{--------}\ \mu=2\ )$
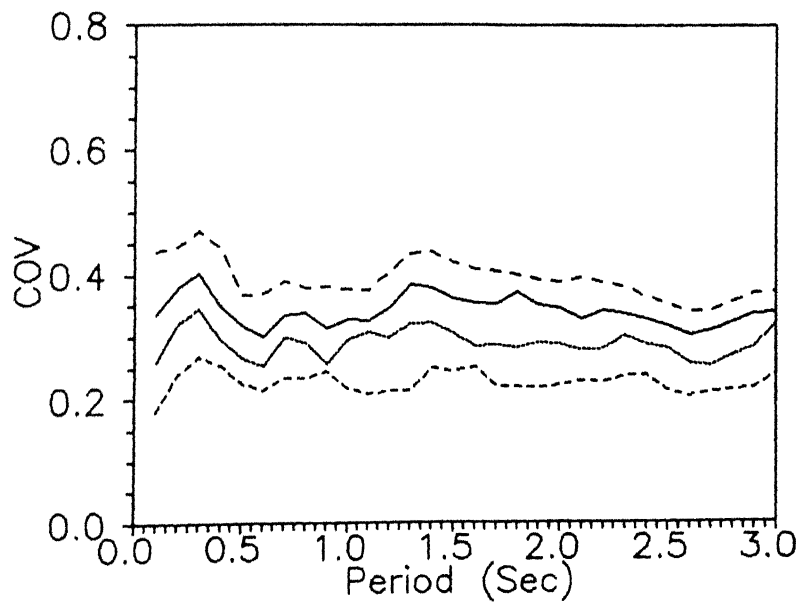
Fig. 5.12   Average COV evaluated by averaging COV of six events.

(- - - - - μ=10, ———— μ=5, ·········· μ=3, -------- μ=2)
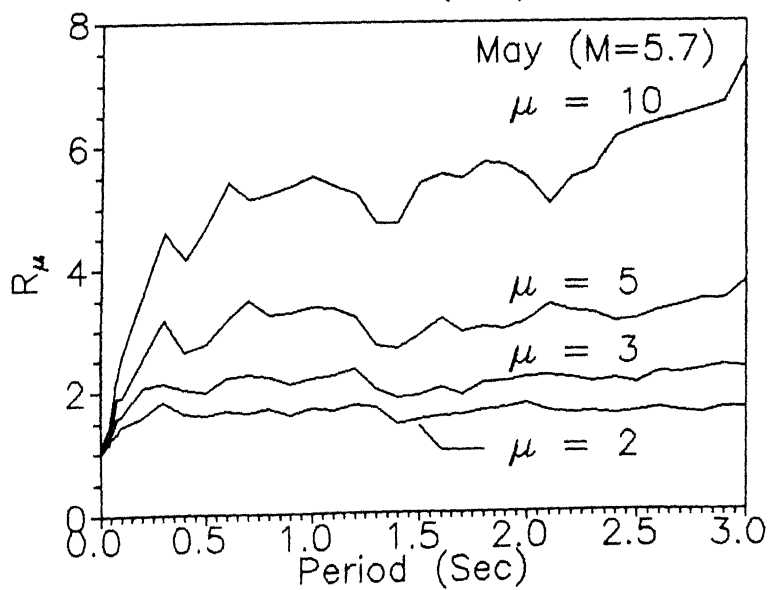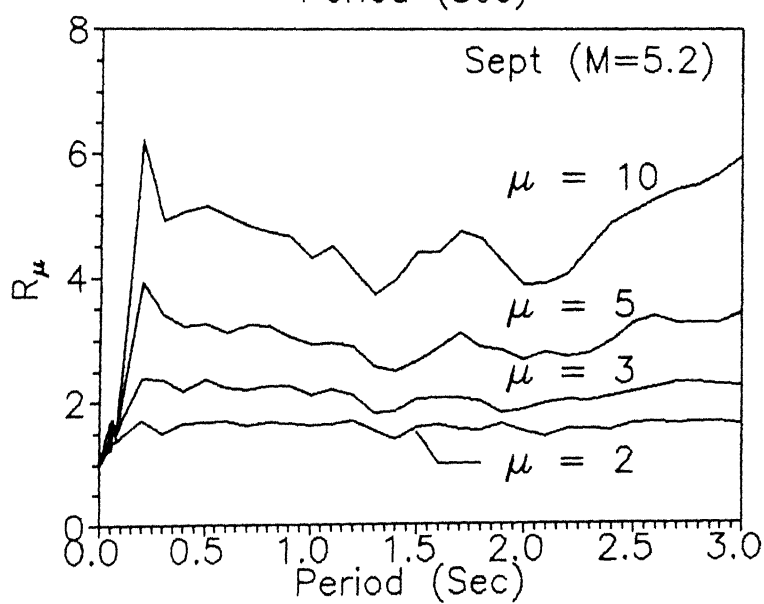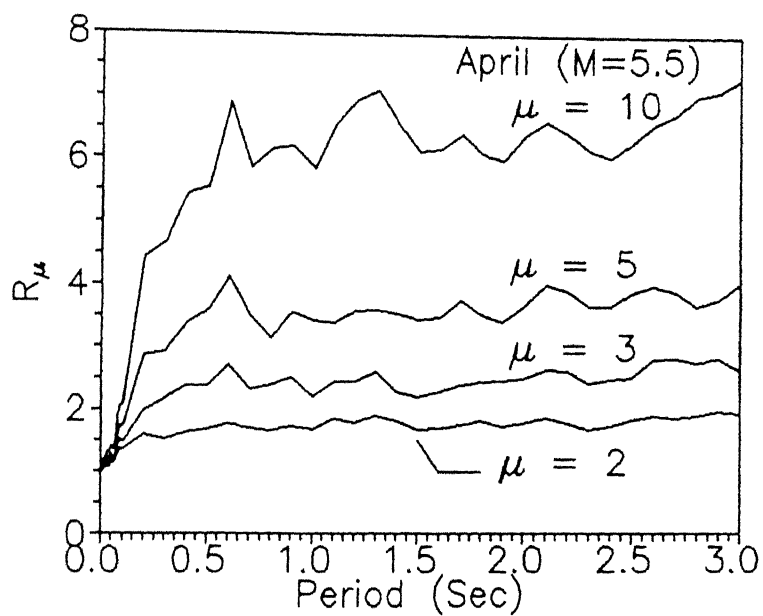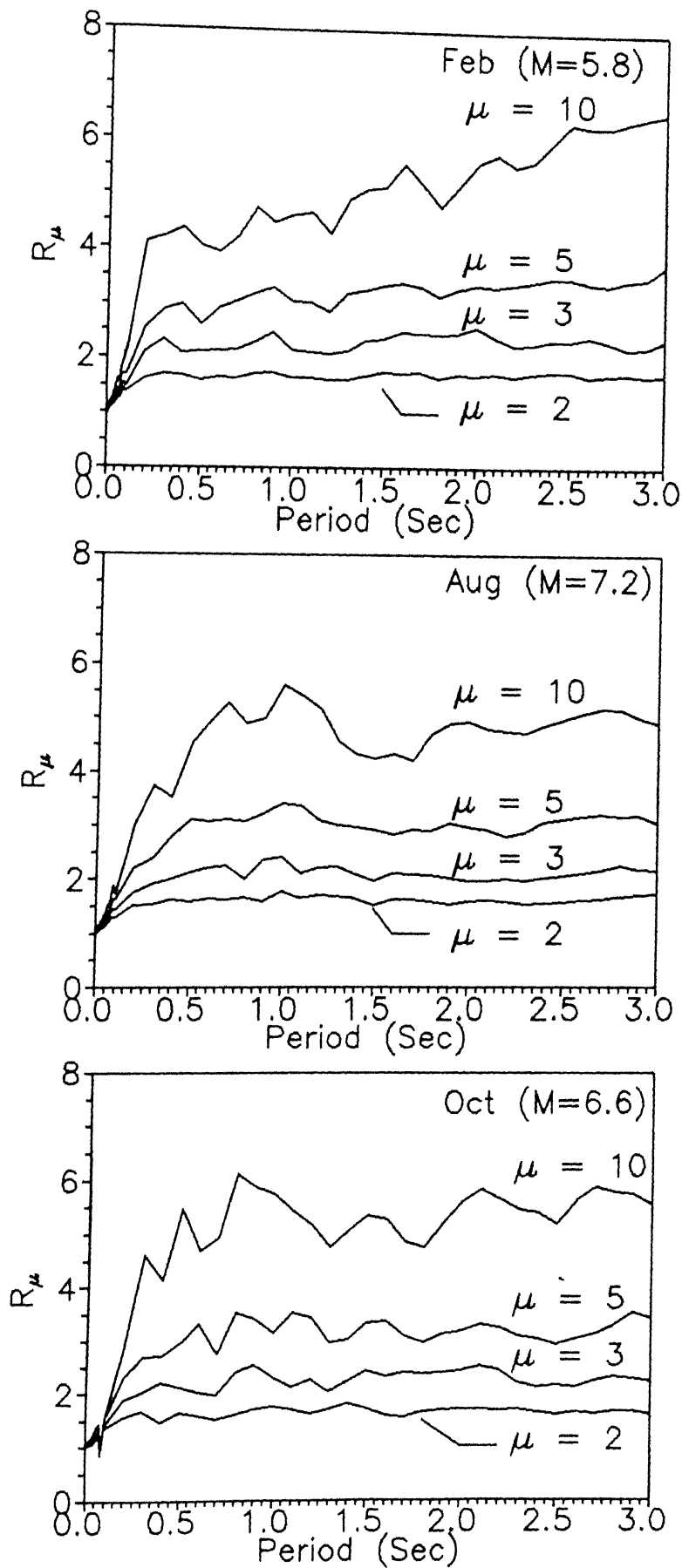
Fig. 5.13   Mean-minus-one-standard-deviation DRF spectra   for
             the six Himalayan earthquakes for 5% damping .
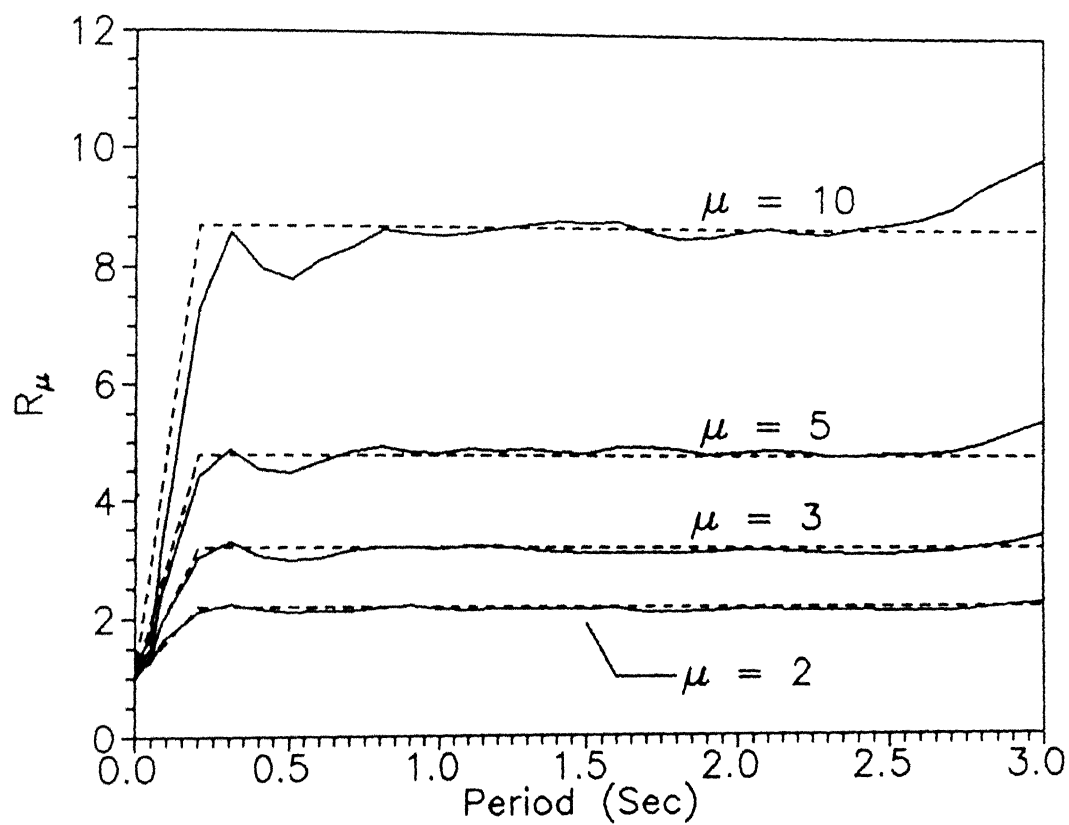
Fig. 5.14   Average mean DRF spectra for the six events and the idealized relationship.
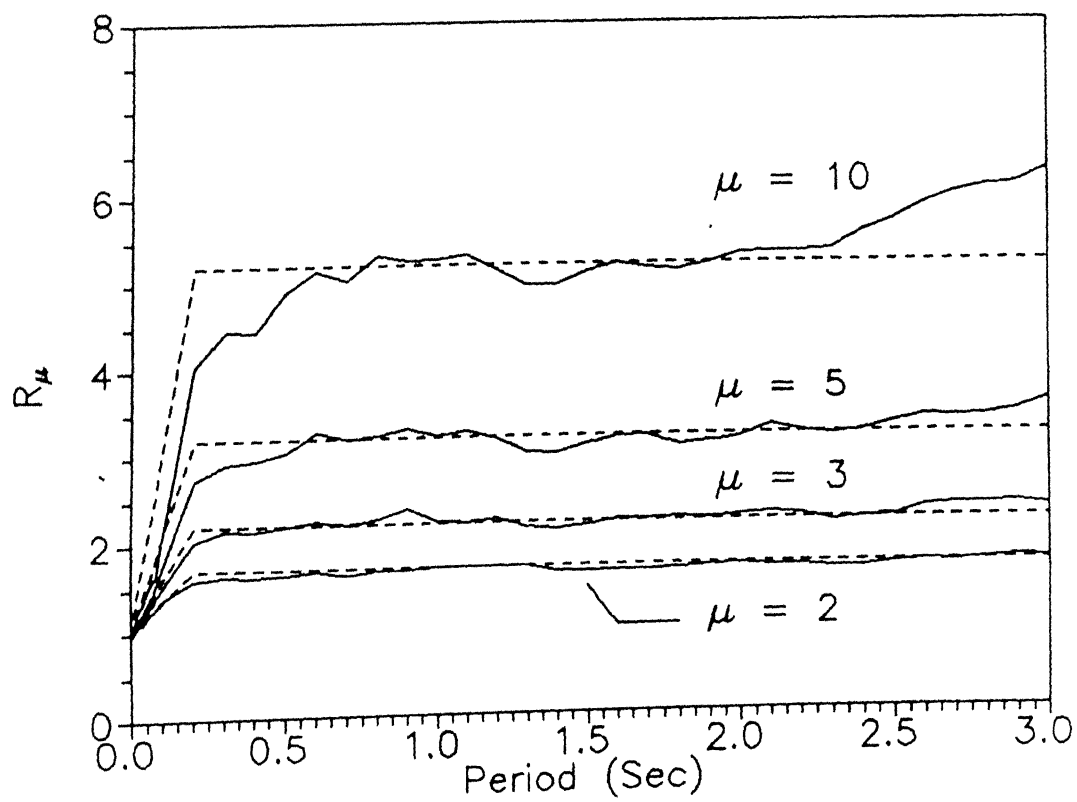
Fig. 5.15   Average mean-minus-one-standard-deviation DRF spectra for the six events and the idealized relationship.
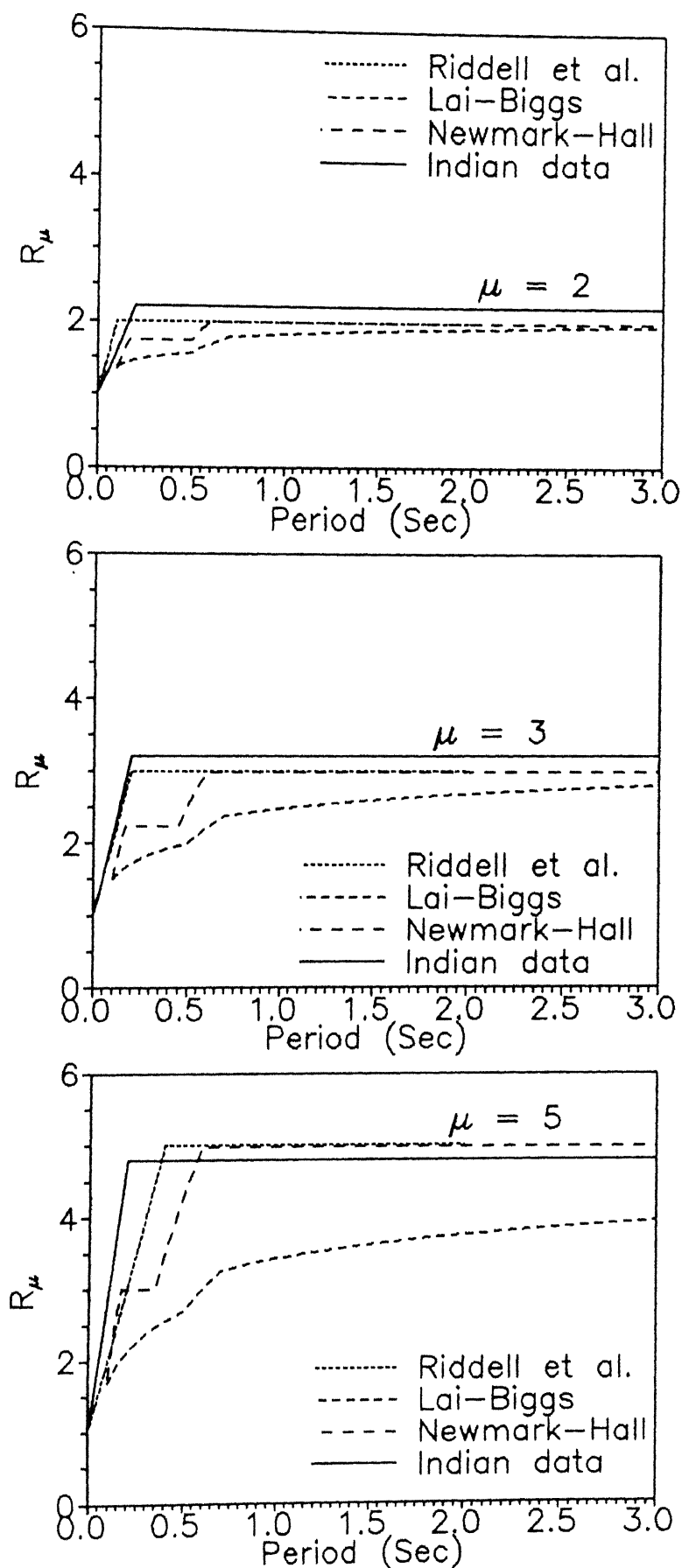
Fig. 5.16 Comparison of obtained DRF spectra with those
obtained in past studies.

CHAPTER VI
SUMMARY AND CONCLUSIONS

When formulating design criteria for aseismic design of structures, it is necessary to specify the ground motion that the structures must be designed to resist. The present knowledge in earthquake engineering and related sciences is not enough to know the exact characteristics of the future ground motion. However, data available from the past earthquakes at the site could be effectively used to estimate the earthquake ground motion in future earthquake.

In the present study, an attempt has been made to study the data available from the six Himalayan earthquakes, which occurred during 1986-1991. A data set consisting of 198 horizontal component and 99 vertical component records is used to study the ground motion characteristics such as peak parameters, duration of strong ground motion, shape of response spectrum, and ductility reduction factor. The results obtained were compared with those available from similar studies on earthquakes elsewhere, and with currently adopted design practices.

Following are the salient conclusions regarding characteristics of ground motions in the Himalayas from the six earthquakes recorded in the region:

- The A/V ratio for the ground motion in the Himalayan region is unusually high. The mean A/V is more like 20.0 sec^{-1} for rock sites; this is quite high when compared to the value of 12-15 sec^{-1} reported for earthquakes elsewhere. The mean-minus-one-standard-deviation A/V value is obtained as 12 sec^{-1}.

- The variation in A/V ratio with the distance from shock-source is

somewhat insignificant for the Himalayan earthquake ground motions. Thus, high A/V value is obtained even at large distances. This suggests that attenuation characteristics of peak ground motions in this region is different from those reported in literature.

- The mean and mean-plus-one-standard-deviation value of AD/V^2 are obtained as 4.6 and 8.0, respectively. No clear trend in variation of AD/V^2 with distance is observed.

- The mean and mean-plus-one-standard-deviation A_V/A_H value is obtained as 0.51 and 0.70, respectively. A conservative value of 0.67 or 0.75 is suggested as against the currently adopted value of 0.5 in Indian code.

- A/V is found to be good indicator of frequency content of ground motion and hence the relative shape of spectra.

- Duration of strong shaking, as evaluated by Trifunac and Brady (1975) definition, shows no definite relationship with A/V or with distance from shock-source, though such relationships are reported in literature.

- Significant variation in elastic spectral shapes in intermediate period range are observed depending on the magnitude of earthquake. Mean elastic spectral shapes for three ranges of earthquake magnitude; (1) small magnitude (M < 5.5), (2) moderate magnitude (5.5 $\leq$ M $\leq$ 6.5), and (3) large magnitude (M > 6.5) are obtained. This could be helpful in deciding the shape of design spectra.

- Spectral shapes do not vary much with distance for moderate magnitude earthquakes within moderate epicentral distances.

- Both, the ratios of peak parameters and the elastic response spectra indicate that with distance the attenuation of waves of different

frequencies is not so different as elsewhere. Hence, for projects in Himalayas, the empirical relationship for peak parameters with magnitude, epicentral distance, etc., of elsewhere are not applicable.

- The design spectral shape provided in UBC (1991) is quite conservative if applied to Himalayan earthquake ground motion as it completely envelops the obtained mean shape. The shape of design spectra currently adopted in IS:1893-1984 is quite different from the mean shape obtained from data. The code spectra underestimates the spectral ordinates in period range of 0.1 to 0.35 sec and overestimates in the period range greater than 0.35 sec. Revision of currently adopted shape in Indian code is urgently required. In order to bring the mean spectral shape of Indian code at par with the shape obtained from the data, the acceleration amplification in the period range of 0.1 to 0.35 sec may be increased, while the presently used shape for longer periods is conservative and can be kept as it is.

- Shapes of AERB "standard spectra" for rock sites and that of mean-plus-one-standard-deviation spectra from the data are in good agreement. This indicates that spectral shapes suggested by AERB are quite satisfactory for the structures which are usually designed using mean-plus-one-standard-deviation spectra.

- The acceleration amplification region mostly ranges between natural periods of 0.12-0.26 sec, while velocity region ranges between periods 0.26 to 2.6 sec. Mean acceleration amplification factor for the data is higher than that for data from earthquakes elsewhere. On the other hand, mean amplification factor in velocity region is lower. However, mean-plus-one-standard-deviation acceleration amplification from Indian data is comparable with those obtained in other studies.

- Straight line correlation between spectrum intensity and peak ground velocity are established. It is found that the slope of straight line correlating spectrum intensity with peak ground velocity increases with the increase in earthquake magnitude.

- A relationship between ductility reduction factor and time period of elasto-plastic single degree of freedom structure is proposed. Except for some difference for periods less than 0.4 sec the proposed spectra is quite similar to the one proposed by Riddell et al. (1989).

Based on the present work, following area for research in future are identified.

- A/V is an excellent indicator of frequency content. Hence, design recommendation can be based on A/V ratio. This approach is adopted by National Building Code of Canada (NBCC 1990). Hence, study of A/V ratio to work out design recommendations can be carried out.

- Amplification factors in displacement region could not be evaluated because of the unexpected shape of spectra in this region. A detailed investigation on this is needed.

- The present work on ductility reduction factor is limited to elasto-plastic single degree of freedom systems, this work could be extended for other load-deformation models and for multi degree of freedom systems.

- Now better strong motion instrumentation is available, to make full use of it the ground motion parameters like magnitude, location of epicentre, etc., are needed with better precision. This will be very helpful in developing the attenuation characteristics of the peak ground motion parameters.

- In India, detailed studies on analysis of available strong motion data

are only few, so many other parameters and characteristics could be studied so that one could reach to the current state-of-art in California or Japan.

REFERENCES

Anderson, J. C., 1989, Dynamic Response of Buildings, The Seismic Design Handbook, Chapter III, Edited by Farzad Naeim, Van Nostrand Reinhold, New York.

ATC 3-06, 1978, Tentative Provisions for the Development of Seismic Regulations, Applied Technology Council, Palo, Alto, California, USA.

Bathe, K. J., and Wilson, E. L., 1978, Numerical Mothods in Finite Element Analysis, Prentice-Hall, Englewood Cliffs, New Jersey.

Blume, J. A., Sharpe, R. L. and Dalal, J. S., 1972, Recommendations for Shape of Earthquake Response Spectra, John A. Blume and Associates, San Francisco, California, Atomic Energy Commission (AEC) Report, WASH-1254.

Bolt, B. A., 1973, Duration of Strong Ground Motion, Proceedings of the Fifth World Conference on Earthquake Engineering, Rome, Italy, pp. 1304-1313.

Briseghella, L., Zaccaria, P. L., and Giuffre, A., 1982, Inelastic response spectra, Preoceedings of the Seventh Symposium on Earthquake Engineering, University of Roorkee, India, Vol.I, pp. 159-162.

Chandrashekaran, A. R., and Das, J. D., 1990, Strong Motion Arrays in India Characterstics of Recent of Recent Recorded Events, Bulletin of the Indian Society of Earthquake Technology, Vol. 27, No. 1, pp. 1-66.

Chandrashekaran, A. R., and Das, J. D., 1992, Analasis of Strong Motion Accelerograms of Uttarkashi Earthquake of October 20, 1991, Bulletin of the Indian Society of Earthquake Technology, Vol. 29, No. 1, pp. 35-55.

Esteva, L., Rascon, O. A., and Gutierrez, A., 1969, Lessons from some Recent Earthquakes in Latin America, Proceedings of the Fourth world Conference on Earthquake Egnineering, Santiago, Chile, Vol. 3, J-2, pp. 58-73.

Gupta, A. K., 1990, Response Spectrum Method in Seismic Analysis and Design of Structures, Blackwell Scietific Publications.

Hays, W. W., 1980, Procedure for Estimating Earthquake Ground Motions, Geological Survey Professional Paper 1114, U.S Government Printing Office, Washington.

Housner, G. W., 1959, Behaviour of Structures During Earthquakes, Journal of Engineering Mechanics Division, Proceedings, ASCE, Vol.85, EM4, pp. 109-129.

Housner, G. W., 1970, Strong Ground Motion, Earthquake Engineering, Chapter IV, R. L. Wiegle, Prentice-Hall, Englewood Cliffs, New Jersey.

Housner, G. W., and Jennings, P. C., 1982, Earthquake Design Criteria, Earthquake Engineering Research Institute, California, Berkeley, CA.

IS:1893-1984, Indian Standard Criteria for Earthquake Resistant Design of Structures, Bureau of Indian Standards, New Delhi.

Iwan, W. D., 1978, Strong-Motion Earthquake Instrument Arrays, Proceedings of the International Workshop on Strong-Motion Earthquake Instrument Arrays in Honolulu, Hawai.

Lai, S. P., and Biggs, J. M., 1980, Inelastic Response Spectra for Aseismic Building Design, Journal of the Structural Division, ASCE, Vol. 106, No. ST6, pp. 1295-1310.

Mahin, S. A., and Bertero, V. V., 1981, An Evaluation of Inelastic Seismic Design Spectra, Journal of the Structural Division, ASCE, Vol. 107, No. ST9, pp. 1777-1795.

McCann, N. W., and Shah, H. C., 1979, Determining Strong-Motion Duration of Earthquakes, Bulletin of Seismological Society of America, Vol.69, pp. 1253-1265.

Miranda, E., 1992, Nonlinear Response Spectra for Earthquake Resistant Design, Proceedings of the Tenth World Conference on Earthquake Engineering, Madrid, Spain, Vol. X, pp. 5835-5840.

Miyama, T., Kanda, J., and Iwadaski, R., Inelastic Response Spectra for Typical Hysteresis Systems Calculated from Elastic Response Spectra, Proceedings of the Ninth World Conference on Earthquake Engineering, Tokyo-Kyoto, Japan, Vol. V, pp. 153-158.

Mohraz, B., Hall, W. J., and Newmark, N. M., 1972, A Study of Vertical and Horizontal Earthquake Spectra, Nathan M. Newmark Consulting Engineering Services, Urbana, Illionos, Atomic Energy Commission (AEC) Report, WASH-1255.

Mohraz, B., 1976, A Study of Earthquake Response Spectra for Different Geological Conditions, Bulletin of Seismological Society of America, Vol.66, No. 3, pp. 915-935.

Mohraz, B., 1978, Influence of the Magnitude of the Earthquake and the Duration of Strong Motion on Earthquake Response Spectra, Proceedings, Central American conference on Earthquake Engineering, San Salvadore, El Salvador.

Mohraz, B., and Elghadamsi, F. E., 1989, Earthquake Ground Motion and Response Spectra, Chapter II, The Seismic Design Handbook, Edited by Farzad Naeim, Van Nostrand Reinhold, New York.

Mohraz, B., and Tiv, M., 1991, Spectral shapes and amplifications for the Loma Prieta earthquake of October 17, 1989. Proceedings, 3rd U.S. Conference Lifeline Earthquake Engineering, Los Angeles, California, pp. 562-571.

Newmark, N. M., and Hall, W. J., 1969, Seismic Design Criteria for Nuclear Reactor Facilities, Proceedings of the Fourth World Conference on Earthquake Engineering, Santiago, Chile, B-4, pp. 37-50.

Newmark, N. M., and Rosenblueth, E., 1971, Fundamentals of Earthquake Engineering, Prentice-Hall, Englewood Cliffs, New Jersey.

Newmark, N. M., and Hall, W. J., 1982, Earthquake Spectra and Design, Earthquake Engineering Research Institute, Berkeley, CA.

Newmark, N. M., and Hall, W. J., 1973, Procedure and Criteria for Earthquake Resistant Design, Building Practices for Disaster Mitigation, Building Science Series 46, U.S. Department of Commerce, National Bureau of Standards, Washignton, DC, February 1973.

Page, R. A., Boore, D. M., Joyner, W. B., and Caulter, H. W., 1972, Ground Motion Values for use in the Seismic Design of the Trans-Alaska Pipeline System, U. S. Geological Survey Circular No. 672.

Pal, S., Dharaka, S. S., and Jain, A. K., 1987, Inelastic Response Spectra, Computers and Structures, Vol. 25, No. 3, pp. 335-344.

Riddell, R., and Newmark, N. M., 1979, Statistical Analysis of the Response of Nonlinear Systems Subjected to Earthquakes, Structural Research, Series No. 468, University of Illinois, Urbana, Illionois.

Riddell. R., Hidalgo, P., and Cruz, E., 1989, Response Modification Factors for Earthquake Resistant Design of Short Period Buildings, Earthquake Spectra, Vol. 5, No. 3, pp. 571-590.

S-11, 1990, Seismic Studies and Design Basis Ground Motion for Nuclear Power Plant Sites, Atomic Energy Regulatory Board, AERB Safety Guide.

Seed, H. B., Ugas, C., and Lysmer, J., 1976, Site Dependent Spectra for Earthquake-Resistance Design, Bulletin of Seismological Society of America, Vol. 66, No.1, pp. 221-243.

Seed, H. B., and Idriss, I. M., 1982, Ground Motion and Soil Liquefaction during Earthquakes, Earthquake Engineering Research Institute, Berkeley, CA.

Trifunac, M. D., and Brady, A. G., 1975, A Study on the Duration of Strong Earthquake Ground Motion, Bulletin of Seismological Society of America, Vol.65, pp. 521-626.

Tso, W. K., Zhu, T. J., and Heidebrecht, A. C., 1992, Engineering Implication of Ground Motion A/V Ratio, Soil Dynamics and Earthquake Engineering, Vol.11, pp. 133-144.

UBC-1991, Uniform Building Code, International Conference of Building officials, whitter, California, USA.

Vanmarcke, E. H., and Lai, S. P., 1977, Strong Motion Duration of Earthquakes, Department of Civil Engineering, M.I.T. Pulication No. R77-16.

Zhu, T. J., Tso, W. K., and Heidebrecht, A. C., 1988, Effect of Peak Ground A/V Ratio on Structural Damage, Journal of the Structural Engineering Division, ASCE, Vol.110, pp. 1019-1037.

EQ 88-16, 1988, Performance of Strong Motion Instruments in Bihar-Nepal Earthquake of August 21, 1988, Earthquake Engineering Studies, Department of Earthquake Engineering, University of Roorkee, Roorkee.

EQ 93-01, 1993, Performance of Strong Motion Instruments in Garhwal (UP) Earthquake of October 20, 1991, Earthquake Engineering Studies, Department of Earthquake Engineering, University of Roorkee, Roorkee.

APPENDIX A

Table A-1 For April 26, 1986 earthquake recorded in Kangra Array.

SR. NO.	LOCATION	EPICENTRAL DISTANCE (Km)		DIRN.*	PEAK GROUND ACCL. (g)	PEAK GROUND VEL. (mm/s)	PEAK GROUND DISPL. (mm)	DURATION TRIFUNAC & BRADY (1975) (sec)	SPECTRUM INTENSITY FOR 5% DAMPING (mm)
1	BHANDLKHAS	Δ1	= 14.8	L	0.145	83.13	20.08	2.82	174.92
		Δ2	= 22.3	T	0.125	90.75	5.85	3.16	147.23
		Δ3	= 26.3	V	0.020	19.03	6.33	9.04	61.93
		Δ4	= 24.8						
2	BAROH	Δ1	= 18.1	L	0.058	36.80	6.55	4.34	89.03
		Δ2	= 13.1	T	0.057	27.00	4.58	6.74	101.74
		Δ3	= 22.2	V	0.020	15.07	3.64	10.50	57.85
		Δ4	= 23.2						
3	BHAWARNA	Δ1	= 14.7	L	0.036	11.70	2.73	9.04	58.39
		Δ2	= 19.1	T	0.035	19.21	4.20	8.08	75.72
		Δ3	= 26.3	V	0.036	9.34	21.13	5.98	36.85
		Δ4	= 25.5						
4	DHARAMSHALA	Δ1	= 9.9	L	0.176	72.97	7.76	2.60	188.37
		Δ2	= 11.3	T	0.186	94.90	24.79	3.94	379.46
		Δ3	= 5.0	V	0.083	27.39	4.19	4.34	99.61
		Δ4	= 2.8						
5	JAWALI	Δ1	= 36.5	L	0.015	19.20	6.90	15.92	78.62
		Δ2	= 29.0	T	0.017	15.18	9.56	13.99	58.34
		Δ3	= 26.4	V	0.011	14.39	7.53	16.14	71.01
		Δ4	= 28.6						
6	KANGRA	Δ1	= 13.5	L	0.148	50.57	5.23	4.84	143.84
		Λ2	= 5.2	T	0.111	95.75	9.67	3.74	248.76
		Δ3	= 11.0	V	0.072	31.93	5.37	5.40	104.75
		Δ4	= 12.5						
7	NAGROTABAGWAN	Δ1	= 3.6	L	0.149	94.17	13.09	4.28	228.38
		Δ2	= 6.4	T	0.080	25.40	6.14	5.14	78.55
		Δ3	= 12.9	V	0.050	18.19	6.51	14.82	89.39
		Δ4	= 12.5						
8	SHAHPUR	Δ1	= 20.4	L	0.200	59.21	7.26	2.70	193.59
		Δ2	= 15.8	T	0.250	147.80	10.85	2.00	309.97
		Δ3	= 6.8	V	0.065	28.04	5.25	6.40	110.13
		Δ4	= 10.3						
9	SIHUNTA	Δ1	= 34.3	L	0.050	26.72	4.71	6.20	96.32
		Δ2	= 30.6	T	0.036	33.88	3.67	6.66	105.27
		Δ3	= 22.4	V	0.039	27.73	4.74	9.34	78.79
		Δ4	= 23.4						

* L : Longitudinal, T : Transverse, V : Vertical

Table A-2 For September 10, 1986 earthquake recorded in Shillong array.

SR. NO.	LOCATION	EPICENTRAL DISTANCE (Km)		DIRN.*	PEAK GROUND ACCL. (g)	PEAK GROUND VEL. (mm/s)	PEAK GROUND DISPL. (mm)	DURATION TRIFUNAC & BRADY (1975) (sec)	SPECTRUM INTENSITY FOR 5% DAMPING (mm)
1	BAITHLANGSO	Δ1	= 139.4	L	0.045	20.58	3.55	10.38	60.31
		Δ2	= 102.1	T	0.042	12.07	2.73	10.78	55.40
		Δ3	= 181.2	V	0.025	10.91	4.74	11.86	39.24
2	DAUKI	Δ1	= 42.7	L	0.089	32.40	3.00	3.92	64.50
		Δ2	= 32.5	T	0.090	37.33	2.56	5.30	67.49
		Δ3	= 48.1	V	0.032	14.14	5.92	14.26	60.31
3	KHLIEHRIAT	Δ1	= 81.6	L	0.031	11.30	2.00	10.56	35.00
		Δ2	= 56.9	T	0.046	18.41	3.86	9.60	49.81
		Δ3	= 54.4	V	0.001	7.71	1.95	11.08	37.01
4	NONGKHAW	Δ1	= 65.4	L	0.055	33.09	9.32	17.24	103.41
		Δ2	= 35.8	T	0.093	48.08	5.47	11.76	120.43
		Δ3	= 28.3	V	0.034	14.11	6.83	23.50	64.77
5	NONGPOH	Δ1	= 93.5	L	0.054	21.13	4.26	8.32	39.04
		Δ2	= 56.4	T	0.056	11.32	4.59	12.86	35.94
		Δ3	= 33.8	V	0.033	11.25	2.84	11.19	27.90
6	NONGSTOIN	Δ1	= 55.8	L	0.019	10.04	4.90	7.76	32.69
		Δ2	= 54.5	T	0.014	6.40	1.66	7.54	24.30
		Δ3	= 64.3	V	0.008	5.95	1.99	7.82	22.68
7	PANIMUR	Δ1	= 134.9	L	0.040	9.37	2.02	8.94	27.08
		Δ2	= 103.8	T	0.048	21.15	2.65	5.78	39.76
		Δ3	= 90.2	V	0.023	5.61	1.40	9.42	27.87
8	PYNURSLA	Δ1	= 37.4	L	0.093	26.75	3.24	5.14	83.82
		Δ2	= 15.0	T	0.076	20.37	4.55	8.68	62.32
		Δ3	= 33.6	V	0.030	9.28	3.80	14.78	35.17
9	SAITSAMA	Δ1	= 104.4	L	0.110	36.69	4.90	6.12	74.97
		Δ2	= 68.3	T	0.140	58.73	4.92	2.44	106.37
		Δ3	= 50.1	V	0.062	20.06	3.22	7.32	54.22
10	UMMULONG	Δ1	= 70.9	L	0.110	26.53	2.38	5.82	46.13
		Δ2	= 36.7	T	0.063	12.10	1.56	9.56	34.91
		Δ3	= 27.4	V	0.050	14.25	3.21	11.42	47.99
11	UMRONGSO	Δ1	= 111.1	L	0.027	9.68	1.30	8.26	32.03
		Δ2	= 82.4	T	0.032	11.84	4.41	9.82	35.96
		Δ3	= 72.5	V	0.014	7.81	2.26	10.66	32.72
12	UMSNING	Δ1	= 76.4	L	0.100	28.72	3.42	4.26	57.56
		Δ2	= 38.3	T	0.076	25.67	3.93	8.78	64.84
		Δ3	= 15.0	V	0.050	10.88	3.75	14.50	41.64

* L : Longitudinal, T : Transverse, V : Vertical

Table A-3 For May 18, 1987 earthquake recorded in Shillong array.

SR. NO.	LOCATION	EPICENTRAL DISTANCE (Km)		DIRN.*	PEAK GROUND ACCL. (g)	PEAK GROUND VEL. (mm/s)	PEAK GROUND DISPL. (mm)	DURATION TRIFUNAC & BRADY (1975) (sec)	SPECTRUM INTENSITY FOR 5% DAMPING (mm)
1	BAITHLANGSO	Δ1 =	121.8	L	0.034	15.53	4.15	16.84	55.89
		Δ2 =	177.5	T	0.027	21.56	8.11	18.50	70.02
		Δ3 =	112.8	V	0.020	12.85	3.80	18.14	59.79
2	BAMUNGAO	Δ1 =	82.1	L	0.020	12.22	4.24	22.58	44.31
		Δ2 =	137.7	T	0.020	22.00	6.78	23.48	57.87
		Δ3 =	73.8	V	0.019	13.62	3.32	25.18	65.10
3	BERLONGFER	Δ1 =	54.0	L	0.072	35.95	5.51	26.52	110.19
		A2 =	109.5	T	0.090	36.20	8.95	22.78	128.03
		₩3 =	46.0	V	0.046	19.24	7.47	30.62	72.52
4	BOKAJAN	Δ1 =	56.4	L	0.030	25.96	9.34	18.88	75.47
		Δ2 =	91.5	T	0.066	34.28	10.31	12.04	107.65
		Δ3 =	58.4	V	0.020	13.20	5.25	21.92	44.61
5	DIPHU	Δ1 =	53.7	L	0.086	27.69	5.80	27.06	94.39
		Δ2 =	104.7	T	0.073	23.92	11.54	27.18	90.79
		Δ3 =	49.6	V	0.054	15.31	6.65	26.68	78.30
6	GUNJUNG	Δ1 =	73.5	L	0.040	23.04	5.55	12.46	84.34
		Δ2 =	120.0	T	0.049	28.56	5.51	11.60	90.31
		Δ3 =	64.0	V	0.019	10.83	3.38	12.08	53.12
7	HAFLONG	Δ1 =	77.9	L	0.055	36.93	8.35	6.62	120.59
		Δ2 =	119.0	T	0.035	20.61	5.38	9.82	107.89
		Δ3 =	69.3	V	0.015	12.15	3.06	11.06	62.22
8	HAJADISA	Δ1 =	42.7	L	0.078	38.07	7.50	12.16	111.86
		Δ2 =	90.5	T	0.086	28.07	5.00	11.24	99.50
		Δ3 =	33.6	V	0.028	15.34	3.49	13.40	74.82
9	HATIKHALI	Δ1 =	62.3	L	0.031	14.55	5.55	27.06	60.68
		Δ2 =	117.5	T	0.038	17.71	3.48	27.26	70.48
		Δ3 =	52.7	V	0.027	18.58	3.64	28.86	74.64
10	LAISONG	Δ1 =	52.2	L	0.042	32.25	7.84	11.28	103.30
		Δ2 =	90.4	T	0.061	23.69	9.42	9.68	109.10
		Δ3 =	45.0	V	0.019	13.54	6.20	13.68	67.30
11	NONGPOH	Δ1 =	188.7	L	0.017	13.12	4.88	16.24	35.71
		Δ2 =	243.4	T	0.047	12.58	5.93	16.46	51.92
		Δ3 =	179.0	V	0.013	9.55	3.13	16.62	54.64
12	PANIMUR	Δ1 =	91.6	L	0.040	18.00	4.10	9.12	53.32
		Δ2 =	146.0	T	0.047	18.11	2.99	9.92	47.74
		Δ3 =	81.7	V	0.017	16.79	5.78	9.52	37.23

.. contd.

SR. NO.	LOCATION	EPICENTRAL DISTANCE		DIRN.*	PEAK GROUND ACCL.	PEAK GROUND VEL.	PEAK GROUND DISPL.	DURATION TRIFUNAC & BRADY (1975)	SPECTRUM INTENSITY FOR 5% DAMPING
		(Km)			(g)	(mm/s)	(mm)	(sec)	(mm)
13	SAITSAMA	$\Delta 1$	= 133.9	L	0.037	13.92	3.36	20.36	39.16
		$\Delta 2$	= 188.1	T	0.050	22.84	8.91	20.38	80.19
		$\Delta 3$	= 124.1	V	0.019	9.29	4.00	21.14	45.12
14	UMRONGSO	$\Delta 1$	= 106.3	L	0.021	13.79	2.76	10.94	44.37
		$\Delta 2$	= 160.2	T	0.026	14.50	5.69	9.90	51.81
		$\Delta 3$	= 98.3	V	0.016	9.13	2.91	10.04	41.11

L : Longitudinal,   T : Transverse,   V : Vertical

Table A-4 For February 6, 1987 earthquake recoded in Shillong Array.

SR. NO.	LOCATION	EPICENTRAL DISTANCE (Km)		DIRN.*	PEAK GROUND ACCL. (g)	PEAK GROUND VEL. (mm/s)	PEAK GROUND DISPL. (mm)	DURATION TRIFUNAC & BRADY (1975) (sec)	SPECTRUM INTENSITY FOR 5% DAMPING (mm)
1	BAIGAO	Δ1 =	190.3	L	0.022	14.14	3.90	11.28	56.19
		Δ2 =	159.0	T	0.024	20.64	6.90	10.72	115.95
		Δ3 =	150.4	V	0.009	11.27	3.26	10.58	73.46
2	BAITHLANGSO	Δ1 =	193.2	L	0.031	13.65	3.81	10.06	59.99
		Δ2 =	184.0	T	0.022	12.26	3.33	9.94	70.49
		Δ3 =	135.5	V	0.014	7.44	1.76	10.46	29.40
3	BAMUNGAO	Δ1 =	223.1	L	0.016	5.08	1.30	7.24	27.01
		Δ2 =	203.9	T	0.013	10.35	2.30	7.72	33.88
		Δ3 =	175.5	V	0.010	6.23	2.33	7.20	26.98
4	DAUKI	Δ1 =	103.7	L	0.027	18.01	2.50	7.50	55.74
		Δ2 =	79.0	T	0.038	18.37	4.41	6.78	57.38
		Δ3 =	75.5	V	0.010	8.57	3.41	8.62	33.73
5	GUNJUNG	Δ1 =	202.8	L	0.036	29.05	6.26	8.68	103.77
		Δ2 =	166.7	T	0.037	24.44	3.87	7.96	74.97
		Δ3 =	166.5	V	0.020	12.87	3.30	10.78	44.54
6	HAFLONG	Δ1 =	202.5	L	0.034	19.42	3.13	8.16	67.35
		Δ2 =	162.3	T	0.027	14.02	3.34	8.04	71.51
		Δ3 =	170.8	V	0.008	7.22	1.99	9.04	22.00
7	HATIKHALI	Δ1 =	222.3	L	0.024	8.78	3.18	8.98	33.11
		Δ2 =	195.3	T	0.025	9.87	3.84	10.18	33.50
		Δ3 =	175.8	V	0.021	7.29	1.98	10.34	28.00
8	KATAKHAL	Δ1 =	164.6	L	0.009	10.64	3.04	8.82	64.70
		Δ2 =	114.9	T	0.008	7.75	1.60	9.28	32.11
		Δ3 =	149.4	V	0.010	9.88	4.00	9.30	44.81
9	KHLIEHRIAT	Δ1 =	142.2	L	0.080	47.46	8.45	3.90	133.52
		Δ2 =	116.9	T	0.066	27.87	3.44	6.12	85.16
		Δ3 =	103.0	V	0.029	15.91	2.94	9.30	49.40
10	MAWPHLANG	Δ1 =	91.7	L	0.081	43.85	7.97	19.90	98.18
		Δ2 =	93.5	T	0.059	24.89	10.14	20.28	100.55
		Δ3 =	42.0	V	0.036	12.33	4.86	23.74	42.19
11	NONGKHLAW	Δ1 =	99.3	L	0.110	42.94	9.58	24.20	89.75
		Δ2 =	116.5	T	0.114	52.63	11.41	13.52	156.09
		Δ3 =	35.0	V	0.104	35.10	11.23	16.58	84.15
12	NONGPOH	Δ1 =	132.9	L	0.027	15.89	4.64	12.28	46.50
		Δ2 =	144.7	T	0.086	26.45	3.75	8.40	74.80
		Δ3 =	68.4	V	0.038	10.64	4.02	12.68	40.16

.. contd.

SR. NO.	LOCATION	EPICENTRAL DISTANCE (Km)		DIRN.*	PEAK GROUND ACCL. (g)	PEAK GROUND VEL. (mm/s)	PEAK GROUND DISPL. (mm)	DURATION TRIFUNAC & BRADY (1975) (sec)	SPECTRUM INTENSITY FOR 5% DAMPING (mm)
13	PYNURSLA	$\Delta1$ =	96.1	L	0.050	21.24	4.99	21.96	72.09
		$\Delta2$ =	83.1	T	0.031	11.95	4.93	22.54	51.90
		$\Delta3$ =	59.4	V	0.015	9.43	3.63	28.44	47.79
14	SAITSAMA	$\Delta1$ =	159.9	L	0.066	22.38	4.50	9.28	71.83
		$\Delta2$ =	148.6	T	0.058	32.43	4.37	9.66	75.86
		$\Delta3$ =	106.1	V	0.032	9.90	2.37	12.52	48.50
15	SHILLONG	$\Delta1$ =	109.1	L	0.047	16.06	5.16	8.82	57.06
		$\Delta2$ =	108.4	T	0.036	15.39	7.86	9.00	64.78
		$\Delta3$ =	55.3	V	0.013	14.42	5.19	10.64	57.49
16	UMMULONG	$\Delta1$ =	127.9	L	0.056	22.48	5.69	19.82	66.66
		$\Delta2$ =	115.3	T	0.055	21.42	6.35	19.18	81.74
		$\Delta3$ =	80.0	V	0.024	10.89	4.37	22.30	40.30
17	UMRONGSO	$\Delta1$ =	171.1	L	0.046	31.43	3.06	7.80	81.06
		$\Delta2$ =	146.7	T	0.037	26.58	6.67	9.32	95.65
		$\Delta3$ =	126.9	V	0.022	12.26	2.38	11.20	47.64
18	UMSNING	$\Delta1$ =	205.5	L	0.040	16.62	3.14	18.19	51.45
		$\Delta2$ =	184.0	T	0.061	36.93	5.03	14.54	78.16
		$\Delta3$ =	155.5	V	0.018	11.95	3.55	20.84	53.25

L : Longitudinal,   T : Transverse,   V : Vertical

able A-5 For August 6, 1988 earthquake recorded in Shillong array.

SR. NO.	LOCATION	EPICENTRAL DISTANCE (Km)		DIRN.*	PEAK GROUND ACCL. (g)	PEAK GROUND VEL. (mm/s)	PEAK GROUND DISPL. (mm)	DURATION TRIFUNAC & BRADY (1975) (sec)	SPECTRUM INTENSITY FOR 5% DAMPING (mm)
1	BAIGAO	Δ1 =	227.5	L	0.221	65.68	10.19	31.919	169.00
		Δ2 =	226.7	T	0.144	63.70	9.80	33.899	182.74
		Δ3 =	165.0	V	0.053	20.11	5.85	38.180	83.00
2	BAITHLANGSO	Δ1 =	268.2	L	0.154	75.52	12.36	28.079	256.94
		Δ2 =	266.2	T	0.165	117.05	15.45	28.839	420.49
		Δ3 =	200.3	V	0.082	36.12	6.98	46.099	136.21
3	BAMUNGAO	Δ1 =	227.6	L	0.093	64.03	8.96	24.319	203.34
		Δ2 =	225.5	T	0.069	49.80	10.23	22.979	200.59
		Δ3 =	159.5	V	0.065	25.06	4.23	23.359	85.14
4	BERLONGFOR	Δ1 =	199.5	L	0.300	217.24	33.40	21.960	898.11
		Δ2 =	197.5	T	0.344	228.19	36.30	20.000	806.13
		Δ3 =	131.6	V	0.174	90.26	13.18	41.599	247.96
5	BOKAJAN	Δ1 =	167.2	L	0.151	86.75	19.91	20.699	345.83
		Δ2 =	163.8	T	0.224	121.36	20.41	20.499	369.27
		Δ3 =	99.5	V	0.148	32.49	9.14	30.819	141.69
6	CHERAPUNJI	Δ1 =	337.2	L	0.052	21.47	3.57	15.839	92.27
		Δ2 =	336.9	T	0.055	26.78	6.22	15.219	111.90
		Δ3 =	277.0	V	0.024	20.45	3.81	17.780	65.50
7	DAUKI	Δ1 =	308.5	L	0.110	46.87	7.56	15.779	152.82
		Δ2 =	308.4	T	0.073	44.53	5.78	14.899	150.53
		Δ3 =	249.5	V	0.031	20.74	6.52	18.139	73.07
8	DIPHU	Δ1 =	190.1	L	0.283	181.48	23.25	19.979	636.62
		Δ2 =	187.5	T	0.338	205.55	22.74	16.779	561.12
		Δ3 =	121.4	V	0.180	56.12	9.00	34.659	196.14
9	DULOO	Δ1 =	232.6	L	0.064	58.89	14.40	18.739	274.51
		Δ2 =	233.1	T	0.062	53.49	12.61	20.099	238.49
		Δ3 =	180.0	V	0.039	33.83	7.63	28.079	156.03
10	GUNJUNG	Δ1 =	211.2	L	0.092	44.19	8.74	28.199	176.73
		Δ2 =	210.7	T	0.133	52.05	8.58	25.239	202.44
		Δ3 =	150.4	V	0.062	25.56	6.74	41.279	88.27
11	HAJADISA	Δ1 =	182.5	L	0.092	42.73	9.72	34.180	175.12
		Δ2 =	181.6	T	0.098	46.43	8.77	32.180	174.97
		Δ3 =	120.1	V	0.046	22.28	5.98	43.599	89.18
12	HARENGJAO	Δ1 =	225.0	L	0.065	40.99	7.57	20.839	167.89
		Δ2 =	225.1	T	0.078	44.39	8.92	19.459	161.06
		Δ3 =	168.4	V	0.032	22.15	6.31	21.260	69.89

SR. NO.	LOCATION	EPICENTRAL DISTANCE (Km)		DIRN.*	PEAK GROUND ACCL. (g)	PEAK GROUND VEL. (mm/s)	PEAK GROUND DISPL. (mm)	DURATION TRIFUNAC & BRADY (1975) (sec)	SPECTRUM INTENSITY FOR 5% DAMPING (mm)
13	HOJAI	$\Delta1$ =	245.8	L	0.108	51.88	14.06	22.439	203.24
		$\Delta2$ =	243.6	T	0.134	65.61	11.61	21.939	260.09
		$\Delta3$ =	177.5	V	0.061	25.25	7.83	41.900	121.04
14	JALLALPUR	$\Delta1$ =	265.2	L	0.029	30.40	4.81	13.559	130.38
		$\Delta2$ =	265.5	T	0.023	20.46	5.18	13.879	82.49
		$\Delta3$ =	209.8	V	0.015	17.07	4.01	13.419	57.62
15	JHIRIGHAT	$\Delta1$ =	202.8	L	0.098	88.30	11.15	18.500	364.48
		$\Delta2$ =	203.8	T	0.089	70.35	10.05	20.779	296.53
		$\Delta3$ =	155.3	V	0.031	30.38	8.21	25.700	148.15
16	KALAIN	$\Delta1$ =	253.8	L	0.057	77.76	15.87	17.979	328.96
		$\Delta2$ =	254.2	T	0.051	51.09	15.71	19.799	223.70
		$\Delta3$ =	199.3	V	0.029	43.21	10.89	22.620	147.82
17	KATAKHAL	$\Delta1$ =	248.7	L	0.067	110.74	23.34	18.360	506.98
		$\Delta2$ =	249.5	T	0.059	93.56	25.26	19.339	366.33
		$\Delta3$ =	197.8	V	0.018	33.72	10.11	21.199	133.94
18	KHLIEHRIAT	$\Delta1$ =	274.8	L	0.070	29.21	4.55	26.780	105.75
		$\Delta2$ =	274.2	T	0.071	31.74	5.42	31.659	112.44
		$\Delta3$ =	213.4	V	0.035	16.11	3.44	46.219	47.66
19	KOOMBER	$\Delta1$ =	210.7	L	0.049	39.04	9.86	16.899	184.96
		$\Delta2$ =	211.2	T	0.037	34.88	7.14	18.920	169.30
		$\Delta3$ =	158.2	V	0.027	23.23	5.57	19.920	98.26
20	LOHARGHAT	$\Delta1$ =	376.1	L	0.058	36.58	8.58	30.879	205.47
		$\Delta2$ =	374.1	T	0.054	48.61	9.91	28.459	255.16
		$\Delta3$ =	303.4	V	0.022	20.42	5.06	27.360	94.73
21	MAWKYRWAT	$\Delta1$ =	364.6	L	0.046	25.18	3.10	17.799	70.94
		$\Delta2$ =	364.1	T	0.046	21.98	4.80	18.920	78.82
		$\Delta3$ =	303.4	V	0.032	17.51	4.69	18.360	66.87
22	MAWPHLANG	$\Delta1$ =	335.6	L	0.115	39.17	6.78	25.359	102.96
		$\Delta2$ =	335.0	T	0.107	38.99	5.34	29.659	83.51
		$\Delta3$ =	273.4	V	0.036	12.52	3.85	30.019	45.56

SR. NO.	LOCATION	EPICENTRAL DISTANCE (Km)		DIRN.*	PEAK GROUND ACCL. (g)	PEAK GROUND VEL. (mm/s)	PEAK GROUND DISPL. (mm)	DURATION TRIFUNAC & BRADY (1975) (sec)	SPECTRUM INTENSITY FOR 5% DAMPING (mm)
23	MAWSYNRAM	Δ1 =	352.3	L	0.085	33.67	8.29	17.399	136.06
		Δ2 =	352.0	T	0.064	28.61	5.47	18.199	124.34
		Δ3 =	292.0	V	0.036	21.45	5.89	17.760	90.86
24	NONGKHLAW	Δ1 =	352.8	L	0.138	64.50	6.02	30.879	149.06
		Δ2 =	351.8	T	0.146	55.66	11.07	28.100	182.58
		Δ3 =	288.4	V	0.083	34.17	9.46	31.399	97.47
25	NONGSTOIN	Δ1 =	385.9	L	0.054	24.09	9.54	28.399	83.96
		Δ2 =	385.3	T	0.052	31.04	11.16	27.779	99.32
		Δ3 =	323.5	V	0.042	14.80	6.14	29.540	65.43
26	PANIMUR	Δ1 =	238.1	L	0.169	55.19	5.29	31.379	132.72
		Δ2 =	236.7	T	0.125	44.38	6.06	41.819	110.47
		Δ3 =	172.3	V	0.073	20.85	6.14	48.159	59.68
27	PYNURSLA	Δ1 =	320.8	L	0.049	42.13	5.92	22.439	138.09
		Δ2 =	320.4	T	0.051	32.24	7.22	24.200	112.20
		Δ3 =	260.2	V	0.036	31.55	6.35	23.159	116.57
28	SAITSAMA	Δ1 =	280.3	L	0.211	87.31	7.83	33.799	218.48
		Δ2 =	279.0	T	0.233	103.63	13.89	32.519	261.50
		Δ3 =	214.6	V	0.099	33.77	4.82	46.840	95.51
29	SHILLONG	Δ1 =	323.9	L	0.075	20.44	3.24	24.319	65.13
		Δ2 =	323.1	T	0.057	17.55	5.86	26.139	58.26
		Δ3 =	260.5	V	0.036	9.75	3.31	26.000	42.02
30	SILCHAR	Δ1 =	233.0	L	0.064	71.52	21.10	22.579	277.62
		Δ2 =	233.0	T	0.091	98.76	21.13	18.079	426.91
		Δ3 =	188.1	V	0.025	29.98	8.62	41.720	98.40
31	UMMULONG	Δ1 =	298.4	L	0.100	30.76	7.86	30.639	87.60
		Δ2 =	297.6	T	0.153	43.95	12.80	25.780	128.93
		Δ3 =	235.3	V	0.062	27.33	11.28	34.859	88.15
32	UMRONGSO	Δ1 =	252.3	L	0.780	51.66	6.46	31.359	197.65
		Δ2 =	251.4	T	0.081	39.98	7.76	31.099	169.49
		Δ3 =	188.7	V	0.045	17.48	4.46	34.159	51.01
33	UMSNING	Δ1 =	329.4	L	0.136	41.46	7.88	29.159	121.41
		Δ2 =	328.2	T	0.153	51.94	10.12	26.439	149.39
		Δ3 =	264.3	V	0.071	38.31	12.50	41.060	61.92

* L : Longitudinal,   T : Transverse,   V : Vertical

Table A-6 For October 20, 1991 earthquake recorded in UttarPradesh Array.

SR. NO.	LOCATION	EPICENTRAL DISTANCE (km)	DIRN.*	PEAK GROUND ACCL. (g)	PEAK GROUND VEL. (mm/sec)	PEAK GROUND DISPL. (mm)	DURATION TRIFUNAC & BRADY (1975) (sec)	SPECTRUM INTENSITY FOR 5% DAMPING (mm)
1	BHATWARI	25.3	L	0.253	178.73	37.54	13.559	128.28
			T	0.247	297.78	53.23	11.699	206.27
			V	0.294	133.65	23.53	17.879	77.09
2	UTTARKASHI	40.2	L	0.242	169.56	21.15	15.119	207.06
			T	0.310	194.68	19.85	14.079	172.11
			V	0.196	141.56	22.98	18.560	134.67
3	GHANSALI	41.1	L	0.118	80.44	13.57	11.119	92.52
			T	0.117	78.21	13.37	11.139	91.21
			V	0.101	95.94	25.90	13.079	83.72
4	RUDRAPRAYAG	54.4	L	0.053	20.70	7.85	6.860	506.97
			T	0.052	27.06	4.01	6.860	579.37
			V	0.045	17.92	3.83	11.56	433.27
5	TEHRI	54.4	L	0.073	42.15	8.17	7.820	709.71
			T	0.062	92.30	19.84	5.460	1382.31
			V	0.059	88.41	23.68	7.660	568.51
6	SRINAGAR	59.4	L	0.067	19.45	5.86	16.279	361.40
			T	0.050	20.20	5.07	17.719	345.22
			V	0.034	35.25	7.62	17.779	395.03
7	BARKOT	62.7	L	0.095	57.87	10.93	14.159	217.77
			T	0.082	44.84	6.98	13.539	428.18
			V	0.044	27.53	5.62	14.299	422.79
8	KOTESHWAR	64.6	L	0.101	51.55	11.14	14.140	227.38
			T	0.066	39.27	6.78	18.330	200.27
			V	0.076	85.25	20.47	19.520	343.09
9	KARNAPRAYAG	65.5	L	0.062	36.90	5.80	25.379	111.96
			T	0.079	37.30	4.02	25.520	93.24
			V	0.026	14.98	2.17	27.719	164.18
10	PUROLA	76.0	L	0.075	48.13	8.44	23.860	77.60
			T	0.093	45.91	9.22	21.739	75.25
			V	0.053	25.57	4.49	22.639	67.10

SR. NO.	LOCATION	EPICENTRAL DISTANCE (km)	DIRN.*	PEAK GROUND ACCL. (g)	PEAK GROUND VEL. (mm/sec)	PEAK GROUND DISPL. (mm)	DURATION TRIFUNAC & BRADY (1975) (sec)	SPECTRUM INTENSITY FOR 5% DAMPING (mm)
11	KOTI	105.4	L	0.021	23.43	4.27	12.920	199.10
			T	0.042	28.60	3.40	14.019	104.79
			V	0.015	17.65	5.05	16.859	49.64
12	KOSANI	143.6	L	0.029	18.82	3.77	11.199	54.75
			T	0.032	15.55	2.86	11.439	52.71
			V	0.011	9.17	2.41	12.139	34.64
13	ALMORA	150.5	L	0.018	13.32	3.42	16.299	45.40
			T	0.021	12.62	4.50	17.440	46.78
			V	0.019	15.48	3.98	18.039	44.25

* L : Longitudinal, T : Transverse, V : Vertical